

Point-by-point Response

*** Note to Editor ***

All line numbers refer to revised manuscript. Line numbers in “tracked changes” at the end of the “Authors Response” document differ.

Reviewer 1

Review of “Detecting the permafrost carbon feedback: Talik formation and increased cold-season respiration as precursors to sink-to-source transitions”

The authors ran the Community Land Model (CLM) version 4.5 up to 2300, using RCP 8.5 forcing. They then perform an in depth analysis of permafrost-region dynamics in this simulation, including identifying key events: Talik formation (related the degradation of permafrost) and sink-to-source transition, i.e. the point at which the land surface changes from a net sink of carbon from the atmosphere, to a net source. It is interesting to note that this behaviour (starting as a sink and transitioning to a source) is identified across a large fraction of the current permafrost zone. However, the total carbon source is apparently only 11.6 GtC by 2300, which is low compared with previous estimates.

The authors extensively analyse different variables such as thawed volume (a newly defined metric), active layer depth, primary production, respiration and fires, and how these influence talik formation and sink-to-source transition. They find three main drivers of sink-to-source transition: 1. Active layer thickening in cold, carbon-rich high Arctic permafrost 2. Talik formation leading to winter respiration in low Arctic, warmer soils 3. Fire driven carbon source in more productive regions which dry out, and a lot of vegetation is burned. They also showed some indicators of talik formation such as a rapid increase in thawed volume immediately preceding talik formation.

This is a very thorough analysis and a well written paper that will make a great publication in The Cryosphere, after some small revisions. In general I would like to see a bit more analysis about the size of the carbon sources, not just the timing of transition. This could comprise a bit of discussion of the cumulative carbon source (11.6 Gt), and the significance of this - compared to previous estimates, and the time trajectory of the cumulative source (i.e. when does the Arctic as a whole become a net source?). And then if they could break that down to say which of the different types of source (driven by AL, talik or fires) has the bigger contribution to the total source or if these are all comparable magnitude, that would be add some value to the paper. It's fine saying that we should monitor the high Arctic systems as they will become a source soonest, but if this source is likely to be very small, there would not be so much point?

We thank the reviewer for the astute observation of the small source and excellent recommendation to enhance our discussion. We found an error in our C source budget calculation with the new total being 120 Pg C by 2300. We have corrected this error, and included more extensive analysis and discussion of cumulative carbon emissions and sources throughout the paper (see responses below).

I also suggest considering the soil types at the boreholes. It would hopefully be possible to get an idea of this from a site description or by asking the PI. For example if these are peaty soils that might explain the very slow progression of freeze-thaw compared with CLM (also relatedly, the water content).

This is a good suggestion. It's difficult to pin down in CLM if mineral soil texture affects thaw rates compared to borehole observations due to the many possible explanation for differences in thaw rates: soil organic content, lateral water flow, surface slope and aspect, ground ice. However, we have looked into soil texture effects at the Alaskan boreholes and find that higher rates of observed soil thawing may be related to 2 factors: (1) relatively dry upper soil at the Gakona and Mould Bay sites, and (2) low surface organic layer and high conductivity of the Barrow2 and Mould Bay soils.

We revised the site descriptions in methods as follows (line 245):

*“Mould Bay is a continuous permafrost tundra site with measurements at 63 depths from 0 - 3 m. **Mould Bay has almost no organic layer (about 2 cm) and then sandy silt with high thermal conductivity.** Barrow is a continuous permafrost tundra site with measurements at 35 depths from 0 - 15 m. **The soil at Barrow is represented by silt with a bit of mix with some organics and almost no organic layer on top. Conductivity of the upper layer is $\sim 1 \text{ W mK}^{-1}$ for unfrozen and $\geq 2 \text{ W mK}^{-1}$ for frozen soil.** Gakona is a continuous permafrost forest tundra site with measurements at 36 depths from 0 - 30 m. **Gakona has a thick organic layer of moss (0 to 5 cm), dead moss (from 5 to 13 cm), and peat (from 13 to 50 cm), then silty clay at depth.**”*

We offer an explanation for high observed thaw rates in Section 3.1 (line 359):

*“Overall, we find that simulated patterns of permafrost thermal state change are consistent with available observations, but that the exact thaw rates are uncertain. **Although there are many possible explanations for differences in observed and simulated thaw rates, we can attribute high observed thaw rates in part to a combination of (1) relatively dry upper soil at Gakona and Mould Bay, and (2) low surface organic layer and high conductivity of the Barrow and Mould Bay soils.** We keep these uncertainties in mind as we examine patterns of change and talik formation simulated into 2300.”*

We offer some advice for future experiments in the discussion (line 586):

“Controlled experiments demonstrating the sensitivity of talik to parameters that control soil drying such ice impedance or baseflow scalars (e.g. Lawrence et al., 2015), and the effect of organic content and mineral soil texture (Lawrence and Slater, 2008), could provide key insight on soil thermal dynamics in frozen or partially frozen conditions.”

We also include an additional column in Table 2 for soil characteristics:

Site	Location	Date Range	Soil Features: Surface organic layer / Soil Type	Depth / Number of Layers	Layer of Deepest Thaw	Month of Latest Thaw
------	----------	------------	-----------------------------------------------------	--------------------------	-----------------------	----------------------

Mould Bay, Canada	119.0°W, 76.0°N	2004- 2012	Low organic layer (~2 cm)/ Sandy silt	3 m / 36	0.69 m	September
Barrow2, Alaska	156.0°W, 71.3°N	2006- 2013	Low organic layer / Sandy silt	15 m / 63	0.58 m	October
Gakona1, Alaska	145.0°W, 62.4°N	2009- 2013	Thick organic layer (50 cm) / Silty clay	30 m / 35	2.5 m	February

Finally the paper is rather long and I would suggest reducing in length where possible. I have indicated a couple of points below.

We removed figures 10 and 11 as suggested by the reviewers, but added a new figure for cumulative carbon sources to address the primary reviewer concerns.

Line-by-line comments

Introduction: L62: ‘Shifts in vegetation community’ is mentioned in the introduction as being an important factor, but is this considered here? Are you running with dynamic vegetation? If you are, this should be mentioned and if not, this omission should be discussed later on. L70: Same for soil organic matter export by rivers.

Since these processes are not considered in this analysis, we added a qualifier statement later on in the discussion (Line 590):

“Other factors affecting soil hydrology and carbon cycling not considered in our CLM4.5 simulations include high spatial resolution in discontinuous permafrost, shifts in vegetation community, lateral flow representation, thermokarst activity and other thaw-related changes to the ground surface, surface slope and aspect, soil heterogeneity, and potentially several other factors (see Jorgenson and Osterkamp (2005) for discussion of some of the many complexities to be considered).”

L86-87: Include more recent references for total permafrost carbon quantity, such as Hugelius et al 2014, Biogeosciences (<https://www.biogeosciences.net/11/6573/2014/bg-11-6573-2014.pdf>), and there is also a new paper by Jackson et al coming out in November with revised estimates, this will be in Annual review of Ecology, Evolution and Systematics (<http://www.annualreviews.org/doi/abs/10.1146/annurev-ecolsys-112414-054234>).

References and carbon totals are updated as follows (Line 91):

“Taliks as well as longer, deeper active layer thaws stimulate respiration of soil C (Romanovsky and Osterkamp, 2000; Lawrence et al., 2008), making the ~1035 Pg soil organic carbon in near surface permafrost (0-3 m) and ~350 Pg soil organic carbon in deep permafrost (> 3 m) vulnerable to decomposition (Hugelius et al., 2014; Jackson et al., 2017).”

Methods: L138-142 The standard RCP 8.5 only goes until 2100 so presumably some extension is used here? Could you mention what this looks like - for example, does it stabilise at some point

or does the global temperature and CO2 just keep increasing? I also think it would be useful for comparing with the permafrost thaw results, to see a plot of the global temperature across the three centuries of future simulation. I suggest adding this at least as a supplementary figure (as there are already a lot of figures in the main manuscript).

We used the ECP8.5 scenario for the period 2100-2300. We added a time series for air temperature in Figure 1A (shown below) and modified our methodology description as follows (Line 165):

“We use an anomaly forcing method to repeatedly force CLM4.5 with observed meteorological from the CRUNCEP dataset for the period 1996–2005 (data available at dods.ipsl.jussieu.fr/igcmg/IGCM/BC/OOL/OL/CRU-NCEP/) and monthly anomalies added based on a single ensemble member from a CCSM4 Representative Concentration Pathway 8.5 (RCP8.5) simulation for the years 2006-2100 and Extended Concentration Pathway 8.5 (ECP8.5) for the years 2100-2300. Land air temperature for the period 2006-2300, shown in Fig. 1A., is projected to increase steadily in our simulation, with a slight decrease in the rate of warming”

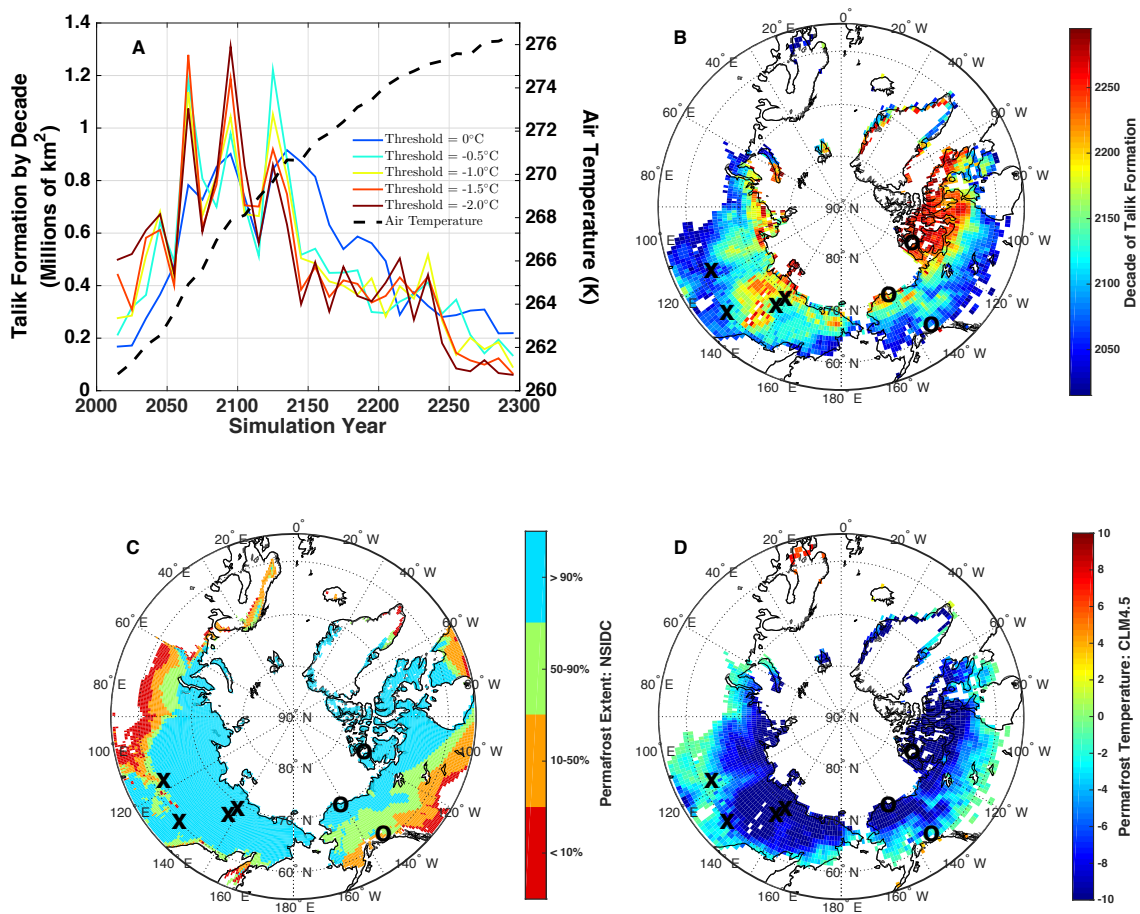


Figure 1. Decade of projected talik formation and correlation to initial state of simulated permafrost temperature and observed permafrost extent. (A) Time series and (B) map of the simulated decade of talik formation are estimated from CLM4.5 as the first decade when the mean temperature of a soil layer exceeds a freeze/thaw threshold of -0.5°C in every month. Additional colors in A represent progression of talik onset for different freeze/thaw threshold. (C) Initial permafrost temperature is defined as the annual mean soil temperature at 3 m depth from 2006-2010. (D) Permafrost extent is taken from (https://nsidc.org/data/docs/fgdc/ggd318_map_circumarctic/; Brown et al., 2001). Crosses in A, C, D represent locations of Siberian borehole measurements along the East Siberian Transect from 1955-1900 (Table 1). Circles represent locations of borehole measurements in Alaska and Canada from 2002-2013 (Table 2). Dashed black line in A shows projected air temperature over the talik region. These results assume a Representative Pathway 8.5 warming scenario through 2100 and an Extended Concentration Pathway 8.5 through 2300. We note that peak talik formation occurs around 2100.

L152-154 “The C source transition represents a shift of ecosystem C balance from a neutral or weak C sink to a long-term source driven by onset of permafrost thaw and respiration of deep SOM” - here you suggest that the deep SOM alone is driving the transition, whereas your analysis suggests that it is driven by different things depending on region. Maybe you can qualify this sentence a bit?

Great point! We have qualified this sentence as follows (L185):

“The C source transition represents a shift of ecosystem C balance from a neutral or weak C sink to a long-term source as C balance shifts to increasing dominance of C source processes including permafrost thaw and fires (Koven, Lawrence and Riley, 2015).”

L 201-204: “For comparison to projected trends in CLM4.5, we recalculate observed trends using the inter-site average from all 9 sites at 3 unique locations: northern Siberia (67°N , 144°E), southwest Siberia (61°N , 115°E), and southeast Siberia (59°N , 131°E).” This is not entirely clear. You were talking about using 6 sites and now it says 9, but then you end up with 3? Can you make it more clear? Did you combine sites into groups based on approximate locations. . .?

We clarified our analysis as follows (L231):

“To assess observed thaw trends from 1955-1990, we analyze individual sites which report at least 10 months yr^{-1} of reported monthly mean soil temperature at each layer, and 55 months across the 5 layers (out of 60 possible layer-months per year). Based on these requirements, we find that 6 of 9 sites yield at least 6 years of data over multiple decades, and are well suited for examining historical thaw trends. For comparison of observed trends to historical and projected trends from 1950-2300, we analyze clusters of sites by combining the 9 sites into 3 groups based on approximate locations, and calculate observed trends using the inter-site average at each location. We use 2 sites in northern Siberia (67°N , 144°E), 6 sites in southwest Siberia (61°N , 115°E), and 1 site in southeast Siberia (59°N , 131°E). Site information is shown in more detail in Table 1.”

Results: L228 Do you mean 2300?

Yes, thank you for identifying this mistake!

L266 “Our simulations show a similar drying pattern in shallow layers (~0-1 m depth) in the 4 decades prior to talik onset (Fig. 2D).” The shallow drying does not appear to be shown on Figure 2D, only the total column soil moisture?

We added a line for shallow soil moisture (see attached revision of Fig 2), and revised the text as follows (L07):

“Our simulations show a *similar, but very slight, drying pattern in shallow layers in the 4 decades prior to talik onset (1.3% loss of soil moisture over 0-1 m depth; Fig. 2D), accounting for about half of total water storage loss in the column. More significant changes in water balance occur following talik onset, including more rapid drying in shallow layers (~10% over 4 decades) and in the column (~16%), and a substantial increase in sub-surface drainage, as discussed below.*”

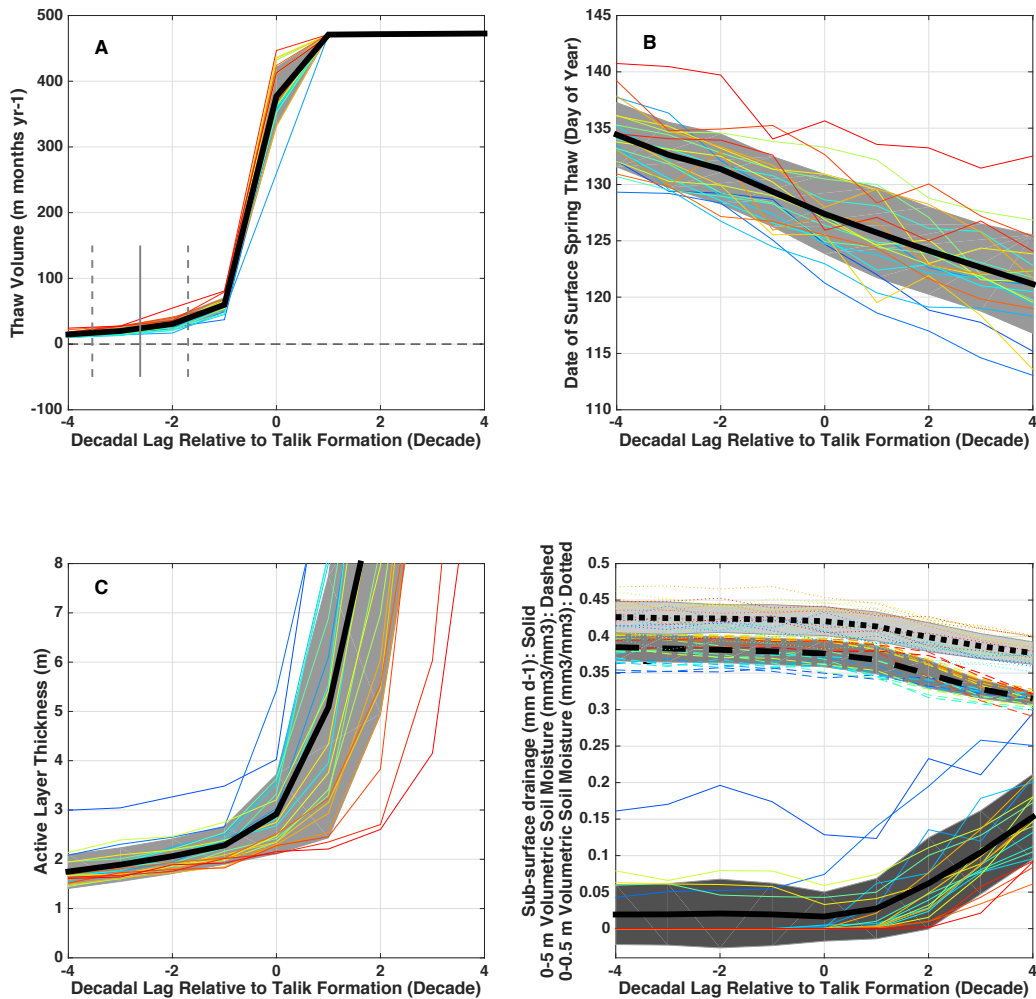


Figure 2. Patterns showing the progression of soil thaw in the decades surrounding talik onset. Individual lines represent averages across the subset of talik forming regions for each decade from the 2050s (darkest red) to the 2250s (darkest blue). (A) Integrated soil thaw volume, where

the vertical solid line represents the mean timing of initial thaw at depth and late into the cold season (Jan-Apr). Note that the upper limit to the thaw volume metric in (A) is an artifact of the arbitrary maximum soil depth of 45.1m in CLM4.5. Other panels show (B) Date of spring surface thaw in the uppermost layer, (C) annual maximum active layer thickness, and (D) annual sub-surface drainage (solid) and volumetric soil moisture averaged over the soil column (dashed) and. Grey shaded areas show the standard deviation of results for individual talik formation decades. Mean behavior exhibits a characteristic pattern: gradual increase in thaw volume and active layer depth prior to talik onset, abrupt shift in thaw volume, active layer depth, followed by stabilization to constant thaw volume as soil drying and sub-surface drainage increases.

L281-2 “we find more pronounced tilting of the thawed layer with time and depth” This is not obvious to me from the plot. I might just suggest deleting this.

“Pronounced tilting” is a misleading description of the thaw pattern. We revised this description as follows (L323):

*“In the 3 decades leading up to talik onset, we find **gradual deepening of the thawed layer to 3-4 m and penetration of thaw period into Jan-Feb.**”*

L290-2 “the rate of thawing and drainage in response to permafrost thaw may be underestimated in deeper CLM4.5 layers near bedrock due to reduced heat capacity.” Sorry if I am missing something here but it doesn’t seem to me like reduced heat capacity would reduce the rate of thawing, but rather than it would thaw more quickly because less heat is needed to thaw? Can you check this? Thanks.

Yes, thanks for catching this inaccurate statement. We clarified as follows (L332).

*“We note that bedrock soil is not hydrologically active in CLM4.5, and thus the rate of thawing and drainage in response to permafrost thaw may be **overestimated** in deeper CLM4.5 layers near bedrock due to reduced heat capacity.”*

L313-315 “however, our comparison to observations suggests that simulated thaw rates in this region and for similar permafrost temperatures are underestimated”. This is not totally clear. Which comparison with obs? Are you referring to the comparison against thaw rates in Siberia which comes in the following section? Or are you inferring this from your comparison against borehole temperatures?

We clarified the discussion as follows (L355):

*“Talik onset in CLM4.5 is variable in **the region containing Gakona (southeast Alaska)** with earliest onset by mid-century (~2050s, Fig. 1A); however, our comparison to **borehole temperature data at Gakona** suggests that simulated thaw rates **in southwest Alaska and across pan-Arctic regions with similar permafrost temperatures** are underestimated, and that earliest onset may occur sooner than predicted.”*

L335-336 “5 Siberian borehole sites which recorded at least 5 years of data spanning multiple decades:” Earlier you were talking about having 6 sites (or 9, or 3) and here it is 5. Please just clarify this a bit!

Should be 6, thank you! We corrected as follows (L383):

*“We focus first on site-specific long-term **historical** trends by analyzing the 6 Siberian borehole sites which recorded at least 5 years of **temperature** data spanning multiple decades: Drughina, Lensk, Macha, **Oimyakon**, Uchur, and Chaingda.”*

L337 “Records at these locations show a decrease in thaw volume” Do you mean an increase? On the next line it also refers to ‘negative trends’, which doesn’t seem to fit with the plots/results (or the expectations!). Maybe these things should read ‘increase in thaw volume’ and ‘positive trends’?

Yes, this should read “increase in thaw volume” and “positive trend”. We corrected as follows (385):

*“Records at these locations show an **increase** in thaw volume with an average positive trend of 0.19 m months yr⁻¹ from 1955 – 1990 (Table 1, Fig 5). All sites except Drughina show **positive** trends”*

L345-346 “(layer thickness increases exponentially with depth along the Siberian tran- C4 sect)” This is not totally clear. Do you mean that active layer thickness increases exponentially with latitude. . .? Is that data shown somewhere? (It doesn’t necessarily need to be, maybe just write ‘data not shown’ if it isn’t)

It’s not clear why we added this statement, and it doesn’t appear to affect the analysis, so we removed it and modified the text as follows (L390):

*“Further examination indicates that active layer thickness at Drughina actually decreased to 0.8 meters from 1989-1990 compared to 1.2 meters in the 1970s (**data not shown**). Drughina also shows smaller average thaw volume magnitude compared to other sites, consistent with shallower thaw. Together, these findings indicate that active layer thickness is decreasing at Drughina.”*

L348-355. I’m not sure how much this is adding overall. It gets a bit confusing. Where you say “(vertical dashed line)”, I would change to ‘(vertical dashed lines on Figure 5)’, assuming this is what you’re referring to? Anyway, it gets confusing when talking about groups of sites and it being hard to identify those groups. I would maybe condense these lines to something along the lines of “There is considerably spatial variability in thaw trends, for example site X is this far from site Y [relatively close] but with Z difference in trends [relatively large]. Talik formation occurs at several sites, at different times between 1957 and 1990 (shown by vertical dashed lines on Figure 5). We acknowledge the difficulty. . .”

This section sets up empirical evidence for increasing permafrost degradation from west to east in Siberia. We therefore clarify and condensed this section as follows (L395):

“There is considerable spatial variability in thaw volume and trends, but in general thaw trends increase from west (0.18 m months yr⁻¹) to east (0.51 m months yr⁻¹). Talik forms at several sites, at different times between 1957 and 1990 (shown by vertical dashed lines on Fig. 5), with earlier talik to the west consistent with higher mean initial thaw volumes.”

L364-366 “The simulated trend in thaw volume shows a change in sign at northern locations (blue), acceleration of thaw at southwest sites (orange), and reduction of thaw at the southeast sites (brown)”. This sentence suggests that the thaw volume reduces at the southeast sites, I guess because the thaw volume in CLM is less than the observations, but I would be inclined to

interpret this instead as: the CLM simulation always had a too-small thaw volume, and there was never any ‘decrease in thaw volume’ in the simulation. But it is not possible to tell from the plot - Why did you not include the historical CLM simulation on the plot so it would overlap with the observed period? I also wouldn’t say there is a “change of sign” at the northern locations. I guess you refer to the fact that the thaw volume is slightly decreasing at the northern sites historically, and increasing in the future? But as you say this is a very small trend so I would probably instead interpret this as a relatively stable site that shifts to degradation towards the end of the century? I also find figure 6 a bit confusing with the symbols and what they represent. So apparently the circle represents ‘thaw onset in January’ but this happens considerably sooner in the simulation than ‘thaw onset in March’, which doesn’t make sense to me? Thaw onset should get earlier each year? In the main text it implies this is actually referring to deep thaw lasting throughout the winter (but this is not implied in the figure caption!). Maybe it would just be best not to include the symbols at all. This would make the plot simpler to interpret. Lines 369 “Our simulations show a shift to accelerated soil thaw beginning in the early 2080s”. This sounds like you are referring to the whole simulation and not just this one particular point - can you make this more clear?

We apologize for the confusion this section created. We added historical thaw simulations from CLM4.5 so the simulated record is continuous from 1950-2300. We also removed the thaw onset symbols, which were meant to represent the progression of thaw later into the cold season (from early winter (Oct-Dec) to deep winter (Jan-Apr)) prior to talik onset. The revised figure and text are shown below (405):

“We recompute observed thaw trends at regional clusters using combined records at the 2 sites in northern Siberia (blue), 6 sites in southwest Siberia (orange), and 1 site in southeast Siberia (brown, Table 1) and compare to historical and projected thaw volume trends in CLM4.5 (Fig. 6). Northern locations show a consistent pattern of low thaw volume ($< 10 \text{ m month yr}^{-1}$) and negligible thaw trend ($\sim 0 \text{ m month yr}^{-1}$) in the historical simulations and observed record from 1950-2000. Thaw projections in northern Siberia indicate continued stability of permafrost through the early 22st century, followed by a shift to accelerated soil thaw in the early 2120, marked by onset of deep soil thaw late in the cold season.

Southern locations show a systematic underestimate of mean thaw volume ($< 20 \text{ m month yr}^{-1}$) compared to observations ($\sim 40 \text{ m month yr}^{-1}$) from 1950-2000. Simulated thaw trends are negligible prior to 2000, but these likely represent an underestimate given low simulated thaw volumes and significant positive observed trends in both southeast and southwest Siberia beginning in the 1960s following talik onset (Fig. 5). Thaw projections show more abrupt shifts in thaw volume in the early 21st century in the southwest (~ 2025) and in the mid 21st century (~ 2050) in the southeast. The strong discrepancy between observed and simulated thaw and talik onset in southern Siberia warrants close monitoring and continued investigation of this region through sustained borehole measurements and additional model realizations of potential future warming.”

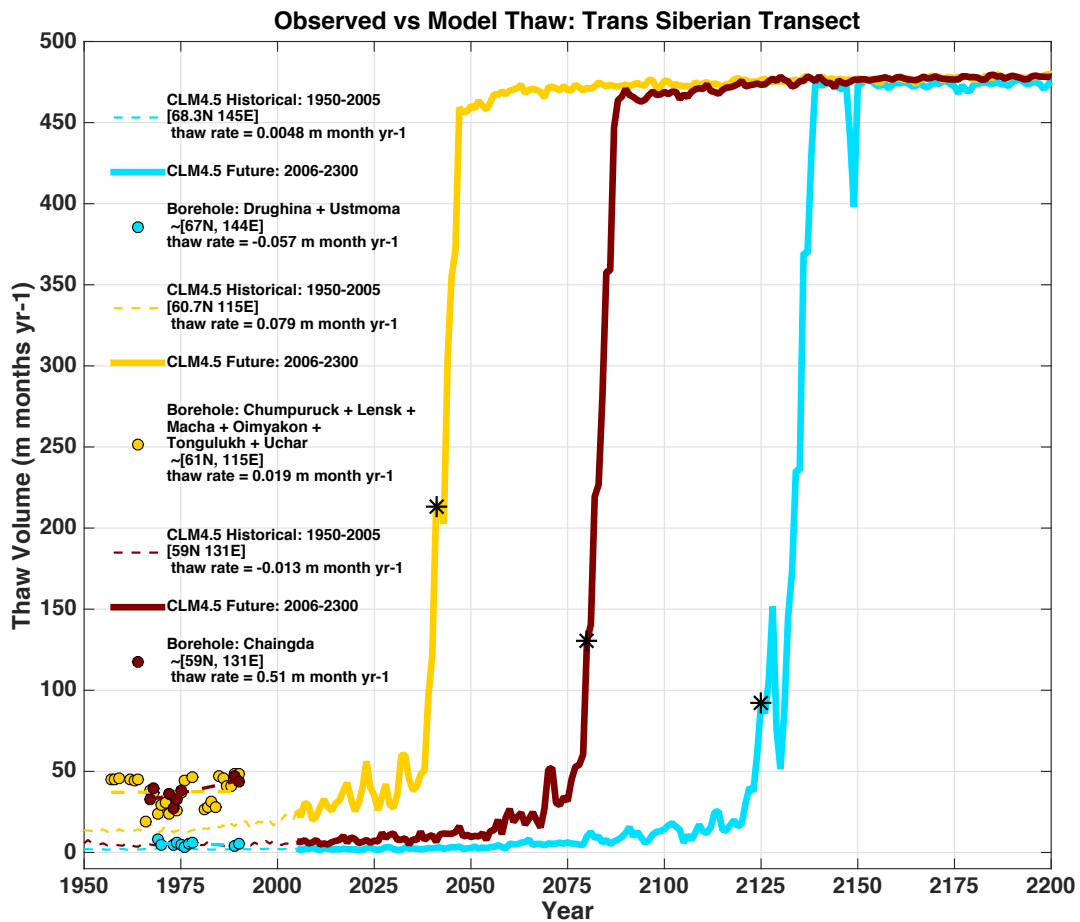


Figure 6. Comparison of observed soil thaw to historical and future simulations at sites along the East Siberian Transect (crosses in Fig. 1). Observed thaw (filled circles) from 1955-1990 is based on soil thaw data in Fig. 5 and on the inter-site average at 3 locations: northern Siberia (blue), southwest Siberia (yellow), and southeast Siberia (brown). Simulated thaw from 1950-2200 is derived from CLM4.5 and sampled at the nearest grid cell of 3 above locations. Asterisks show simulated talik onset. Observed and simulated thaw trends are derived from soil thaw volume, and estimated over the same period 1955-1990. We note a key discrepancy between observed and simulated thaw volume: Simulated thaw volume is integrated over depths from 0-40 meters; observed thaw volume is integrated from 0-3.6 meters. The effect of this selection bias is a potential low bias in observed thaw volume. In general, soil thaw is projected to remain stable in northern Siberia but become increasingly unstable in southern Siberia. L382 “A total of 6.8 million km² of land is projected to transition”. This is not clear in the abstract which reads like it’s only around 3 million km².

6.8 million km² refers to all NHL regions, within and outside the permafrost zone. This is clarified in Section 3.3 (L425).

“A total of 6.8 million km² of land is projected to transition, peaking in the late 21st century, with most regions transitioning prior to 2150 (4.8 million km² or 70%, Fig. 7B, solid black). C source transitions which occur in the permafrost zone, accounting for 6.2 million km² of land (91% of all C source transitions), also form talik at some time from 2006-2300 (Fig. 7C). The remaining C source transitions (0.6 million km², or 9%) occur outside the permafrost zone, primarily in eastern Europe.”

We also rephrase the abstract to be more consistent with this section (L29):

“Widespread talik at depth is projected across most of the NHL permafrost region (14 million km²) by 2300, 6.2 million km² of which is projected to become a long term C source, emitting 10 Pg C by 2100, 50 Pg C by 2200, and 120 Pg C by 2300, with few signs of slowing. Roughly half of the projected C source region occurs in predominantly warm sub-Arctic permafrost following talik onset. This region emits only 20 Pg C by 2300, but the CLM4.5 estimate may be biased low by not accounting for deep C in yedoma. Accelerated decomposition of deep soil C following talik onset shifts the ecosystem C balance away from surface dominant processes (photosynthesis and litter respiration), but sink-to-source transition dates are delayed by 20-200 years by high ecosystem productivity, such that talik peaks early (~2050s, borehole data suggests sooner) and C source transition peaks late (~2150-2200). The remaining C source region is in cold northern Arctic permafrost, which shifts to a net source early (late 21st century), emits 5 times more C (95 Pg C) by 2300, and prior to talik formation due to the high decomposition rates of shallow, young C in organic rich soils coupled with low productivity.”

L388 “followed by gradual decline to 0.5 Pg C by 2300”. Does this suggest the temperature has stabilised and things are moving back towards equilibrium or is it more complicated than that? Could you comment? Including the supplementary plots of temperature trajectories that I suggested earlier might clear this one up.

Temperatures continue to rise based on ECP8.5 which suggests it is more complicated. We clarify this section, including more detailed analysis of C source magnitudes and categories, as follows (L431):

“Net C emissions from C source transition regions are a substantial fraction of the total NHL C budget over the next 3 centuries (Fig. 8). The cumulative pan-Arctic C source increases slowly over the 21st century, reaching 10 Pg C by 2100 with RCP8.5 warming, then increases more rapidly to 70 Pg C by 2200 and 120 Pg by 2300 with sustained ECP8.5 warming (Fig. 8, solid black). This pan-Arctic source represents 86% of cumulative emissions in 2300 from the larger NHL talik region (crosses), despite the 2 fold smaller land area, and exceeds the talik region through 2200 due to mitigating widespread vegetation C gains (Koven et al., 2015). Cumulative emissions over all NHL land regions (diamonds, > 55N) increase in similar fashion to the talik region, reaching 120 Pg C by 2200 and 220 by 2300, with no sign of slowing.”

L405-412. Here you are talking about NBP as positive, increasing, but in the plot (and according to your stated sign convention), a source is represented by negative NBP, decreasing. Please make this paragraph consistent.

Corrected as follows (L458):

“In these regions, thaw volume is low (< 50 m months yr^{-1}) and shows a weak relationship to NBP (NBP decreases much faster than thaw volume) prior to C source onset (indicated by large green circle in Fig. 8A).”

L437 - Again wrong sign convention for NBP?

Corrected as follows (489):

“and talik formation occurs when these regions are weak sinks (NBP > 0 g C m^{-2} yr^{-1}).”

We have also revised Figure 8 (now Figure 9) with arrows indicating C source or sink for clarification:

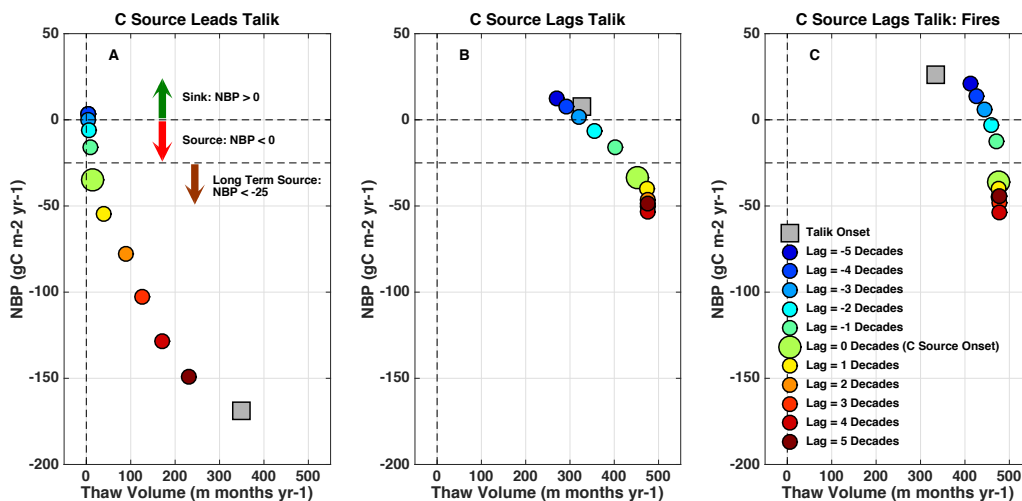


Figure 9. Net biome production (NBP) as a function of thaw volume. Symbols represent NBP and thaw volume values averaged over regions which transition to long term C source from 2060-2140, binned into regions where the decade of C source transition (A) leads talik onset, (B) lags talik onset, and (C) lags talik onset AND where fires exceed $25 \text{ g C m}^{-2} \text{ yr}^{-1}$. Colors indicate decade relative to C Source transition, denoted by the large green marker, which occurs when NBP exceeds $-25 \text{ g C m}^{-2} \text{ yr}^{-1}$ (grey horizontal dashed line). The grey square marker indicates the mean NBP and thaw volume values during talik onset. Cases where C source leads talik (A) show small thaw volumes during C source transition, and amplified C sources during talik onset. Cases where C source lags talik (B-C) show large thaw volumes during C source transition, and C sinks during talik onset.

L437-438 “In general, C sources in these regions are more sensitive to C emissions from deep soil thaw” Have you actually quantified how much of the C is coming from deep soil. . .?

Unfortunately, we can’t quantify C from deep soils since vertical resolved C flux output is not available. We have revised the statement to reflect an inferred contribution from deep soils (L490):

“In general, C source onset under high thaw volume indicates these regions are more sensitive to C emissions from deep soil thaw.”

Figure 10: I think this could also be a supplementary figure or removed altogether, maybe giving slightly more detail on the numbers where it's mentioned in the text.

We have removed Figure 10 and revised the text as follows (L470):

*“A broader analysis of soil thaw statistics over all regions and periods indicates **that most C source transitions (~2.3 million km², or 77% of land where C source leads talik) occur at active layer depths below 3 m and thaw season penetration into November.**”*

Figure 11 / Lines 453-461. I am struggling to interpret the upper plot on this Figure, and I am wondering whether this part adds much to the analysis. Since the analysis is already long I might suggest removing this paragraph and figure.

Agreed. The main point is the difference in GPP between warm and cold permafrost regions, which is discussed in previous sections. We have removed this paragraph and figure.

I suggest doing a bit more quantification of the contribution to total carbon sources. If there is a total of 11PgC emitted by 2300, what fraction of that comes from the three different 'categories' of points in the trimodal distribution? I think it would be really useful to know which are the important carbon sources - or whether they are all similar. (I have made this comment again above)

We have added a new figure (Figure 8) quantifying the different carbon sources (below). We also found that our cumulative C emission estimate was off by a factor of 10 (didn't convert from year to decade), bringing our new C emission to 120 PgC by 2300.

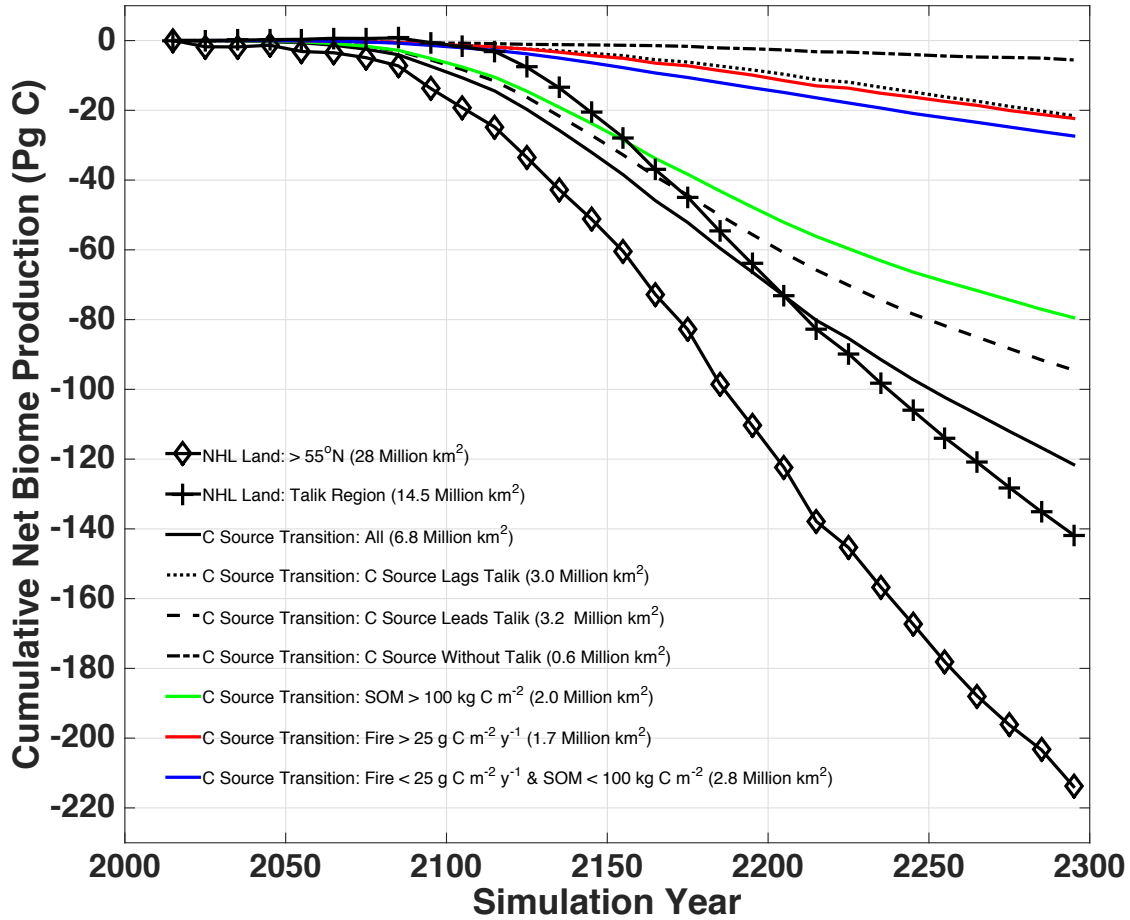


Figure 8. Cumulative net biome production (NBP) over northern high latitude (NHL) regions (> 55°N) from 2010 to 2300, where NBP < 0 is a net source. NHL regions are divided into the following categories: All NHL land (diamonds), NHL land regions which from talik from 2010-2300 (crosses), and regions which transition to long term C sources from 2010-2300 (black solid). C source transition regions are further broken down based on the lag relationship between talik onset and C source transition as follows: Regions where the C source transition lags talik onset (dotted), lead talik onset (dashed), and occurs in the absence of talik (dashed dotted). C source transition regions also divided by soil C content and fire activity: Regions where soil organic matter (SOM) exceeds 100 kg C m⁻² (green), fire emissions exceed 25 g C m⁻² yr⁻¹ (red), and SOM and Fires don't exceed these thresholds (blue). Regions which transition to C sources prior to talik formation make up half of the total C source area, but account for most of the cumulative C source (~80%) in large part due to high soil C.

We have revised the text as follows:

Abstract, to include total and regional contributions:

“Widespread talik at depth is projected across most of the NHL permafrost region (14 million km²) by 2300, 6.2 million km² of which is projected to become a long term C source, **emitting 10 Pg C by 2100, 50 Pg C by 2200, and 120 Pg C by 2300, with few signs of slowing**. Roughly half of the projected C source region occurs in predominantly warm sub-Arctic permafrost following talik onset. **This region emits only 20 Pg C by 2300, but the CLM4.5 estimate may be biased low by not accounting for deep C in yedoma**. Accelerated decomposition of deep soil C following talik onset shifts the ecosystem C balance away from surface dominant processes (photosynthesis and litter respiration), but sink-to-source transition dates are delayed by 20-200 years by high ecosystem productivity, such that talik peaks early (~2050s, borehole data suggests sooner) and C source transition peaks late (~2150-2200). The remaining C source region is in cold northern Arctic permafrost, which shifts to a net source early (late 21st century), **emitting 80 Pg C by 2300, and prior to talik formation due to the high decomposition rates of shallow, young C in organic rich soils coupled with low productivity.**”

The opening of section 3.3 to include total emissions and different categories:

“Fig. 7A plots the decade in which NHL ecosystems are projected to transition to long-term C sources over the next 3 centuries (2010-2300). A total of 6.8 million km² of land is projected to transition, peaking in the late 21st century, with most regions transitioning prior to 2150 (4.8 million km² or 70%, Fig. 7B, solid black). **C source transitions which occur in the permafrost zone, accounting for 6.2 million km² of land (91% of all C source transitions), also form talik at some time from 2006-2300 (Fig. 7C). The remaining C source transitions (0.6 million km², or 9%) occur outside the permafrost zone, primarily in eastern Europe.**”

“**Net C emissions from C source transition regions are a substantial fraction of the total NHL C budget over the next 3 centuries (Fig. 8). The cumulative pan-Arctic C source increases slowly over the 21st century, reaching 10 Pg C by 2100 with RCP8.5 warming, then increases more rapidly to 70 Pg C by 2200 and 120 Pg by 2300 with sustained ECP8.5 warming (Fig. 8, solid black). This pan-Arctic source represents 86% of cumulative emissions in 2300 from the larger NHL talik region (crosses), despite the 2 fold smaller land area, and exceeds the talik region through 2200 due to mitigating widespread vegetation C gains (Koven et al., 2015). Cumulative emissions over all NHL land regions (diamonds, > 55N) increase in similar fashion to the talik region, reaching 120 Pg C by 2200 and 220 by 2300, with no sign of slowing.**”

“The geographic pattern of C sink-to-source transition date is reversed compared to that of talik formation, with earlier transitions at higher latitudes (the processes driving these patterns are discussed in detail below). Overall, the lag relationship between talik onset and C source transition exhibits a tri-modal distribution (Fig. 7D), with peaks at negative time lag (C source leads talik onset; Median Lag = -5 to -6 decades), neutral time lag (C source synchronized with talik onset; Median Lag = -2 to 1 decade), and positive time lag (C source lags talik; Median Lag = 12 decades; red shading in Fig. 7C). Roughly half of these regions (3.2 million km²) show neutral or positive time lag (lag ≥ 0). This pattern, characteristic of the sub-Arctic (< 65°N), represents the vast majority of C source transitions after 2150 (Fig. 7B, dotted), **but only accounts for 17% of cumulative emissions (20 Pg C by 2300, Fig. 8, dotted)**. The remaining regions (3.0 million km²) in the Arctic and high Arctic (> 65°N) show negative time lag and account for most of late 21st century sources (Fig. 7B, dashed) **and cumulative emissions (95 Pg C by 2300, or 79%; Fig. 8, dashed)**. C sources in regions not identified as talik (0.63 million km²) either show talik presence at the start of our simulation, or are projected to transition in the

*absence of permafrost or in regions of severely degraded permafrost (Fig. 7C, dash dotted). **This region contributes only 5 Pg C (4%) of cumulative C emissions in 2300.***

And the following statements on line 479 referring to high SOM emissions:

*“The total area of land in which SOM exceeds 100 kg C m⁻² represents 2/3 of all land where C sources lead talik onset (2.0 million km²), and peaks at a negative time lag of -5 to -6 decades (Fig. 7D, green bars), which perfectly aligns with the peak distribution of negative time lags. **Cumulative C emissions from regions of SOM > 100 kg C m⁻² are also 2/3 of total C emissions (80 Pg C; Fig 8, green).**”*

And line 495 for fire emissions:

*“The regions where fire C emissions exceed 25 g C m⁻² yr⁻¹, representing our threshold for C source transition, are exclusively boreal ecosystems, account for 1/3 of all land with negative lags (~1.1 million km²), and align perfectly with the peak distribution of positive time lags (Fig. 7D, red bars) **and cumulative C emissions (20 Pg C in 2300, Fig. 8, red).**”*

Lines 608 and 635 in the discussion:

*“**About half of this region (3.2 million km²) shows a pattern of accelerated soil C respiration following talik onset, which shifts the surface C balance of photosynthetic uptake and litter respiration from net C sinks to long term net sources totaling 20 Pg C across 3.2 million km² of NHL land by 2300.**”*

*“We identify an equally large region of land in the high Arctic, representing ~3.0 million km², which is projected to transition to a long term C source much sooner than the sub-Arctic in the absence of talik, **and emit 5 times as much carbon by 2300 (~95 Pg C).**”*

And line 688 in the conclusions

*“6.8 million km² of land impacted in Siberia and North America will produce an integrated C source of **90 Pg C by 2100 and 120 Pg C by 2200.**”*

L472 “GPP and total respiration show nearly linear increases (~15% per decade)” Minor point but an increase of 15% per decade would be exponential, not linear.

Revised as follows (L527):

*“GPP and combined respiration **increase by ~15% per decade for each permafrost regime surrounding the decade of C source transition with peak fluxes in the growing season (Fig. 11 A - D).**”*

L485-487 “The trend in soil vs litter respiration explains almost the entire trend in net ecosystem C balance from neutral to net source (Fig. 12 G – H).” I’m not sure what you mean by this. I would have thought the trend in NBP is determined by the difference between GPP and total respiration, rather the difference between soil and litter respiration? And how do you draw these conclusions from the plots? Please could you make this clearer! Thanks.

We have revised as follows (L541):

“The trend in the respiration difference in warm and cold permafrost, which increase by similar amounts (~100 g C m⁻² yr⁻¹), thus reflects an increasing dominance of respiration from younger and older soil C pools, respectively. These trends are identical to the corresponding NBP trends, which decrease by 100 g C m⁻² yr⁻¹ over the same period from neutral to net

source (Fig. 12 G – H), such that the differences between GPP and respiration driving the NBP trends are explained almost entirely by the increasing fraction of soil vs litter respiration.”

L494 NF was only defined at the beginning of the paper and never used again until this point, which means that I had forgotten what it meant by now. You don't use this abbreviation much so I suggest you don't need it.

NF has been changed to non-frozen.

Discussion: L526-529 “Experiments demonstrating the sensitivity of talik to soil drying within the active layer across soil hydrology schemes in previous (CLM4), current (CLM4.5), and newly available (CLM5) versions of CLM could provide key insight on soil thermal dynamics in frozen or partially frozen conditions.” This comes out of the blue a bit, and I am also not clear about why this would be useful? Comparing different hydrology schemes could be useful if one is more realistic than the others or includes different processes? But it is not clear that this would be the case in different CLM versions? It might be better to look at a purpose-built permafrost model, for example, or a model that resolves discontinuous permafrost.

We agree it's not clear how exactly this would be useful since the model differences in soil hydrology and snow are not systematically differences. We don't think a purpose-built permafrost model is likely to be any better since the processes represented are typically the same as in CLM. We agree that resolving discontinuous permafrost would be good, but it's unclear how to do that other than with increased resolution, but this would miss other important processes such as lateral flow. Something more controlled like a parameter sensitivity study with variable ice impedance or baseflow scalar, such as examined in Lawrence et al., 2015, is likely to provide the best insight. We therefore replace our comment with a more general comment about uncertainties, and suggest more controlled experiments similar to Lawrence (L586):

“Controlled experiments demonstrating the sensitivity of talik to parameters that control soil drying such ice impedance or baseflow scalars (e.g. Lawrence et al., 2015), and the effect of organic content and mineral soil texture (Lawrence and Slater, 2008), could provide key insight on soil thermal dynamics in frozen or partially frozen conditions. Other factors affecting soil hydrology and carbon cycling not considered in our CLM4.5 simulations include high spatial resolution in discontinuous permafrost, shifts in vegetation community, lateral flow representation, thermokarst activity and other thaw-related changes to the ground surface, surface slope and aspect, soil heterogeneity, and potentially several other factors (see Jorgenson and Osterkamp (2005) for discussion of some of the many complexities to be considered).”

L538-540 “thus appears to be driven by combination of warming and increased nitrogen availability resulting from permafrost thaw”. I would suggest changing “appears to be” to “may be”. . . you haven't looked at nitrogen here, and it is not totally clear/agreed that permafrost thaw will increase nitrogen availability.

We have revised as suggested

L605 “Our main results emphasize an emergence of cold season processes” Not sure what you mean by ‘an emergence of cold season processes’. . .? Rephrase?

Rephrased as follows (L692):

“Our main results emphasize an increasingly important impact of NHL cold season warming on earlier spring thaw, longer non-frozen seasons, and increased depth and seasonal duration of soil thaw.”

L629-630 “Active-layer deepening leads to C sink-to-source transitions in some regions, talik-driven permafrost loss in others, . . .” This should be rephrased, “C sink-to-source transitions are caused by active layer deepening in some regions, talik-driven permafrost loss in others, . . .” Otherwise the sentence doesn’t quite make sense, it sounds like active-layer deepening is causing all of the other things!

Rephrased as suggested.

Hope you find these comments helpful. Best wishes!

Thank you, much improved now!

Reviewer 2

Overall impression

In the current study, Parazoo and colleagues have used the land surface model CLM4.5 to simulate permafrost state and changes from 2010 to 2300 under strong warming following the RCP8.5 scenario. They have investigated how permafrost degradation evolves in space and time, with a special focus on how talik formation affects thaw dynamics. Further, the authors have used their model experiment to analyse how future C fluxes in permafrost regions will evolve and when a carbon sink to source transition is likely to occur along different regions of the permafrost domain.

The presented analyses are helpful for increasing our process understanding of how individual factors explain inferred differences in simulated carbon fluxes between cold and warmer permafrost regions. E.g. the authors find that cold permafrost locations become C sources due to altered thaw-season dynamics while transitions of warm permafrost regions are mainly affected by changes in cold season dynamics. Further, the authors discuss how the presented results of this study can help finding an (optimal) design for monitoring the thermal and carbon state and changes in permafrost regions. The paper is well structured and written, and model analyses were performed elaborately. Adding new insights into permafrost degradation and carbon dynamics, this study can be considered of broad interest to the readership of The Cryosphere.

General comments

1) Initial SOC storages The initialized soil C stocks play a key role in affecting simulated future C release and the timing for a sink to source transition. In the study presented, no information is given how these C stocks were initialized for the simulation setting used here (besides referring to two previous CLM4.5 studies). Information should be provided in a sub-section on how SOC stocks were initialized, and on how these stocks compare to observed data (e.g. NCSCD - in terms of total storages and with regard to CLM4.5 inferred high (peaty) SOC storages at northern grid cells). As talik formation down to some meters are analysed in this study, I wonder how deep SOC is initialized in the soil column? Can e.g. soil thaw deeper than 3 meters further increase the pool of thawed carbon available for decomposition? A further key factor not

discussed in the manuscript concerns assumptions about SOM lability made in the model. As especially uncertainty in slowly decomposing SOM is very high, I wonder how different settings of a humus timescale parameter (or different partitioning between labile and less labile pools) would affect inferred sink to source transition times? If feasible, this would be worth exploring by an extra sensitivity run, or at least by discussing qualitatively the impact of uncertainty in assumed SOM decomposition timescales on the findings discussed here.

We thank the reviewer for the recommendation to include the very important discussion of soil C stocks and decomposition controls in CLM. Deep soil decomposition experiments in CLM have been run in previous studies by the co-authors, to decouple changing dynamics of surface soils from deep soils, to determine the potential contribution from permafrost layers, and to calibrate initial soil C stocks against observations.

We have elaborated on these details in the methods (L139) as follows:

“CLM is spunup to C equilibrium for the year 1850 by repeatedly cycling through 20 years of pre-industrial climate forcing with CO₂ and N-deposition set at 1850 levels. C initialization is achieved via slow mixing by cryoturbation between the seasonally thawed active layers and deeper permafrost layers (Koven et al., 2009). Including vertically resolved processes leads to a sign change in the projected high-latitude C response to warming, from net C gains driven by increased vegetation productivity to net C losses from enhanced SOM decomposition (Koven et al., 2011). The soil grid includes 30 vertical levels that has a high-resolution exponential grid in the interval 0–0.5 m and fixed 20-cm layer thickness in the range of 0.5–3.5 m to maintain resolution through the base of the active layer and upper permafrost, and reverts to exponentially increasing layer thickness in the range 3.5–45 m to allow for large thermal inertia at depth. Soil C turnover in CLM4.5 is based on a vertical discretization of first-order multipool SOM dynamics (Koven et al., 2013; Oleson et al., 2013) where decomposition rates as a function of soil depth are controlled by a parameter $Z\tau$ (Koven et al., 2015; Lawrence et al., 2015). This depth control of decomposition represents the net impacts of unresolved depth dependent processes. In this study, we utilize $Z\tau=10$ m, which yields a weak additional depth dependence of decomposition beyond the environmental controls and, as discussed and evaluated relative to $Z\tau=1$ m and $Z\tau=0.5$ m in Koven et al (2015), results in CLM permafrost-domain soil C stocks that are in closest agreement (1582 Pg for $Z\tau=0.5$ m, 1331 Pg for $Z\tau=1$ m, and 1032 Pg for $Z\tau=10$ m) with observed estimates (1060 Pg C to 3 m depth; Hugelius et al 2013). This reduction in initial C is due to higher decomposition rates at depth during the model initialization period. There is no C below 3.5 m, so additional thaw below 3 meters has a small impact on the C cycle. We note that the relationship applied in CLM4.5, which implies multiplicative impacts of limitations to decomposition, is commonly applied in land biogeochemical models, but is quite uncertain.”

We also discuss implications of 3.5 m C limit in discussion (Line 626):

“Our estimate of C emissions following talik onset (~20 Pg C) is low compared to the cumulative emissions from all long term C source transitions (120 Pg C), but likely strongly underestimated. Soil C is not permitted below 3.5 m in CLM4.5, or in most analogous models, such that potential decomposition of the ~350 Pg soil organic C in deep permafrost (> 3 m) is not accounted for (Hugelius et al., 2014; Jackson et al., 2017). This is significant for our simulations, which show frequent talik formation and accelerating thaw volumes below 3 m (e.g., Fig. 3). We therefore caution the reader in the interpretation of the timing and

magnitude of permafrost C emissions following talik onset in our simulations, which represent a lower bound of potential emissions based on the current formulation of CLM4.5.”

Talik formation

The study focuses on talik formation as a key process which leads to abrupt permafrost degradation. The discussion (and the model simulation) is done for non-lake environments. Talik formation through thermokarst lake initialisation is not considered and mentioned. Yet this process is known to lead to rapid thaw through pronounced sub-lake talik formation, which can strongly affect carbon release from thawed sub-lake sediments. Although it is questionable to which extent future Arctic landscapes will be affected by thermokarst formation, this process should be discussed in the context of future permafrost degradation and permafrost carbon release.

We agree that thermokarst is an important process which is not considered in our simulations. We added the following discussion of thermokarst effects to the intro (Line 87)

“More abrupt processes such as thermokarst lake initialization can also lead to rapid thaw through pronounced sub-lake talik formation (Jorgenson and Osterkamp, 2005). These processes can initiate formation of a talik zone (perennially thawed sub-surface soils) during active layer adjustment to new thermal regimes (Jorgenson et al., 2010) in lake and non-lake environments.”

And methods (Line 135)

“More abrupt thaw processes affecting permafrost C dynamics and talik formation such as the effect of thermokarst or other thaw related landscape dynamics changes in wetland or lake distribution are not accounted for (see Riley et al (2011) for more discussion).”

and discussion (Line 590):

*“Other factors that are necessary for more accurate simulation of soil hydrology and carbon cycling but not considered in CLM4.5 and analogous models include: enhanced spatial resolution in complex topography and in discontinuous permafrost, sophisticated vegetation community definitions including trait based representation, shifts in vegetation community, lateral flow representation, **thermokarst activity and other thaw-related changes to the ground surface**, surface slope and aspect, soil heterogeneity, and potentially several other factors (see Jorgenson and Osterkamp (2005) for discussion of some of the many complexities to be considered).”*

Vegetation distribution

As discussed extensively in the presented paper, the Arctic land carbon balance is determined by changes in the net flux of vegetation carbon uptake and respiration losses. To what extent is CLM4.5 able capturing high latitude vegetation distribution/patterns? Some short discussion on simulated high latitude vegetation in CLM4.5 would be interesting to include.

The use of static vegetation distributions and simple vegetation community definitions is a major source of uncertainty in CLM4.5. We have acknowledged this model weakness in the response above.

Cumulated C fluxes

I guess you want to discuss C source numbers as PgC per year? (L387). Please specify in the text and in Fig.7B y-axis label. How does the cumulative C source from 2010- 2300 of 11.6 PgC relate to shown C release rates in Fig. 7B? If I interpret numbers shown correctly, these suggest much larger cumulative release. Given published work on total C release from future permafrost degradation under RCP8.5 in other studies (suggesting much larger release), this number (total C release) should be discussed in the context of existing estimates.

We thank the reviewer for correctly pointing out our y-axis error and suggesting to compare our cumulative releases to existing estimates. We corrected the y-axis error by moving the C source numbers from Fig. 7B to Fig. 8 for more in depth analysis (Figure 7 below; Figure 8 provided in Reviewer 1 responses). Our cumulated emission is 120 Pg C which is more in line with existing estimates. We summarize in the discussion as follows (Line 596):

“Our simulations show increasing C emissions over time across the talik region (Fig. 1B), as cumulative NBP becomes increasingly negative (NBP < 0 equals a net C source), reaching a net source of 140 Pg C by 2300 (Fig. 8, crosses), consistent with previous estimates of net C balance across the larger pan-Arctic region from CLM4.5 (~160 Pg C, Koven et al., 2015; Lawrence et al., 2015). Ecosystems which transition from net C sinks to net C sources represent less than half the total talik area (6.8 of 14.5 Million km², Fig. 7A), but account for most (~85%) of the cumulative emissions, reaching 10 Pg C in 2100, 70 Pg C in 2200, and 120 Pg C by 2300 (Fig. 8, solid black). Removing the effect of vegetation C gain (~20 Pg C in 2100 and 40 Pg C in 2200 and 2300 according Koven et al., 2015), we estimate a cumulative permafrost emission for C source transition regions of 30 Pg C in 2100, 110 Pg C in 2200, and 160 Pg C in 2300. These numbers are on the low end but consistent with estimates of permafrost C emissions summarized by Schuur et al. (2015), which range from 37-174 Pg C by 2100 and 100-400 Pg C by 2300.”

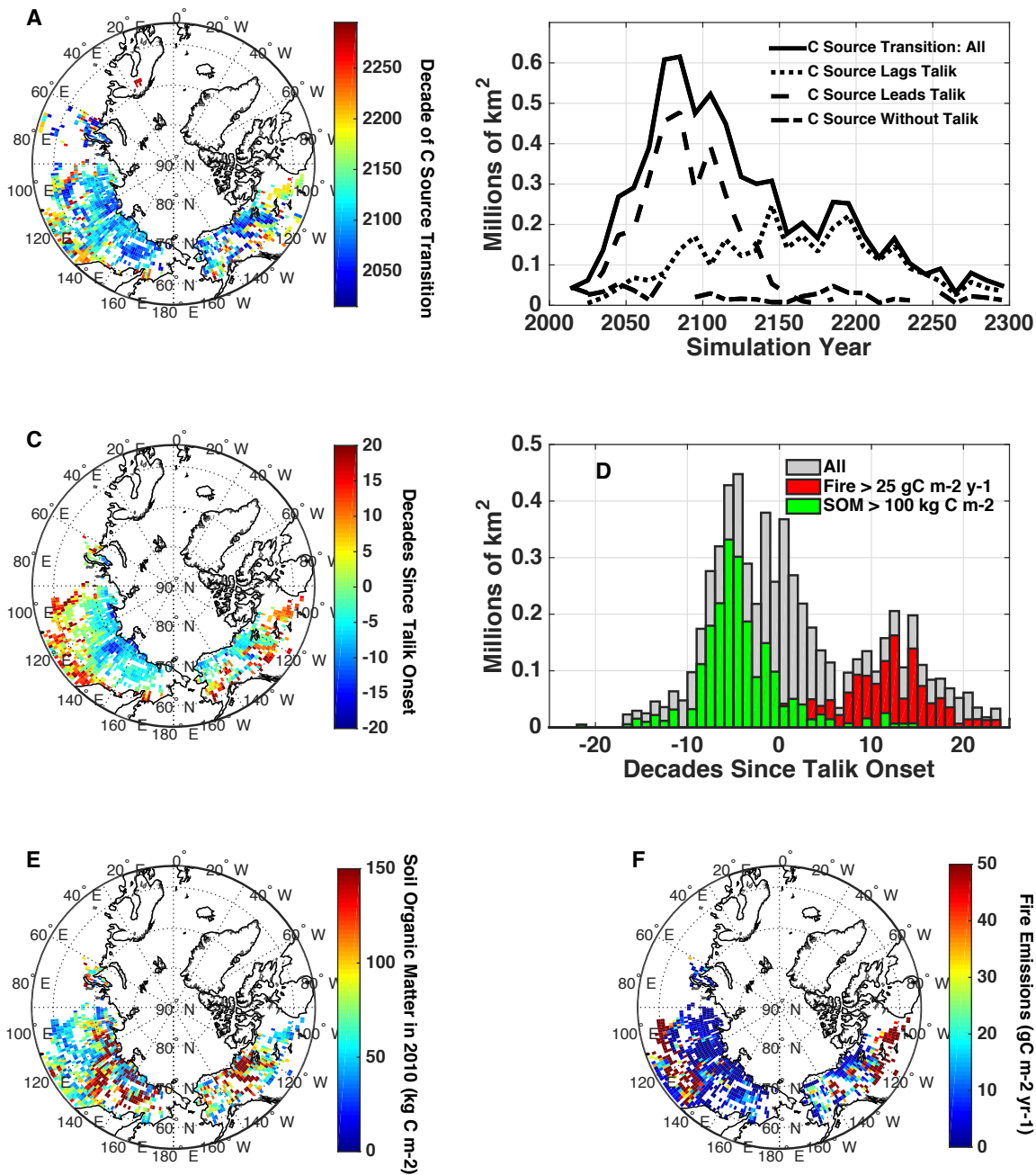


Figure 7. Projected decade when permafrost regions shift to long-term C sources over the period 2010-2300, and relation to talik onset, soil C, and fire emissions. (A) Map of the decade of transition to C source, reflected in the color code, showing earlier transitions in cold northern permafrost. (B) The area of land that transitions peaks in the late 21st century, and is driven by regions where the C source leads talik onset (dashed). (C) The decadal time lag from talik onset to C source transition shows positive lags in warm southern permafrost (C source lags talik) and negative lags in cold northern permafrost (C source leads talik). (D) Histogram shows trimodal distribution of permafrost area as a function of decadal time lag, with negative lags related to high soil organic matter (green bars and map in E), and large positive lags related to fires (red bars and map in F) but delayed by high productivity. See text for details. These results assume a

Representative Pathway 8.5 warming scenario through 2100 and an Extended Concentration Pathway 8.5 through 2300.

Specific comments

Results presented in this study are inferred for the RCP8.5 scenario. This should be made more clear in the text (when discussing future evolution of permafrost and carbon fluxes), and in some of the figure legends.

We have added RCP8.5 and ECP8.5 information throughout the text:

L263 Section 3.1:

“Our simulations show widespread talik formation throughout Siberia and northern North America over the period 2010-2300 (Fig. 1B), impacting ~14.5 million km² of land in NHLs (55°-80°N) assuming a freeze/thaw threshold of -0.5°C and RCP8.5 and ECP8.5 warming scenarios.”

L432 Section 3.3:

“The cumulative pan-Arctic C source increases slowly over the 21st century, reaching 10 Pg C by 2100 with RCP8.5 warming, then increases more rapidly to 70 Pg C by 2200 and 120 Pg by 2300 with sustained ECP8.5 warming (Fig. 8, solid black).”

We also included information in the first talik figure (Fig. 1) and carbon figure (Fig. 7):

“These results assume a Representative Pathway 8.5 warming scenario through 2100 and an Extended Concentration Pathway 8.5 through 2300.”

Please check for consistent/correct use of NBP sink/source definition (e.g. L410) Fig.8: Did you intend to put the dashed horizontal NBP threshold line at -25 gCm⁻²yr⁻¹ - in accordance with your definition?

The definition of NBP has been corrected in the text and in the figures.

I wonder whether a discussion of a bi-modal distribution (Fig. 7D) seems more likely than a tri-modal distribution.

We thank the reviewer for this suggestion and understand the motivation, since 2 clearly defined peaks exist on either side of the talik onset lag = 0 line. However, we argue that a tri-modal distribution is appropriate here since each peak falls into a distinct category associated with a unique process: High SOM (left peak), High Fires (right peak), and low SOM and low fires (middle peak). We have added the following discussion on L507 to justify the trimodal distribution:

“The decadal time lag between talik onset and C source transition is more normally distributed in the remaining region, represented by the residual grey bars visible in Fig. 7D, which occurs predominantly in cold northern permafrost in northwest Siberia where low SOM (<100 Kg m⁻²) and fire emission (<25 g C m⁻² yr⁻¹) prevail. This region has a mean lag of 1 decade from talik onset to C source, with high standard deviation of lags (± 8 decades) reflecting a skewed distribution of GPP; low productivity in cold permafrost (GPP = 385 g C m⁻² yr⁻¹) increases the likelihood that soil thaw will lead to C source transition prior to talik onset, and high productivity in warm permafrost (GPP = 1111 g C m⁻² yr⁻¹) increasing the

likelihood of a transition after talik onset. Cumulative C emissions from this region are on the low end (27 Pg C by 2300; Fig. 8, blue) due to low soil C (SOM = 59 kg C m⁻²). “

Maybe a shifting of some figures (e.g. Fig 10., Fig.11) to an appendix section would be good?

Based on comments from both reviewers that Figures 10 and 11 do not add much to the paper, they have been removed, and replaced with more details describing the results of these figures

L338/339 you mean positive trends?

Yes, this has been corrected

L 365 and following Given the small (statistically insignificant?) trend at Drughina, probably discussing “unchanged” conditions (instead of discussing a “change in sign”) is more appropriate.

Thanks for the excellent suggestions. We have modified the text as follows (L410):

*“Thaw projections in northern Siberia indicate an **unchanged** trend and continued stability of permafrost through the early 22nd century, followed by a shift to accelerated soil thaw in the early 2120, marked by onset of deep soil thaw late in the cold season.”*

L 362 and following Please check colour specifications (in my printed version lines are yellow instead of orange, “blue” and “cyan” are used to refer to the same line, ...)

Color specifications have been corrected.

L494 define “NF” - or better avoid abbreviation

NF has been expanded to non-frozen

Fig.12 legend how were error bars inferred / what do they describe? Spelling

We have included a description of error bars in figure 12, which represent the multi-decadal standard deviation of seasonal and C source transition time series from 2040 – 2270.

L29 IS -> is

Corrected, thank you

L458 form -> from

This paragraph has been removed

L470 = -> -

Corrected, thank you

List of Changes

- L29: “Widespread talik at depth is projected across most of the NHL permafrost region (14 million km²) by 2300, 6.2 million km² of which is projected to become a long term C source, **emitting 10 Pg C by 2100, 50 Pg C by 2200, and 120 Pg C by 2300, with few signs of slowing**. Roughly half of the projected C source region occurs in predominantly warm sub-Arctic permafrost following talik onset. **This region emits only 20 Pg C by 2300, but the CLM4.5 estimate may be biased low by not accounting for deep C in yedoma**. Accelerated decomposition of deep soil C following talik onset shifts the ecosystem C balance away from surface dominant processes (photosynthesis and litter respiration), but sink-to-source transition dates are delayed by 20-200 years by high ecosystem productivity, such that talik peaks early (~2050s, borehole data suggests sooner) and C source transition peaks late (~2150-2200). The remaining C source region is in cold northern Arctic permafrost, which shifts to a net source early (late 21st century), **emitting 80 Pg C by 2300**, and prior to talik formation due to the high decomposition rates of shallow, young C in organic rich soils coupled with low productivity.”
- Line 87: “**More abrupt processes such as thermokarst lake initialization can also lead to rapid thaw through pronounced sub-lake talik formation (Jorgenson and Osterkamp, 2005)**. These processes can initiate formation of a talik zone (perennially thawed sub-surface soils) during active layer adjustment to new thermal regimes (Jorgenson et al., 2010) **in lake and non-lake environments**.”
- L91: “Talik as well as longer, deeper active layer thaw stimulate respiration of soil C (Romanovsky and Osterkamp, 2000; Lawrence et al., 2008), making the **~1035 Pg soil organic carbon in near surface permafrost (0-3 m) and ~350 Pg soil organic carbon in deep permafrost (> 3 m) vulnerable to decomposition (Hugelius et al., 2014; Jackson et al., 2017)**.”
- Line 135: “More abrupt thaw processes affecting permafrost C dynamics and talik formation such as the effect of thermokarst or other thaw related landscape dynamics changes in wetland or lake distribution are not accounted for (see Riley et al (2011) for more discussion).”
- L139: “CLM is spunup to C equilibrium for the year 1850 by repeatedly cycling through 20 years of pre-industrial climate forcing with CO₂ and N-deposition set at 1850 levels. C initialization is achieved via slow mixing by cryoturbation between the seasonally thawed active layers and deeper permafrost layers (Koven et al., 2009). Including vertically resolved processes leads to a sign change in the projected high-latitude C response to warming, from net C gains driven by increased vegetation productivity to net C losses from enhanced SOM decomposition (Koven et al., 2011). The soil grid includes 30 vertical levels that has a high-resolution exponential grid in the interval 0–0.5 m and fixed 20-cm layer thickness in the range of 0.5–3.5 m to maintain resolution through the base of the active layer and upper permafrost, and reverts to exponentially increasing layer thickness in the range 3.5–45 m to allow for large thermal inertia at depth. Soil C turnover in CLM4.5 is based on a vertical discretization of first-order multipool SOM dynamics (Koven et al., 2013; Oleson et al., 2013) where decomposition rates as a function of soil depth are controlled by a parameter $Z\tau$ (Koven et al., 2015; Lawrence et al., 2015). This depth control of decomposition represents the net

impacts of unresolved depth dependent processes. In this study, we utilize $Z\tau=10$ m, which yields a weak additional depth dependence of decomposition beyond the environmental controls and, as discussed and evaluated relative to $Z\tau=1$ m and $Z\tau=0.5$ m in Koven et al (2015), results in CLM permafrost-domain soil C stocks that are in closest agreement (1582 Pg for $Z\tau=0.5$ m, 1331 Pg for $Z\tau=1$ m, and 1032 Pg for $Z\tau=10$ m) with observed estimates (1060 Pg C to 3 m depth; Hugelius et al 2013). This reduction in initial C is due to higher decomposition rates at depth during the model initialization period. There is no C below 3.5 m, so additional thaw below 3 meters has a small impact on the C cycle. We note that the relationship applied in CLM4.5, which implies multiplicative impacts of limitations to decomposition, is commonly applied in land biogeochemical models, but is quite uncertain.”

- L165: “We use an anomaly forcing method to repeatedly force CLM4.5 with observed meteorological from the CRUNCEP dataset for the period 1996–2005 (data available at dods.ipsl.jussieu.fr/igcm/IGCM/BC/OOL/OL/CRU-NCEP/) and monthly anomalies added based on a single ensemble member from a CCSM4 Representative Concentration Pathway 8.5 (RCP8.5) simulation for the years 2006-2100 and Extended Concentration Pathway 8.5 (ECP8.5) for the years 2100-2300. Land air temperature for the period 2006-2300, shown in Fig. 1A., is projected to increase steadily in our simulation, with a slight decrease in the rate of warming”
- L185: “The C source transition represents a shift of ecosystem C balance from a neutral or weak C sink to a long-term source as C balance shifts to increasing dominance of C source processes including permafrost thaw and fires (Koven, Lawrence and Riley, 2015).”
- L231: “To assess observed thaw trends from 1955-1990, we analyze individual sites which report at least 10 months yr^{-1} of reported monthly mean soil temperature at each layer, and 55 months across the 5 layers (out of 60 possible layer-months per year). Based on these requirements, we find that 6 of 9 sites yield at least 6 years of data over multiple decades, and are well suited for examining historical thaw trends. For comparison of observed trends to historical and projected trends from 1950-2300, we analyze clusters of sites by combining the 9 sites into 3 groups based on approximate locations, and calculate observed trends using the inter-site average at each location.
- L238: We use 2 sites in northern Siberia (67°N, 144°E), 6 sites in southwest Siberia (61°N, 115°E), and 1 site in southeast Siberia (59°N, 131°E). Site information is shown in more detail in Table 1.”
- L245: “Mould Bay is a continuous permafrost tundra site with measurements at 63 depths from 0 - 3 m. Mould Bay has almost no organic layer (about 2 cm) and then sandy silt with high thermal conductivity. Barrow is a continuous permafrost tundra site with measurements at 35 depths from 0 - 15 m. The soil at Barrow is represented by silt with a bit of mix with some organics and almost no organic layer on top. Conductivity of the upper layer is $\sim 1 \text{ W mK}^{-1}$ for unfrozen and $\geq 2 \text{ W mK}^{-1}$ for frozen soil. Gakona is a continuous permafrost forest tundra site with measurements at 36 depths from 0 - 30 m. Gakona has a thick organic layer of moss (0 to 5 cm), dead moss (from 5 to 13 cm), and peat (from 13 to 50 cm), then silty clay at depth.”
- L263: “Our simulations show widespread talik formation throughout Siberia and northern North America over the period 2010-2300 (Fig. 1B), impacting ~ 14.5 million km^2 of land in

NHLs (55°-80°N) assuming a freeze/thaw threshold of -0.5°C and RCP8.5 and ECP8.5 warming scenarios.”

- L307: “Our simulations show a **similar, but very slight**, drying pattern in shallow layers in the 4 decades prior to talik onset (**1.3% loss of soil moisture over 0-1 m depth**; Fig. 2D), **accounting for about half of total water storage loss in the column. More significant changes in water balance occur** following talik onset, including **more rapid drying in shallow layers (~10% over 4 decades) and in the column (~16%), and a substantial increase in sub-surface drainage**, as discussed below.”
- L323: “In the 3 decades leading up to talik onset, we find **gradual deepening of the thawed layer** to 3-4 m and penetration of thaw period into Jan-Feb.”
- L332: “We note that bedrock soil is not hydrologically active in CLM4.5, and thus the rate of thawing and drainage in response to permafrost thaw may be **overestimated** in deeper CLM4.5 layers near bedrock due to reduced heat capacity.”
- L355: “Talik onset in CLM4.5 is variable in **the region containing Gakona (southeast Alaska)** with earliest onset by mid-century (~2050s, Fig. 1A); however, our comparison to **borehole temperature data at Gakona** suggests that simulated thaw rates **in southwest Alaska and across pan-Arctic regions with similar permafrost temperatures are underestimated**, and that earliest onset may occur sooner than predicted.”
- L359: “Overall, we find that simulated patterns of permafrost thermal state change are consistent with available observations, but that the exact thaw rates are uncertain. **Although there are many possible explanations for differences in observed and simulated thaw rates, we can attribute high observed thaw rates in part to a combination of (1) relatively dry upper soil at Gakona and Mould Bay, and (2) low surface organic layer and high conductivity of the Barrow and Mould Bay soils.** We keep these uncertainties in mind as we examine patterns of change and talik formation simulated into 2300.”
- L383: “We focus first on site-specific long-term **historical** trends by analyzing the **6 Siberian borehole sites** which recorded at least 5 years of **temperature** data spanning multiple decades: Drughina, Lensk, Macha, **Oimyakon**, Uchur, and Chaingda.”
- L385: “Records at these locations show an **increase** in thaw volume with an average positive trend of 0.19 m months yr⁻¹ from 1955 – 1990 (Table 1, Fig 5). All sites except Drughina show **positive** trends”
- L390: “Further examination indicates that active layer thickness at Drughina actually decreased to 0.8 meters from 1989-1990 compared to 1.2 meters in the 1970s (**data not shown**). Drughina also shows smaller average thaw volume magnitude compared to other sites, consistent with shallower thaw. Together, these findings indicate that active layer thickness is decreasing at Drughina.”
- L395: “**There is considerable spatial variability in thaw volume and trends, but in general thaw trends increase from west (0.18 m months yr⁻¹) to east (0.51 m months yr⁻¹).** Talik forms at several sites, at different times between 1957 and 1990 (shown by vertical dashed lines on Fig. 5), with earlier talik to the west consistent with higher mean initial thaw volumes.”
- L405: “We recompute observed thaw trends at regional clusters using combined records at the 2 sites in northern Siberia (blue), 6 sites in southwest Siberia (orange), and 1 site in southeast Siberia (brown, Table 1) and compare to historical and projected thaw volume trends in CLM4.5 (Fig. 6). Northern locations show a consistent pattern of low thaw

volume ($< 10 \text{ m month yr}^{-1}$) and negligible thaw trend ($\sim 0 \text{ m month yr}^{-1}$) in the historical simulations and observed record from 1950-2000. Thaw projections in northern Siberia indicate continued stability of permafrost through the early 22nd century, followed by a shift to accelerated soil thaw in the early 2120, marked by onset of deep soil thaw late in the cold season.

- L410: “Thaw projections in northern Siberia indicate an **unchanged** trend and continued stability of permafrost through the early 22nd century, followed by a shift to accelerated soil thaw in the early 2120, marked by onset of deep soil thaw late in the cold season.”
- L413: *Southern locations show a systematic underestimate of mean thaw volume ($< 20 \text{ m month yr}^{-1}$) compared to observations ($\sim 40 \text{ m month yr}^{-1}$) from 1950-2000. Simulated thaw trends are negligible prior to 2000, but these likely represent an underestimate given low simulated thaw volumes and significant positive observed trends in both southeast and southwest Siberia beginning in the 1960s following talik onset (Fig. 5). Thaw projections show more abrupt shifts in thaw volume in the early 21st century in the southwest (~ 2025) and in the mid 21st century (~ 2050) in the southeast. The strong discrepancy between observed and simulated thaw and talik onset in southern Siberia warrants close monitoring and continued investigation of this region through sustained borehole measurements and additional model realizations of potential future warming.”*
- L424: “Fig. 7A plots the decade in which NHL ecosystems are projected to transition to long-term C sources over the next 3 centuries (2010-2300). A total of 6.8 million km² of land is projected to transition, peaking in the late 21st century, with most regions transitioning prior to 2150 (4.8 million km² or 70%, Fig. 7B, solid black). C source transitions which occur in the permafrost zone, accounting for 6.2 million km² of land (91% of all C source transitions), also form talik at some time from 2006-2300 (Fig. 7C). The remaining C source transitions (0.6 million km², or 9%) occur outside the permafrost zone, primarily in eastern Europe.”
- L431: “Net C emissions from C source transition regions are a substantial fraction of the total NHL C budget over the next 3 centuries (Fig. 8). The cumulative pan-Arctic C source increases slowly over the 21st century, reaching 10 Pg C by 2100 with RCP8.5 warming, then increases more rapidly to 70 Pg C by 2200 and 120 Pg by 2300 with sustained ECP8.5 warming (Fig. 8, solid black). This pan-Arctic source represents 86% of cumulative emissions in 2300 from the larger NHL talik region (crosses), despite the 2 fold smaller land area, and exceeds the talik region through 2200 due to mitigating widespread vegetation C gains (Koven et al., 2015). Cumulative emissions over all NHL land regions (diamonds, $> 55\text{N}$) increase in similar fashion to the talik region, reaching 120 Pg C by 2200 and 220 by 2300, with no sign of slowing.”
- L440: “The geographic pattern of C sink-to-source transition date is reversed compared to that of talik formation, with earlier transitions at higher latitudes (the processes driving these patterns are discussed in detail below). Overall, the lag relationship between talik onset and C source transition exhibits a tri-modal distribution (Fig. 7D), with peaks at negative time lag (C source leads talik onset, Median Lag = -5 to -6 decades), neutral time lag (C source synchronized with talik onset; Median Lag = -2 to 1 decade), and positive time lag (C source lags talik; Median Lag = 12 decades; red shading in Fig. 7C). Roughly half of these regions (3.2 million km²) show neutral or positive time lag (lag ≥ 0). This pattern, characteristic of the sub-Arctic ($< 65\text{N}$), represents the vast majority of C source transitions after 2150 (Fig.

7B, dotted), **but only accounts for 17% of cumulative emissions (20 Pg C by 2300, Fig. 8, dotted)**. The remaining regions (3.0 million km²) in the Arctic and high Arctic (> 65°N) show negative time lag and account for most of late 21st century sources (Fig. 7B, dashed) **and cumulative emissions (95 Pg C by 2300, or 79%; Fig. 8, dashed)**. C sources in regions not identified as talik (0.63 million km²) either show talik presence at the start of our simulation, or are projected to transition in the absence of permafrost or in regions of severely degraded permafrost (Fig. 7C, dash dotted). **This region contributes only 5 Pg C (4%) of cumulative C emissions in 2300.**

- L458: **“In these regions, thaw volume is low (< 50 m months yr⁻¹) and shows a weak relationship to NBP (NBP decreases much faster than thaw volume) prior to C source onset (indicated by large green circle in Fig. 8A).”**
- L470: **“A broader analysis of soil thaw statistics over all regions and periods indicates that most C source transitions (~2.3 million km², or 77% of land where C source leads talik) occur at active layer depths below 3 m and thaw season penetration into November.”**
- L479: **“The total area of land in which SOM exceeds 100 kg C m⁻² represents 2/3 of all land where C sources lead talik onset (2.0 million km²), and peaks at a negative time lag of -5 to -6 decades (Fig. 7D, green bars), which perfectly aligns with the peak distribution of negative time lags. Cumulative C emissions from regions of SOM > 100 kg C m⁻² are also 2/3 of total C emissions (80 Pg C; Fig 8, green).”**
- L489: **“and talik formation occurs when these regions are weak sinks (NBP > 0 g C m⁻² yr⁻¹).”**
- L490: **“In general, C source onset under high thaw volume indicates these regions are more sensitive to C emissions from deep soil thaw.”**
- L495: **“The regions where fire C emissions exceed 25 g C m⁻² yr⁻¹, representing our threshold for C source transition, are exclusively boreal ecosystems, account for 1/3 of all land with negative lags (~1.1 million km²), and align perfectly with the peak distribution of positive time lags (Fig. 7D, red bars) and cumulative C emissions (20 Pg C in 2300, Fig. 8, red).”**
- L507: **“The decadal time lag between talik onset and C source transition is more normally distributed in the remaining region, represented by the residual grey bars visible in Fig. 7D, which occurs predominantly in cold northern permafrost in northwest Siberia where low SOM (< 100 Kg m⁻²) and fire emission (< 25 g C m⁻² yr⁻¹) prevail. This region has a mean lag of 1 decade from talik onset to C source, with high standard deviation of lags (± 8 decades) reflecting a skewed distribution of GPP; low productivity in cold permafrost (GPP = 385 g C m⁻² yr⁻¹) increases the likelihood that soil thaw will lead to C source transition prior to talik onset, and high productivity in warm permafrost GPP = 1111 g C m⁻² yr⁻¹) increasing the likelihood of a transition after talik onset. Cumulative C emissions from this region are on the low end (27 Pg C by 2300; Fig. 8, blue) due to low soil C (SOM = 59 kg C m⁻²).”**
- L527: **“GPP and combined respiration increase by ~15% per decade for each permafrost regime surrounding the decade of C source transition with peak fluxes in the growing season (Fig. 11 A - D).”**
- L541: **“The trend in the respiration difference in warm and cold permafrost, which increase by similar amounts (~100 g C m⁻² yr⁻¹), thus reflects an increasing dominance of respiration from younger and older soil C pools, respectively. These trends are identical to the corresponding NBP trends, which decrease by 100 g C m⁻² yr⁻¹ over the same period**

from neutral to net source (Fig. 12 G – H), such that the differences between GPP and respiration driving the NBP trends are explained almost entirely by the increasing fraction of soil vs litter respiration.”

- *L586: “Controlled experiments demonstrating the sensitivity of talik to parameters that control soil drying such ice impedance or baseflow scalars (e.g. Lawrence et al., 2015), and the effect of organic content and mineral soil texture (Lawrence and Slater, 2008), could provide key insight on soil thermal dynamics in frozen or partially frozen conditions. Other factors affecting soil hydrology and carbon cycling not considered in our CLM4.5 simulations include high spatial resolution in discontinuous permafrost, shifts in vegetation community, lateral flow representation, thermokarst activity and other thaw-related changes to the ground surface, surface slope and aspect, soil heterogeneity, and potentially several other factors (see Jorgenson and Osterkamp (2005) for discussion of some of the many complexities to be considered).”*
- *L596: “Our simulations show increasing C emissions over time across the talik region (Fig. 1B), as cumulative NBP becomes increasingly negative (NBP < 0 equals a net C source), reaching a net source of 140 Pg C by 2300 (Fig. 8, crosses), consistent with previous estimates of net C balance across the larger pan-Arctic region from CLM4.5 (~160 Pg C, Koven et al., 2015; Lawrence et al., 2015). Ecosystems which transition from net C sinks to net C sources represent less than half the total talik area (6.8 of 14.5 Million km², Fig. 7A), but account for most (~85%) of the cumulative emissions, reaching 10 Pg C in 2100, 70 Pg C in 2200, and 120 Pg C by 2300 (Fig. 8, solid black). Removing the effect of vegetation C gain (~20 Pg C in 2100 and 40 Pg C in 2200 and 2300 according Koven et al., 2015), we estimate a cumulative permafrost emission for C source transition regions of 30 Pg C in 2100, 110 Pg C in 2200, and 160 Pg C in 2300. These numbers are on the low end but consistent with estimates of permafrost C emissions summarized by Schuur et al. (2015), which range from 37-174 Pg C by 2100 and 100-400 Pg C by 2300.”*
- *L608: “About half of this region (3.2 million km²) shows a pattern of accelerated soil C respiration following talik onset, which shifts the surface C balance of photosynthetic uptake and litter respiration from net C sinks to long term net sources totaling 20 Pg C across 3.2 million km² of NHL land by 2300.”*
- *Line 626: “Our estimate of C emissions following talik onset (~20 Pg C) is low compared to the cumulative emissions from all long term C source transitions (120 Pg C), but likely strongly underestimated. Soil C is not permitted below 3.5 m in CLM4.5, or in most analogous models, such that potential decomposition of the ~350 Pg soil organic C in deep permafrost (> 3 m) is not accounted for (Hugelius et al., 2014; Jackson et al., 2017). This is significant for our simulations, which show frequent talik formation and accelerating thaw volumes below 3 m (e.g., Fig. 3). We therefore caution the reader in the interpretation of the timing and magnitude of permafrost C emissions following talik onset in our simulations, which represent a lower bound of potential emissions based on the current formulation of CLM4.5.”*
- *L635: “We identify an equally large region of land in the high Arctic, representing ~3.0 million km², which is projected to transition to a long term C source much sooner than the sub-Arctic in the absence of talik, and emit 5 times as much carbon by 2300 (~95 Pg C).”*

- L688: “6.8 million km² of land impacted in Siberia and North America will produce an integrated C source of **90 Pg C by 2100 and 120 Pg C by 2200.**”
- L692: “Our main results emphasize **an increasingly important impact of NHL cold season warming on earlier spring thaw, longer non-frozen seasons, and increased depth and seasonal duration of soil thaw.**”

Figure Changes:

- We also included information in the first talik figure (Fig. 1) and carbon figure (Fig. 7): **“These results assume a Representative Pathway 8.5 warming scenario through 2100 and an Extended Concentration Pathway 8.5 through 2300.”**
- The definition of NBP has been corrected in the text and in the figures.
- Revised Figure 8 (now Figure 9) with arrows indicating C source or sink for clarification:
- Corrected y-axis error on Fig. 7 by moving the C source numbers from Fig. 7B to Fig. 8 for more in depth analysis (Figure 7 below; Figure 8 provided in Reviewer 1 responses). Added Figure 8
- Removed Figures 10 and 11
- Color specifications have been corrected in all figures.
- New Fig. 11: We have included a description of error bars in figure 12, which represent the multi-decadal standard deviation of seasonal and C source transition time series from 2040 – 2270.
- Removed the thaw onset symbols from Figure 6
- We also include an additional column in Table 2 for soil characteristics:

Tracked Changes

1
2
3
4
5
6
7
8
9
10
11
12
13
14
15
16
17

Detecting the permafrost carbon feedback: Talik formation and increased cold-season
respiration as precursors to sink-to-source transitions

Nicholas C Parazoo¹, Nicholas.c.parazoo@jpl.nasa.gov

Charles D. Koven², cdkoven@lbl.gov

David M. Lawrence³, dlawren@ucar.edu

Vladimir Romanovsky⁴, veromanovsky@alaska.edu

Charles E. Miller¹, Charles.E.Miller@jpl.nasa.gov

¹Jet Propulsion Laboratory, California Institute of Technology, Pasadena, California, 91109, USA

²Lawrence Berkeley National Laboratory, Berkeley, California, USA

³National Center for Atmospheric Research, Boulder, Colorado, USA

⁴Geophysical Institute UAF, Fairbanks, Alaska, 99775, USA

18 **Abstract**

19 Thaw and release of permafrost carbon (C) due to climate change is likely to offset increased
20 vegetation C uptake in Northern High Latitude (NHL) terrestrial ecosystems. Models project
21 that this permafrost C feedback may act as a slow leak, in which case detection and attribution
22 of the feedback may be difficult. The formation of talik, a sub-surface layer of perennially
23 thawed soil, can accelerate permafrost degradation and soil respiration, ultimately shifting the
24 C balance of permafrost affected ecosystems from long-term C sinks to long-term C sources. It
25 is imperative to understand and characterize mechanistic links between talik, permafrost thaw,
26 and respiration of deep soil C to detect and quantify the permafrost C feedback. Here, we use
27 the Community Land Model (CLM) version 4.5, a permafrost and biogeochemistry model, in
28 comparison to long term deep borehole data along North American and Siberian transects, to
29 investigate thaw driven C sources in NHL (> 55°N) from 2000-2300. Widespread talik at depth is
30 projected across most of the NHL permafrost region (14 million km²) by 2300, 6.2 million km² of
31 which is projected to become a long term C source, emitting 10 Pg C by 2100, 50 Pg C by 2200,
32 and 120 Pg C by 2300, with few signs of slowing. Roughly half of the projected C source region
33 is in predominantly warm sub-Arctic permafrost following talik onset. This region emits only 20
34 Pg C by 2300, but the CLM4.5 estimate may be biased low by not accounting for deep C in
35 yedoma. Accelerated decomposition of deep soil C following talik onset shifts the ecosystem C
36 balance away from surface dominant processes (photosynthesis and litter respiration), but sink-
37 to-source transition dates are delayed by 20-200 years by high ecosystem productivity, such
38 that talik peaks early (~2050s, borehole data suggests sooner) and C source transition peaks
39 late (~2150-2200). The remaining C source region in cold northern Arctic permafrost, which
40 shifts to a net source early (late 21st century), emits 5 times more C (95 Pg C) by 2300, and prior
41 to talik formation, due to the high decomposition rates of shallow, young C in organic rich soils
42 coupled with low productivity. Our results provide important clues signaling imminent talik
43 onset and C source transition including: (1) late cold season (Jan-Feb) soil warming at depth (~2
44 m), (2) increasing cold season emissions (Nov-Apr), (3) enhanced respiration of deep, old C in
45 warm permafrost and young, shallow C in organic rich cold permafrost soils. Our results suggest
46 a mosaic of processes that govern carbon source-to-sink transitions at high latitudes, and

- Deleted: IS
- Formatted: Superscript
- Deleted: correlated to increased cold season warming, earlier spring thaw, and growing active layers
- Deleted: Talik formation peaks in the 2050s in warm permafrost regions in the sub-Arctic. Comparison to borehole data suggests talik formation may even occur sooner.
- Deleted: A
- Deleted: the
- Deleted: balance of
- Deleted: tic
- Deleted: uptake
- Deleted: into long-term C sources
- Deleted: across 3.2 million km² of permafrost. Talik driven sources occur predominantly in warm permafrost, but s
- Deleted: decades to centuries
- Deleted: due to
- Deleted: y.
- Deleted: In contrast
- Deleted: , most of the
- Deleted: region in the northern Arctic (3 million km²)
- Deleted: by the end of the
- Deleted: in the absence of
- Deleted:

72 emphasize the urgency of monitoring soil thermal profiles, organic C age and content, cold
73 season CO₂ emissions, and atmospheric ¹⁴C as key indicators of the permafrost C feedback.

74

75 **1. Introduction**

76 The future trajectory of the Arctic Boreal Zone (ABZ) as a carbon (C) sink or source is of global
77 importance due to vast quantities of C in permafrost and frozen soils (Belshe, Schuur and Bolker,
78 2013). Cold and waterlogged conditions in the ABZ have hindered soil organic material (SOM)
79 from microbial decomposition and led to long-term C accumulation at soil depths below 1 m (Ping
80 *et al.*, 2015). Arctic warming, which stimulates plant growth as well as respiration in tundra
81 ecosystems (Mack *et al.*, 2004; Euskirchen *et al.*, 2012; Natali, Schuur and Rubin, 2012; Barichivich
82 *et al.*, 2013; Commane *et al.*, 2017), has driven a period of C cycle intensification over the last 50
83 years with greater C inputs and outputs across high latitude ecosystems (Graven *et al.*, 2013).
84 Expert assessments of site-level observations, inversion studies, and process models suggest that
85 Arctic C balance is near neutral, but large uncertainties allow for solutions ranging from small
86 sources to moderate sinks; however, most assessments favor an overall strengthening of the
87 regional C sink, with productivity gains exceeding respiration losses on average (McGuire *et al.*,
88 2012).

89 The effect of continued warming on future northern high latitude (NHL) ecosystem C balance is
90 uncertain but appears to be increasingly dependent on responses to changes in cold season
91 emissions, soil moisture, shifts in vegetation community, and permafrost degradation (Abbott *et al.*,
92 2016). These vulnerabilities are likely driven by disproportionate warming during the cold
93 season (Fraser *et al.*, 2014), which is projected to increase at twice the rate of summer warming
94 over the next century (Christensen *et al.*, 2013). For example, winter warming during the long
95 cold season promotes increased soil respiration, offsetting C uptake during the short Arctic
96 growing season (Oechel *et al.* 2014; Euskirchen *et al.* 2016; Commane *et al.* 2017), and shifting
97 tundra ecosystems from C sink to source (Webb *et al.*, 2016). Winter warming also promotes
98 earlier and more rapid snow melt and landscape thawing (Goulden, 1998; Schuur *et al.*, 2015).
99 This can impact seasonal C balance through increased hydrological export of SOM by Arctic rivers

100 (Olefeldt and Roulet, 2014), which is projected to increase by 75% by end of century (Abbott *et*
101 *al.*, 2016). Early snow melt can also cause increased exposure of the land surface to solar
102 absorption (Lawrence, Slater and Swenson, 2012) resulting in increased evapotranspiration and
103 summer drought risk (Zhang *et al.*, 2011), which decreases terrestrial biomass through reduced
104 plant growth and increased intensity and frequency of boreal fire emissions and fire disturbance
105 (Yi *et al.* 2014; Veravebeke *et al.*, 2017). ABZ fire-driven C losses are expected to increase four-
106 fold by 2100 (Abbott *et al.*, 2016).

107 On longer time scales, permafrost degradation and resulting C losses from deep, old C is expected
108 to be the dominant factor affecting future Arctic C balance (McGuire *et al.*, 2012; Lawrence *et al.*,
109 2015; Schuur *et al.*, 2015). In addition to these effects, warmer temperatures and longer non-
110 frozen seasons caused by earlier spring thaw and later autumn freezing can promote accelerated
111 deepening and increased duration of the active layer (layer of soil near the surface which is
112 unfrozen in summer and frozen in winter) and thawing permafrost. More abrupt processes such
113 as thermokarst lake initialization can also lead to rapid thaw through pronounced sub-lake talik
114 formation (Jorgenson and Osterkamp, 2005). These processes can initiate formation of a talik
115 zone (perennially thawed sub-surface soils) during active layer adjustment to new thermal
116 regimes (Jorgenson *et al.*, 2010) in lake and non-lake environments. Talik as well as longer,
117 deeper active layer thaw stimulate respiration of soil C (Romanovsky and Osterkamp, 2000;
118 Lawrence *et al.*, 2008), making the ~1035 Pg soil organic carbon in near surface permafrost (0-3
119 m) and ~350 Pg soil organic carbon in deep permafrost (> 3 m) vulnerable to decomposition
120 (Hugelius *et al.*, 2014; Jackson *et al.*, 2017).

121 Climate models used in the Coupled Model Intercomparison Project Phase 5 (CMIP5) consistently
122 project widespread loss of permafrost in the future due to climate warming (Slater and Lawrence,
123 2013), though the ESMS that participated in the CMIP5 also project NHL terrestrial C uptake
124 rather than losses due to warming (Ciais *et al.*, 2013). This projection conflicts with expectations
125 from field studies (Schuur *et al.*, 2009; Natali *et al.*, 2014), but newer approaches, such as
126 explicitly representing the vertical structure of soil respiration and its coupling to deep soil
127 thermal changes, lead to changes in the model-projected response from a net C gain with
128 warming to a net loss, and hence a positive carbon-climate feedback (Koven *et al.* 2011).

Deleted: (NF)

Deleted: .

Deleted: is

Deleted:

Deleted: ~1000

Deleted: C

Deleted:

Deleted: (Tamocai *et al.* 2009; Harden *et al.* 2012)

Deleted: [Slater and Lawrence, 2013]

Deleted: (Ciais *et al.*, 2013)

Deleted: A

Deleted: (Schuur *et al.*, 2009; Natali *et al.*, 2014)

141 Permafrost C emissions are likely to occur gradually over decades to centuries, and therefore are
142 unlikely to cause abrupt and easily detected signals in the global C cycle or climate (Schuur *et al.*,
143 2015). We use the coupled permafrost and biogeochemistry Community Land Model Version 4.5
144 (CLM4.5) to investigate in detail the subsurface thermal processes driving C emissions from
145 shallow (0-3m) and deep (>3m) permafrost C stocks and to project the rate of NHL permafrost C
146 feedbacks (> 55°N) over the 21st century. Using CLM4.5 in the framework of an observing system
147 simulation experiment (Parazoo *et al.*, 2016), we ask how we might be able to (1) identify
148 potential thresholds in soil thaw, (2) detect the specific changes in soil thermal regimes that lead
149 to changes in ecosystem C balance, and (3) project future C sources following talik onset. We
150 hypothesize that talik formation in permafrost triggers accelerated respiration of deep soil C and,
151 ultimately, NHL ecosystem transition to long-term C sources.

Deleted: (e.g., Parazoo et al., 2016)

152 Comparison to observed thaw at selected tundra and forested ecosystems along north-south
153 transects in Siberia and North America in the 20th and early 21st century provides a reference to
154 evaluate historical thaw patterns and projected thaw rates. The remainder of our paper is
155 organized as follows: Section 2.1 describes our methods to simulate and analyze soil thaw and C
156 balance in CLM4.5; Section 2.2 describes borehole datasets used to analyze CLM4.5 soil thermal
157 regime; Section 3.1 presents results of talik formation in CLM4.5 and comparison of simulated
158 thaw profiles to borehole data in North America; Section 3.2 evaluates projected thaw rates
159 against long-term borehole data in Siberia; Section 3.3 identifies timing and location of C source
160 onset and discusses formation mechanisms in the presence and absence of talik; Section 3.4
161 presents a projection of future C sources at talik locations; Sections 4 discusses the main findings.

162

163 **2. Methods**

164 *2.1 Simulations*

165 CLM4.5 provides an accurate characterization of the physical and hydrological state of
166 permafrost needed to evaluate permafrost vulnerability and identify key processes (Lawrence *et al.*,
167 2008; Swenson, Lawrence and Lee, 2012). CLM4.5 includes a basic set of permafrost
168 processes to allow projection of permafrost carbon–climate feedbacks, including snow schemes,

170 vertically resolved SOM dynamics and soil hydrology, coupled hydraulic and thermal properties
171 in frozen and unfrozen soils allowing realistic seasonal evolution of the active layer, and
172 interaction with shallow (0-3m) and deep (>3m) permafrost C (Swenson et al. 2012; Oleson et al.
173 2013; Koven et al. 2013, 2015; Lawrence et al. 2008). More abrupt thaw processes affecting
174 permafrost C dynamics and talik formation such as thermokarst or other thaw related landscape
175 dynamics changes in wetland or lake distribution are not accounted for in CLM4.5 (see Riley et
176 al. (2011) for more discussion).

177 CLM is spunup to C equilibrium for the year 1850 by repeatedly cycling through 20 years of pre-
178 industrial climate forcing with CO₂ and N-deposition set at 1850 levels. C initialization is achieved
179 via slow mixing by cryoturbation between the seasonally thawed active layers and deeper
180 permafrost layers (Koven et al., 2009). Including vertically resolved processes leads to a sign
181 change in the projected high-latitude C response to warming, from net C gains driven by
182 increased vegetation productivity to net C losses from enhanced SOM decomposition (Koven et
183 al., 2011). The soil grid includes 30 vertical levels that has a high-resolution exponential grid in
184 the interval 0–0.5 m and fixed 20-cm layer thickness in the range of 0.5–3.5 m to maintain
185 resolution through the base of the active layer and upper permafrost, and reverts to
186 exponentially increasing layer thickness in the range 3.5–45 m to allow for large thermal inertia
187 at depth. Soil C turnover in CLM4.5 is based on a vertical discretization of first-order multipool
188 SOM dynamics (Koven et al., 2013; Oleson et al., 2013) where decomposition rates as a function
189 of soil depth are controlled by a parameter Z_τ (Koven et al., 2015; Lawrence et al., 2015). This
190 depth control of decomposition represents the net impacts of unresolved depth dependent
191 processes. In this study, we utilize Z_τ=10 m, which yields a weak additional depth dependence of
192 decomposition beyond the environmental controls and, as discussed and evaluated relative
193 to Z_τ=1m and Z_τ=0.5m in Koven et al (2015), results in CLM permafrost-domain soil C stocks that
194 are in closest agreement (1582 Pg for Z_τ=0.5 m, 1331 Pg for Z_τ=1m, and 1032 Pg for Z_τ=10m)
195 with observed estimates (1060 Pg C to 3 m depth; Hugelius et al 2013). This reduction in initial C
196 is due to higher decomposition rates at depth during the model initialization period. There is no
197 C below 3.5 m, so additional thaw below 3 meters has a small impact on the C cycle. We note

Deleted: (

Deleted: ,

Formatted: Font:+Theme Body (Calibri), 12 pt

Formatted: Font:+Theme Body (Calibri)

Formatted: Font:+Theme Body (Calibri), 12 pt

Formatted: Font:+Theme Body (Calibri)

Formatted: Font:+Theme Body (Calibri), 12 pt

Formatted: Font:+Theme Body (Calibri), 12 pt

Formatted: Font:+Theme Body (Calibri), 12 pt

Formatted: Font:+Theme Body (Calibri)

Formatted: Font:+Theme Body (Calibri), 12 pt

Formatted: Font:+Theme Body (Calibri)

Formatted: Font:+Theme Body (Calibri), 12 pt

Formatted: Font:+Theme Body (Calibri)

Formatted: Font:+Theme Body (Calibri), 12 pt

Formatted: Font:+Theme Body (Calibri)

200 that the relationship applied in CLM4.5, which implies multiplicative impacts of limitations to
201 decomposition, is commonly applied in land biogeochemical models, but is quite uncertain.

202 We use CLM4.5 configured as described in two recent permafrost studies (Lawrence et al. 2015;
203 Koven et al. 2015) using time-varying meteorology, N deposition, CO₂ concentration, and land
204 use change to capture physiological (i.e., CO₂ fertilization) and climate effects of increasing CO₂
205 over the period 2006-2300. We use an anomaly forcing method to repeatedly force CLM4.5
206 with observed meteorological from the CRUNCEP dataset for the period 1996–2005 (data
207 available at dods.ipsl.jussieu.fr/igcmg/IGCM/BC/OOL/OL/CRU-NCEP/) and monthly anomalies
208 added based on a single ensemble member from a CCSM4 Representative Concentration
209 Pathway 8.5 (RCP8.5) simulation for the years 2006-2100 and Extended Concentration Pathway
210 8.5 (ECP8.5) for the years 2100-2300. The period from 1996 to 2015 represents a base
211 climatological period used for calculating monthly anomalies, with a 20-y record chosen to
212 minimize large anomalies in the first few years. This process is repeated for all variables and all
213 times from 2006 to 2300 (constantly cycling through the same 1996–2005 observed data). Land
214 air temperature for the period 2006-2300, shown in Fig. 1A, is projected to increase steadily
215 over our simulation, with a slight decrease in the rate of warming.

216 We caution that we are using only a single ensemble member from CCSM4, and hence our
217 results represent one realization from one model forced with one climate scenario. This results
218 in uncertainties from the historical climate/weather forcing, the structure and parameterization
219 of the model, and climate scenarios (both across models and across emissions scenarios).

220 Simulations are carried out on a global domain at a grid resolution of 1.25° longitude x 0.9375°
221 latitude and saved as monthly averages. Simulation output is collected into decadal averages
222 from 2011-2300 (e.g., 2011-2020 averages for the 2010s, 2021-2030 for the 2020s, etc). Our
223 method to link C balance changes to permafrost thermal state relies on identifying the timing of
224 two key processes: (1) talik formation, and (2) C source transition. Talik formation represents a
225 critical threshold of permafrost thaw. The C source transition represents a shift of ecosystem C
226 balance from a neutral or weak C sink to a long-term source as C balance shifts to increasing
227 dominance of C source processes including permafrost thaw and fires. (Koven, Lawrence and
228 Riley, 2015). Using the hypothesis that talik formation triggers a transition to long-term C

Deleted: driven by onset of permafrost thaw and respiration of deep SOM

Deleted: (

232 sources, we quantify the extent of talik formation and rate of transition to C source once talik
233 has formed in permafrost-affected NHL ecosystems.

234 Following Koven et al. (2015), we define the timing of C source transition from net annual sink
235 to net source as the first decade when annual net biome production (NBP) decreases below -25
236 $\text{g C m}^{-2} \text{ y}^{-1}$ and remains a source ($\text{NBP} < 0 \text{ g C m}^{-2} \text{ y}^{-1}$) through 2300. Here, we use the sign
237 convention of $\text{NBP} < 0$ to represent net C flux from land to atmosphere (e.g., source). The
238 timing of talik formation is defined as the first decade when soil temperature (T_s) for any layer
239 between 0 and 40 m exceeds -0.5°C for all months in a calendar year (Jan-Dec), assuming that
240 soils start off as permafrost at the beginning of our simulations in 2006. We use a negative
241 freezing point threshold to account for availability of liquid water below 0°C due to freezing
242 point depression. We note the real threshold temperature at which liquid water remains
243 available varies depending on the soil salinity or mineral content, the latter effect of which is
244 included in the actual respiration calculations used by CLM. Here we use -0.5°C as the
245 freeze/thaw cutoff, and examine cutoffs at 0.5°C increments from 0°C to -2.0°C .

246 We introduce the thawed volume-time integral, or “thaw volume”, as a metric to better
247 understand thaw dynamics and help identify thaw instability thresholds. We integrate
248 permafrost in both time (month of year) and depth (soil layer from the surface to 40 m) into a
249 logical function that is one for thawed layers ($T_s > -0.5^\circ\text{C}$), zero for frozen layers, and multiply
250 each thawed layer by layer thickness to convert to units of meter months. This conversion
251 accounts for non-uniform layer thicknesses, providing a consistent metric for comparing
252 simulated and observed thaw.

253 Our analysis focuses on NHL grid points within the ABZ north of 55°N . We analyze talik
254 formation and C source transitions in the context of the simulated initial state of SOM, and
255 published maps of permafrost conditions from NSIDC
256 (https://nsidc.org/data/docs/fgdc/ggd318_map_circumarctic/) and described in Brown et al.
257 (2001). Permafrost extent is classified as continuous (90-100%), discontinuous (50-90%),
258 sporadic (10-50%).

259 *2.2 Observations*

260 We compare simulated patterns of active layer dynamics and soil thaw to patterns observed
261 from contemporary and historical borehole measurements of permafrost temperature profiles.
262 We focus on sites in western North America and eastern Siberia with daily continuous
263 observations year-round (Jan-Dec) over multiple consecutive years. The primary focus of data in
264 North America (2004-2013) is to evaluate seasonal progression of soil thaw and talik formation
265 near the surface (0-3 m). Siberian data, which have a longer record on average (1950-1994), are
266 used to evaluate long term trends in soil thaw at 0.0 - 3.6 m depth. Site locations are shown in
267 Fig. 1.

268 Siberian data are based on measurements along the East Siberian Transect (EST)
269 (<https://arcticdata.io/metacat/metacat/doi:10.5065/D6Z036BQ/default>). The EST consists of 13
270 sites that cover a southwest-to-northeast transect in east Siberia [60.7°N, 114.9°E to 68.3°N,
271 145°E] during the period 1882-1994 (Romanovsky et al. 2007). For this study, we focus on the 9
272 sites which report measurements as monthly averages at regular depths of 0.2, 0.4, 0.8, 1.6,
273 and 3.2 m. Unfortunately, data gaps of years to decades exist on a site-by-site basis, and many
274 years do not report the full annual cycle over multiple layers. To assess observed thaw trends
275 from 1955-1990, we analyze individual sites which report at least 10 months yr⁻¹ of reported
276 monthly mean soil temperature at each layer, and 55 months across the 5 layers (out of 60
277 possible layer-months per year). Based on these requirements, we find that 6 of 9 sites yield at
278 least 6 years of data over multiple decades, and are well suited for examining historical thaw
279 trends. For comparison of observed trends to historical and projected trends from 1950-2300,
280 we analyze clusters of sites by combining the 9 sites into 3 groups based on approximate
281 locations, and calculate observed trends using the inter-site average at each location. We use 2
282 sites in northern Siberia (67°N, 144°E), 6 sites in southwest Siberia (61°N, 115°E), and 1 site in
283 southeast Siberia (59°N, 131°E). Site information is shown in more detail in Table 1.

284 North American transect data are taken from the global terrestrial network for permafrost
285 (GTNP) borehole database (<http://gtnpdatabase.org/boreholes>): (1) Borehole 1108 at Mould
286 Bay in Canada [119°W, 76°N] from 2004-2012; (2) Borehole 33 in Barrow along the northern
287 coast of Alaska [156°W, 71.3°N] from 2006-2013; and (3) Borehole 848 in Gakona in southeast
288 Alaska [145°W, 62.39°N] from 2009-2013. Mould Bay is a continuous permafrost tundra site

Deleted: W
Deleted: therefore only
Deleted: years with

Deleted: comparison to
Deleted: i
Deleted: n CLM4.5
Deleted: re
Deleted: from all 9 sites at 3 unique
Deleted: s
Deleted: :

Formatted: Font:Calibri

299 with measurements at 63 depths from 0 - 3 m. Mould Bay has almost no organic layer (about 2
300 cm) and then sandy silt with high thermal conductivity. Barrow is a continuous permafrost
301 tundra site with measurements at 35 depths from 0 - 15 m. The soil at Barrow is represented by
302 silt with a bit of mix with some organics and almost no organic layer on top. Conductivity of the
303 upper layer is $\sim 1 \text{ W mK}^{-1}$ for unfrozen and $\geq 2 \text{ W mK}^{-1}$ for frozen soil. Gakona is a continuous
304 permafrost forest tundra site with measurements at 36 depths from 0 - 30 m. Gakona has a
305 thick organic layer of moss (0 to 5 cm), dead moss (from 5 to 13 cm), and peat (from 13 to 50
306 cm), then silty clay at depth.

307 All North American transect datasets are reported as daily averages. For each site, we
308 aggregate from daily to monthly averages requiring at least 20 days month⁻¹ at each layer and
309 for each year. Measurements are reported at multiple depths and high vertical resolution (up to
310 0.1 m in shallow layers) but are generally non-uniform in depth (multiple layers missing,
311 different layers reported for each site). Given these inconsistencies and records ≤ 8 years, we
312 use these data for qualitative analysis of seasonal and vertical patterns in permafrost thaw. Site
313 information and soil characteristics are summarized in Table 2.

314 3. Results

315 3.1 Simulated Talik Onset in the 21st Century

316 Our simulations show widespread talik formation throughout Siberia and northern North
317 America over the period 2010-2300 (Fig. 1B), impacting ~ 14.5 million km² of land in NHL's (55°-
318 80°N) assuming a freeze/thaw threshold of -0.5°C and RCP8.5 and ECP8.5 warming scenarios.
319 10.6 million km² of land in Europe, southwest Asia, and N. America (below 60°N) either formed
320 talik prior to the start of our simulation in 2010 in regions already experiencing degraded
321 permafrost (e.g., Fig. 1D, permafrost extent $< 90\%$ in southwest Siberia and southern N.
322 America), or did not have permafrost to begin with. A small amount of land along northern
323 coastal regions (~ 1.6 million km²) show no talik formation prior to 2300.

324 The long-term trend and decadal variability of talik formation are quantitatively and
325 qualitatively similar for freeze/thaw thresholds at or below -0.5°C (Fig. 1A). Peak formation
326 generally occurs over the period 2050-2150, accelerating rapidly early in the 21st century, and

Formatted: Font:Calibri, Font color: Text 1

Formatted: Font:Calibri

Formatted: Font:Calibri, Font color: Text 1

Formatted: Font:Calibri

Formatted: Font:Calibri, Font color: Text 1

Formatted: Font:Calibri

Deleted: is

Deleted: shown in more detail

Deleted: A

Deleted: 2

Deleted: B

332 leveling off in the late 22nd century. The timing and location of talik formation correlates with
333 the annual mean temperature of permafrost at 3 m ($T_{\text{soil-3m}}$) (Fig. 1C) and observed permafrost
334 state (Fig. 1D, from Brown et al. 2001) at the start of our simulation; we see earlier talik
335 formations in sub-Arctic regions (< 66N) with warm simulated permafrost ($T_{\text{soil-3m}} > 0^{\circ}\text{C}$) and
336 permafrost extent less than 90%, and later formation in northern regions with cold permafrost
337 ($T_{\text{soil-3m}} < 0^{\circ}\text{C}$) and continuous permafrost. Talik formation progresses northward from the sub-
338 Arctic to the Arctic over time, starting in the warm/discontinuous permafrost zone in the 21st
339 century then to the cold/continuous permafrost zone the 22nd century. This suggests a shift in
340 permafrost state across the pan-Arctic from continuous to discontinuous over the next 2
341 centuries.

342 Our simulations demonstrate consistent patterns of changing thaw volume leading up to and
343 following initial talik formation, independent of the decade of talik onset. Time series of thaw
344 volume as a function of decade relative to talik onset (Fig. 2A) show a steady rise in thaw
345 volume of 1-2 m months yr^{-1} in the decades prior to talik formation, with thaw limited primarily
346 to shallow soils (< 1.5 m) and summer/early fall. Thaw volume accelerates to 10-20 m months
347 yr^{-1} within 1-4 decades of talik onset, coinciding with thaw penetration at depth (~2 meters on
348 average, Fig. 2B) and deeper into the cold season (~Jan-Apr). Thaw penetration into the Jan-Apr
349 period occurs for the first time at 2.6 ± 0.9 decades prior to talik onset (vertical grey lines in Fig.
350 2A). At talik onset, thaw volume jumps from mean values of 60 ± 10.7 m months yr^{-1} to $377 \pm$
351 44 m months yr^{-1} at a mean depth of 4.1 meters. Thaw volume levels out within one decade
352 following initial talik formation and accelerated thaw of all soil layers; this leveling is an artifact
353 of the maximum depth of soils in CLM4.5 (equal to 45.1 meters), and represents the complete
354 transition from permafrost to seasonally-frozen ground in the model. The transition to deep
355 cold season thaw and rapidly increasing thaw volume represent key threshold signaling
356 imminent talik onset.

357 Onset of surface thaw in the uppermost soils during the spring freeze/thaw transition provides
358 another reliable predictor for talik onset. In particular, we find consistent dates and trends of
359 spring thaw in the surface soil layer in the decades leading up to talik onset (Fig. 2C), shifting by

360 about 1 week over 4 decades from Day of Year (DOY) 134 ± 2.8 (~mid May) to $DOY 127 \pm 3.5$
361 during talik formation (~early May).

362 Changes in total column soil water and sub-surface drainage following talik onset may provide
363 clues a posteriori that talik is already present. Lawrence et al. (2015) show that deepening of
364 the active layer and thawing of permafrost allows water to drain deeper into the soil column,
365 which dries out near surface soils. Our simulations show a similar, but very slight, drying pattern
366 in shallow layers in the 4 decades prior to talik onset (1.3% loss of soil moisture over 0-1 m
367 depth; Fig. 2D), accounting for about half of total water storage loss in the column. More
368 significant changes in water balance occur following talik onset, including more rapid drying in
369 shallow layers (~10% over 4 decades) and in the column (~16%), and a substantial increase in
370 sub-surface drainage, as discussed below.

371 The time evolution of soil vertical thermal and hydrological structure for the subset of grid cells
372 that form talik in the 2090s is shown in more detail in Fig. 3. Here, we have subtracted the
373 thermal and hydrological profiles in the 2040s to show relative change. The 4 decades prior to
374 talik onset are shown in Fig. 3A-D (2050s – 2080s), the decade of talik onset in Fig. 3E (2090s),
375 and the 4 decades following talik onset in Fig. 3F-I (2100s – 2130s). CLM4.5 represents the
376 process of soil thawing as passage of a “thaw front” in space and time through soil layers,
377 penetrating and warming colder, deeper layers, and bringing the frozen soil environment at
378 depth closer to thermodynamic equilibrium with the warming atmosphere. At 4 decades prior
379 to talik onset (Fig. 3A), our simulated thawed layer exhibits a tilted time-depth profile with
380 earlier thaw and longer thaw duration (~4-5 months) in the near surface (< 1 m) compared to
381 later thaw and reduced thaw duration (1-2 months) at maximum thaw depth (~ 2 m). In the 3
382 decades leading up to talik onset, we find gradual deepening of the thawed layer to 3-4 m and
383 penetration of thaw period into Jan-Feb.

384 Our simulations indicate an increased rate of heat transfer and thawing at depth following talik
385 onset, leading to rapid subsequent thawing, drying, and decrease in the thickness of the
386 seasonally frozen layer above talik (Fig. 3 E-I). This rapid thawing is depicted in Fig 2A as the
387 large jump in thaw volume, and in Fig. 2D as enhanced drying and drainage, with drying peaking
388 at 3.5-4.5 m depth. In our simulations, talik onset effectively pulls the “bath plug” that was the

- Deleted:
- Deleted: similar
- Deleted: (~0-1 m depth)
- Deleted: .
- Deleted: This does not significantly impact
- Deleted: as it is primarily a redistribution of water within
- Deleted: ; however,
- Deleted: there are
- Deleted: and decrease in volumetric soil moisture
- Deleted: , as

- Deleted: more pronounced tilting of the thawed layer with time and depth, with

401 ice filled pore space at depth, with year round ice-free conditions allowing soil water to
402 percolate and be diverted to sub-surface drainage (Lawrence et al., 2015). We note that
403 bedrock soil is not hydrologically active in CLM4.5, and thus the rate of thawing and drainage in
404 response to permafrost thaw may be overestimated in deeper CLM4.5 layers near bedrock due
405 to reduced heat capacity.

Deleted: underestimated

406 Our simulated pattern of phase lag for heat transfer to depth mimics observed thaw profiles in
407 N. America (Fig. 4), which are sensitive to latitude and ecosystem, but with more “vertical”
408 time-depth tilt in CLM4.5 compared to observations. Borehole data shows shallow (~0.5 m) and
409 seasonally short (~3-4 months from Jun-Sep) thaw at the northernmost tundra site in the
410 Canadian Archipelago (Fig. 4A; 76°N, Mould Bay), shallow but longer thaw (5 months from Jun-
411 Oct) moving slightly south to North Slope Alaska (Fig. 4B; 71.3°N, Barrow), and deep (~3 m) and
412 seasonally long (May-Feb) thaw at the low latitude continental boreal site in southeast Alaska
413 (Fig. 4C; 62.4°N, Gakona). CLM4.5 shows reduced depth and seasonal duration of thaw when
414 sampled at these specific geographical points, although the north-south gradient of increasing
415 thaw moving south is preserved (Fig. 4D-F). Given the challenging task of comparing point
416 locations with grid cell means, we also examine the mean behavior of CLM4.5 at locations
417 where soil temperature at depth is similar to that observed. Accounting for permafrost
418 temperature at 3 meters (by sampling all locations with $T_{\text{soil-3m}}$ within 0.5°C of the observed
419 temperature) better reproduces thaw depth, but with reduced seasonal duration throughout
420 the soil column (Fig. 4G-I). These results suggest the current ensemble CLM4.5 run
421 overestimates the rate of soil refreeze in early fall.

422 Based on the pattern of January and February thaw/freeze dynamics observed at Gakona in the
423 2010s and the time lag of 1-3 decades from this occurrence to talik onset in our simulations, we
424 project that Gakona will form talik as early as the 2020s, assuming the atmosphere continues to
425 warm as prescribed in CLM4.5. Talik onset in CLM4.5 is variable in the region containing Gakona
426 (southeast Alaska), with earliest onset by mid-century (~2050s, Fig. 1A); however, our
427 comparison to borehole temperatures at Gakona suggests that simulated thaw rates in
428 southwest Alaska and across pan-Arctic regions with similar permafrost temperatures are
429 underestimated, and that earliest onset may occur sooner than predicted. Overall, we find that

Deleted: is region

Deleted: observations

Deleted: this region

Deleted: for

Deleted:

436 simulated patterns of permafrost thermal state change are consistent with available
437 observations, but that the exact thaw rates are uncertain. Although there are many possible
438 explanations for differences in observed and simulated thaw rates, we can attribute high
439 observed thaw rates in part to a combination of (1) relatively dry upper soil at Gakona and
440 Mould Bay, and (2) low surface organic layer and high conductivity of the Barrow and Mould
441 Bay soils. We keep these uncertainties in mind as we examine patterns of change and talik
442 formation simulated into 2300.

443 3.2 Evaluation of Simulated Thaw Rates and Talik Onset Against Siberian Borehole Data

444 The Siberian borehole locations have similar permafrost extent (> 50%) to the North American
445 locations according to the Circumpolar Permafrost Map (Brown, 2001) and similar mean annual
446 air temperature (~ -13.6°C) in the 2000s according to CLM4.5. However, air temperature is
447 more seasonal in Siberia, including colder winters (4°C colder) and warmer summers (6°C
448 warmer). Spring thaw for the Siberian sites occurs two weeks earlier on average than for the
449 North American sites in the 2000s, but follows the same pattern of later thaw date moving
450 north along the borehole transect.

451 Next we examine thaw trends observed from borehole soil temperature data in Siberia in the
452 20th century and evaluate patterns of CLM4.5 projected trends in the 21st century. We note
453 several caveats in these comparisons: (1) model simulations are based on only one realization
454 (i.e., model ensemble member) of historic and future warming and projected permafrost thaw,
455 (2) availability and access of long term records in Siberia is limited, and (3) there is significant
456 variability in space and time in simulated and observed thaw rates, making direct comparisons
457 challenging. These comparisons thus serve primarily as a first benchmark for future model
458 analysis and development.

459 We focus first on site-specific long-term historical trends by analyzing the 6 Siberian borehole
460 sites which recorded at least 5 years of temperature data spanning multiple decades: Drughina,
461 Lensk, Macha, Oimyakon, Uchur, and Chaingda. Records at these locations show an increase in
462 thaw volume with an average positive trend of 0.19 m months yr⁻¹ from 1955 – 1990 (Table 1,
463 Fig 5). All sites except Drughina show positive trends, with larger trends in southern locations,

Deleted: 5

Deleted: 5

Deleted: decrease

Deleted: negative

468 ranging from 0.51 m months yr⁻¹ from 1957-1990 at Chaingda in southern Siberia, to a
469 statistically insignificant trend of -0.083 months yr⁻¹ from 1969-1990 at Druzhina in
470 northeastern Siberia, suggesting a more or less constant thermal state at this site. Further
471 examination indicates that active layer thickness at Druzhina actually decreased to 0.8 meters
472 from 1989-1990 compared to 1.2 meters in the 1970s (data not shown). Druzhina also shows
473 smaller average thaw volume magnitude compared to other sites, consistent with shallower
474 thaw. Together, these findings indicate that active layer thickness is decreasing at Druzhina.

475 There is considerable spatial variability in thaw volume and trends, but in general thaw trends
476 increase from west (0.18 m months yr⁻¹) to east (0.51 m months yr⁻¹). Talik forms at several
477 sites, at different times between 1957 and 1990 (shown by vertical dashed lines on Fig. 5), with
478 earlier talik to the west consistent with higher mean initial thaw volumes. We acknowledge the
479 difficulty in identifying talik onset due to discontinuities in the dataset and limited vertical
480 information; however, we note that the 15-30 year gap between talik formation in the western
481 site cluster vs Chaingda 15° east is geographically consistent with model simulations of later
482 talik formation in eastern Siberia in the 21st century (Fig. 1B) and thus may represent a gradual
483 expansion of warming into the east. In general, permafrost appears to be degrading more
484 rapidly at the southern locations compared to the northern location.

485 We recompute observed thaw trends at regional clusters using combined records at the 2 sites
486 in northern Siberia (blue), 6 sites in southwest Siberia (yellow), and 1 site in southeast Siberia
487 (brown, Table 1) and compare to historical and projected thaw volume trends in CLM4.5 (Fig.
488 6). Northern locations show a consistent pattern of low thaw volume (< 10 m month yr⁻¹) and
489 negligible thaw trend (~0 m month yr⁻¹) in the historical simulations and observed record from
490 1950-2000. Thaw projections in northern Siberia indicate an unchanged trend and continued
491 stability of permafrost through the early 22st century, followed by a shift to accelerated soil
492 thaw in the early 2120, marked by onset of deep soil thaw late in the cold season.

493 Southern locations show a systematic underestimate of mean thaw volume (< 20 m month yr⁻¹)
494 compared to observations (~40 m month yr⁻¹) from 1950-2000. Simulated thaw trends are
495 negligible prior to 2000, but these likely represent an underestimate given low simulated thaw
496 volumes and significant positive observed trends in both southeast and southwest Siberia

Deleted: (layer thickness increases exponentially with depth along the Siberian transect)

Deleted: The average trend at 3 long term stations in southwest Siberia clustered at [60.7°N, 114.9°E] is -0.18 m months yr⁻¹, which is a factor of 3 weaker compared to Chaingda station (thaw rate = 0.51 m months yr⁻¹; p < 0.05) slightly south and 15° to the east (59.0°N 130.6°E). Each of these permafrost sites exhibits talik at various times between 1957 and 1990 (vertical dashed line), with earlier talik onset to the west (1957 at Lensk, 1970 at Macha, 1974 at Uchur) and later talik onset to the east (1989 at Chaingda). The presence of talik reflects an increase in the depth and duration of thaw late into the cold season, rather than a physical decrease in soil thaw as appears to be the case at Druzhina.

Formatted: Highlight

Deleted: A

Deleted: We recompute observed thaw trends at regional clusters using combined records at the 2 sites in northern Siberia, 6 sites in southwest Siberia, and 1 site in southeast Siberia (Table 1) and compare these to thaw projections in CLM4.5 (Fig. 6). The simulated trend in thaw volume shows a change in sign at northern locations (blue), acceleration of thaw at southwest sites (orange), and reduction of thaw at the southeast sites (brown). Despite the change in sign in northern Siberia representing a possible shift from net permafrost accretion to net thaw in the mid 21st century, thaw projections indicate continued stability of permafrost through the early 22st century. Our simulations show a shift to accelerated soil thaw beginning in the early 2080s, marked by onset of deep soil thaw late in the cold season (January, denoted by cyan circle).

Formatted: Highlight

528 beginning in the 1960s following talik onset (Fig. 5). Thaw projections show more abrupt shifts
529 in thaw volume in the early 21st century in the southwest (~2025) and in the mid 21st century
530 (~2050) in the southeast. The strong discrepancy between observed and simulated thaw and
531 talik onset in southern Siberia warrants close monitoring and continued investigation of this
532 region through sustained borehole measurements and additional model realizations of
533 potential future warming.

534 3.3 Carbon Cycle Responses to Changing Ground Thermal Regime

535 Fig. 7A plots the decade in which NHL ecosystems are projected to transition to long-term C
536 sources over the next 3 centuries (2010-2300). A total of 6.8 million km² of land is projected to
537 transition, peaking in the late 21st century, with most regions transitioning prior to 2150 (4.8
538 million km² or 70%, Fig. 7B, solid black). C source transitions which occur in the permafrost
539 zone, accounting for 6.2 million km² of land (91% of all C source transitions), also form talik at
540 some time from 2006-2300 (Fig. 7C). The remaining C source transitions (0.6 million km², or 9%)
541 occur outside the permafrost zone, primarily in eastern Europe.

542 Net C emissions from C source transition regions are a substantial fraction of the total NHL C
543 budget over the next 3 centuries (Fig. 8). The cumulative pan-Arctic C source increases slowly
544 over the 21st century, reaching 10 Pg C by 2100 with RCP8.5 warming, then increases more
545 rapidly to 70 Pg C by 2200 and 120 Pg C by 2300 with sustained ECP8.5 warming (Fig. 8, solid
546 black). This pan-Arctic source represents 86% of cumulative emissions in 2300 from the larger
547 NHL talik region (crosses), despite the 2 fold smaller land area, and exceeds the talik region
548 through 2200 due to mitigating widespread vegetation C gains (Koven et al., 2015). Cumulative
549 emissions over all NHL land regions (diamonds, > 55N) increase in similar fashion to the talik
550 region, reaching 120 Pg C by 2200 and 220 by 2300, with no sign of slowing.

551 The geographic pattern of C sink-to-source transition date is reversed compared to that of talik
552 formation, with earlier transitions at higher latitudes (the processes driving these patterns are
553 discussed in detail below). Overall, the lag relationship between talik onset and C source
554 transition exhibits a tri-modal distribution (Fig. 7D), with peaks at negative time lag (C source
555 leads talik onset, Median Lag = -5 to -6 decades), neutral time lag (C source synchronized with

Deleted: in the southern locations

Deleted: the

Deleted: magnitude of thaw volume

Deleted: . Projected thaw volume is generally on track with borehole data at the western locations, but deviate strongly from the single record at Chaingda. Despite observed talik onset as early as the 1970s in the southwest (Macha and Uchar) and late 1980s in the southeast (Chaingda), simulated talik onset is not projected to occur until the 2030s

Deleted: at the western sites (orange)

Deleted: the 2080s

Formatted: Superscript

Deleted: at the eastern sites (brown)

Formatted: Font:Not Italic

Deleted: At first, pan-Arctic C fluxes remain neutral on average over the early- to mid- 21st century (2010-2070) as increasing productivity and C sinks dominate large scale C balance (Fig. 7B, purple). The spatially integrated pan-Arctic C balance increasingly favors net C source dominance over the next 100 years, peaking at 0.7-0.8 Pg C in the mid- to late- 22nd century, followed by gradual decline to 0.5 Pg C by 2300. The cumulative C source over the entire simulated period (2010-2300) is 11.6 Pg C. ... IT

Deleted: regions (6.2 million km² of land, or 91%) identified as a C source also form

Deleted: talik at some time during

Deleted: the simulation

Deleted: .

Formatted: Not Highlight

Deleted: However, t

585 talik onset; Median Lag = -2 to 1 decade), and positive time lag (C source lags talik; Median Lag
586 = 12 decades; red shading in Fig. 7C), each of which is associated with a distinct process based
587 on soil C and fire emissions as discussed below. Roughly half of these regions (3.2 million km²)
588 show neutral or positive time lag (lag ≥ 0). This pattern, characteristic of the sub-Arctic (< 65°N),
589 represents the vast majority of C source transitions after 2150 (Fig. 7B, dotted), but only
590 accounts for 17% of cumulative emissions (20 Pg C by 2300, Fig. 8, dotted). The remaining
591 regions (3.0 million km²) in the Arctic and high Arctic (> 65°N) show negative time lag and
592 account for most of late 21st century sources and cumulative emissions (95 Pg C by 2300, or
593 79%; Fig. 8, dashed). C sources in regions not identified as talik (0.63 million km²) either show
594 talik presence at the start of our simulation, or are projected to transition in the absence of
595 permafrost or in regions of severely degraded permafrost (Fig. 7C, dash dotted). This region
596 contributes only 5 Pg C (4%) of cumulative C emissions in 2300.

597 Here, we investigate biological and soil thermal processes driving these relationships, focusing
598 first on regions where C source transition leads talik onset (blue shading in Fig. 7C). In these
599 regions, thaw volume is low (< 50 m months yr⁻¹) and shows a weak relationship to NBP (NBP
600 decreases much faster than thaw volume) prior to C source onset (indicated by large green
601 circle in Fig. 9A). By the time thaw volume reaches 300 m months yr⁻¹ and talik formation
602 occurs, these regions are already very strong sources (NBP > 150 g C m⁻² yr⁻¹). This suggests that
603 C sources in these regions are not driven by respiration of old C from deep soil thaw, and thus
604 alternative explanations are needed.

605 Closer examination of thermal and moisture dynamics in shallow soils reveals three potential
606 indicators of C source transition: (1) seasonal duration of thaw, (2) depth of thaw, and (3) soil
607 drying. For example, vertical profiles of soil temperature and moisture (Fig. 10) in regions which
608 transition to C sources in the 2090s show deeper seasonal penetration of soil thaw, a jump in
609 active layer growth, and enhanced year round soil drying during the C source transition decade
610 (Fig. 10D). A broader analysis of soil thaw statistics over all regions and periods indicates that
611 most C source transitions (~2.3 million km², or 77% of land where C source leads talik) occur at
612 active layer depths below 3 m and thaw season penetration into November.

Deleted: (Fig. 7B, dashed)

Deleted: the

Deleted: increases

Formatted: Not Highlight

Deleted: 8

Deleted: 9

Deleted: 9

Deleted:

Deleted: are most common

Deleted: when active layers grow to 1-2 meter depth

Deleted: duration penetrates to Oct or Nov for the first time (Fig. 10)

624 Further examination of ecosystem biogeochemistry also shows high initial C stocks in these
625 regions (red shading in Fig. 7E). The median initial state of soil organic matter (SOM), 109 kg C
626 m^{-2} , is nearly a factor of 2 larger than the median value in regions where C source lags talik
627 onset (SOM = 59 kg C m^{-2}). These regions also show 40% less gross primary production (median
628 GPP = 755 vs 1296 g C $m^{-2} yr^{-1}$) and higher over saturation prior to C source onset (water filled
629 pore space at 0.5 m depth at 10, 5, and 2 decades prior = 0.63, 0.59, and 0.57 $mm^3 mm^{-3}$ for
630 cold permafrost, vs a near constant value of 0.57 $mm^3 mm^{-3}$ in warm permafrost). The total
631 area of land in which SOM exceeds 100 kg C m^{-2} represents 2/3 of all land where C sources lead
632 talik onset (2.0 million km^2), and peaks at a negative time lag of -5 to -6 decades (Fig. 7D, green
633 bars), which perfectly aligns with the peak distribution of negative time lags. Cumulative C
634 emissions from regions of SOM > 100 kg C m^{-2} are also 2/3 of total C emissions (80 Pg C; Fig 8,
635 green). These results indicate peat like conditions characterized by saturated soils, high C
636 stocks, and low annual productivity which allow low thaw volumes (active layer depth < 2 m
637 and peak thaw month of October, on average) and rapid soil drying to produce early C losses in
638 colder environments in the absence of talik.

639 In regions where C source transitions lag talik onset (red shading in Fig. 7C), NBP is strongly
640 sensitive to changes in thaw volume until C source onset occurs (Fig. 9B), and talik formation
641 occurs when these regions are weak sinks (NBP > 0 g C $m^{-2} yr^{-1}$). In general, C source onset
642 under high thaw volume indicates these regions are more sensitive to C emissions from deep
643 soil thaw. However, as noted above, neutral and positive time lags show a bimodal distribution
644 peaking near 0 and 15 decades, and thus additional explanations are needed. Further
645 examination shows high fire activity in these regions at the time of C source onset (red shading
646 in Fig. 7F). The regions where fire C emissions exceed 25 g C $m^{-2} yr^{-1}$, representing our threshold
647 for C source transition, are exclusively boreal ecosystems, account for 1/3 of all land with
648 negative lags (~ 1.1 million km^2), and align perfectly with the peak distribution of positive time
649 lags (Fig. 7D, red bars) and cumulative C emissions (20 Pg C in 2300, Fig. 8, red). NBP is less
650 sensitive to thaw volume in regions where fire dominates the C balance, which are strong C
651 sinks at talik onset (Fig. 9C), where soil C respiration is 13% less than non-fire regions (median
652 SOM-HR = 331 vs 382 g C $m^{-2} yr^{-1}$), and productivity is 25% more (median GPP = 1548 vs 1216 g

Deleted: 8

Deleted: <

Deleted: In general,

Deleted: C sources

Deleted: in

Deleted: 8

659 C m⁻² yr⁻¹). Fire regions are also 28% drier on average in the surface layer than non fire regions
660 (volumetric soil moisture = 0.28 vs 0.39 mm³ mm⁻³ in summer (May-Sep) in the upper 10 cm of
661 soil). These results suggest that soil thermal processes and talik formation are significant factors
662 driving C source transition in regions with reduced productivity, but fire activity, spurred by soil
663 drying, drives C source transition in higher productivity regions.

664 The decadal time lag between talik onset and C source transition is more normally distributed
665 in the remaining region, represented by the residual grey bars visible in Fig. 7D, which occurs
666 predominantly in cold northern permafrost in northwest Siberia where low SOM (< 100 Kg m⁻²)
667 and fire emission (< 25 g C m⁻² yr⁻¹) prevail. This region has a mean lag of 1 decade from talik
668 onset to C source, with high standard deviation of lags (± 8 decades) reflecting a skewed
669 distribution of GPP; low productivity in cold permafrost (GPP = 385 g C m⁻² yr⁻¹) increases the
670 likelihood that soil thaw will lead to C source transition prior to talik onset, and high
671 productivity in warm permafrost GPP = 1111 g C m⁻² yr⁻¹) increasing the likelihood of a
672 transition after talik onset. Cumulative C emissions from this region are on the low end (27 Pg C
673 by 2300; Fig. 8, blue) due to low soil C (SOM = 59 kg C m⁻²).

674 Independent of the presence of talik, a key effect of an increasing number of thaw months is an
675 increasing rate of respiration from soil C pools. Warming and CO₂ fertilization increase the rate
676 of photosynthetic C uptake, increasing soil respiration mainly from younger near-surface C
677 pools; whereas deeper thawing affects both young and old C pools, so that the depth of thaw
678 dictates the timing and dominant C age of the net respiration flux. Fig. 11 illustrates this with a
679 comparison of decadal respiration trends for SOM (SOMHR) and litter (LITHR) C pools for C
680 source transitions in the mid 21st century, for scenarios where C source leads talik onset (blue
681 line, cold permafrost) and lags talik (red lines, warm permafrost). Here, we examine combined
682 respiration (SOMHR+LITHR) and respiration difference (SOMHR-LITHR) from soil and litter C
683 pools.

684 GPP and combined respiration increase by ~15% per decade for each permafrost regime
685 surrounding the decade of C source transition with peak fluxes in the growing season (Fig. 11A
686 - D). Combined respiration in cold permafrost is systematically larger than in warm permafrost
687 in the growing season (May – Sep) and smaller in the cold season (Oct – Apr). In particular,

Deleted: . [2]

Deleted: 2

Deleted: total

Deleted: =

Deleted: total

Deleted: show nearly linear

Deleted: s (~

Deleted:)

Deleted: 2

Deleted: Total

699 combined respiration is effectively zero for the late cold season (Jan – Apr) in cold permafrost
700 and significantly positive in warm permafrost over the same period. The respiration difference
701 also increases surrounding the C source transition (Fig. 11 E - F), but with 2 key differences from
702 combined respiration: (1) the decadal increase is exponential, starting from a value near zero
703 just 3 decades prior to C source transition, and (2) peak respiration difference occurs in late
704 summer and early fall. Because litter respiration in the model is mainly drawing from C pools
705 with short turnover times, the litter respiration flux equilibrates rapidly to changes in
706 productivity and thus its change primarily reflects changes to inputs rather than decomposition
707 rates. Conversely, soil C pools, which have much longer turnover times, equilibrate much more
708 slowly to the productivity changes and thus primarily reflect changes to the turnover times.

709 The trend in the respiration difference in warm and cold permafrost, which increase by similar
710 amounts ($\sim 100 \text{ g C m}^{-2} \text{ yr}^{-1}$), thus reflects an increasing dominance of respiration from younger
711 and older soil C pools, respectively. These trends are identical to the corresponding NBP trends,
712 which decrease by $100 \text{ g C m}^{-2} \text{ yr}^{-1}$ over the same period from neutral to net source (Fig. 11 G –
713 H), such that the differences between GPP and respiration driving the NBP trends are explained
714 almost entirely by the increasing fraction of soil vs litter respiration. Furthermore, warm
715 permafrost shows sustained dominance of soil respiration during the entire cold season. These
716 results are consistent with an increasing thaw effect on C budgets during C source transitions,
717 but where shallow thaw of young soil C dominates in cold permafrost, and where talik
718 formation and deep thaw of old soil C dominate warm permafrost.

719 These results suggest that where talik forms, soil respiration increases throughout the year as
720 talik and perennial thaw mobilize deeper old soil C to respiration. In the absence of talik in
721 colder environments, soil respiration increases primarily in the non-frozen season due to
722 increased availability of thawed shallow soil C. The lower GPP in colder regions suggests that
723 increased availability of substrate for respiration due to plant growth and soil C accumulation
724 has less impact on C source transition in our simulations than soil thaw dynamics and the initial
725 state of soil C. Thus, cold permafrost locations become C sources due only to thaw-season
726 dynamics while warmer permafrost locations transition to C sources due largely to changes in
727 cold season dynamics.

Deleted: total

Deleted: 2

Deleted: total

Deleted: /

Deleted: The trend in soil vs litter respiration explains almost the entire trend in net ecosystem C balance from neutral to net source (Fig. 12 G – H)

Deleted: .

Formatted: Font:(Default) Times, Font color: Auto

Deleted: NF

737

738 **4 Discussion**

739 Talik formation is widespread in our simulations, affecting [half of all Northern High Latitude](#)
740 [\(NHL\) land \(~14.5 million km²\) from 2010 through 2300](#). Simulations of the vertical thermal
741 structure of soil thaw leading to talik in CLM4.5 qualitatively reproduce deep soil temperature
742 data from borehole measurements in Siberia and western North America, although rates of
743 thaw at these and similar permafrost locations are underestimated. Space-for-time
744 comparisons along the north-south borehole transect in Alaska and the Canadian Archipelago
745 show a pattern of deepening and seasonal expansion of thaw moving from the coldest location
746 of the transect in northern Canada (Mould Bay) to the warmest location in southeast Alaska
747 (Gakona). Gakona shows the characteristic late cold season thaw penetration into February at
748 2-3 meters depth which in our simulations signals imminent talik onset (in the case of Gakona,
749 as soon as the 2020s). Likewise, projected soil thaw trends in east Siberia are in line with long
750 term borehole measurements along the East Siberian Transect, but the rate of talik formation
751 here is also underestimated.

752 These comparisons indicate stable permafrost conditions in the colder sites in Siberia and N.
753 America through the 21st century, where thaw is generally slow, seasonally short, and stable.
754 This suggests talik formation in the northern Arctic is decades to centuries away, but potentially
755 sooner than the early 22nd century as projected by the CLM4.5 simulation. Our analysis finds
756 more unstable permafrost conditions to the south, with observed talik in the late 20th century
757 although simulated talik is delayed until the early 21st century.

758 Due to the potential for early 21st century talik and discrepancy between observed and
759 simulated trends in warm permafrost, continued model investigation of factors controlling the
760 rate of soil thaw is critically needed. In particular, large scale drying as projected in CLM4.5 near
761 the surface (Lawrence et al., 2015) may be restricting heat penetration and active layer growth
762 in the growing season, especially in organic rich soils which have very low thermal conductivity
763 (O'Donnell et al., 2009; Lawrence et al., 2011; 2012). [Controlled experiments demonstrating the](#)
764 [sensitivity of talik to parameters that control soil drying such ice impedance or baseflow scalars](#)

- Deleted:
- Deleted: of
- Deleted: NHL land
- Deleted: in the 21st century

769 (e.g. Lawrence et al., 2015), and the effect of organic content and mineral soil texture
770 (Lawrence and Slater, 2008), could provide key insight on soil thermal dynamics in frozen or
771 partially frozen conditions. Other factors affecting soil hydrology and carbon cycling not
772 considered in our CLM4.5 simulations include high spatial resolution in discontinuous
773 permafrost, shifts in vegetation community, lateral flow representation, thermokarst activity
774 and other thaw-related changes to the ground surface, surface slope and aspect, soil
775 heterogeneity, and potentially several other factors (see Jorgenson and Osterkamp (2005) for
776 discussion of some of the many complexities to be considered).
777 Our simulations show increasing C emissions over time across the talik region (Fig. 1B), as
778 cumulative NBP becomes increasingly negative (NBP < 0 equals a net C source), reaching a net
779 source of 140 Pg C by 2300 (Fig. 8, crosses), consistent with previous estimates of net C balance
780 across the larger pan-Arctic region from CLM4.5 (~160 Pg C, Koven et al., 2015; Lawrence et al.,
781 2015). Ecosystems which transition from net C sinks to net C sources represent less than half
782 the total talik area (6.8 of 14.5 Million km², Fig. 7A), but account for most (~85%) of the
783 cumulative emissions, reaching 10 Pg C in 2100, 70 Pg C in 2200, and 120 Pg C by 2300 (Fig. 8,
784 solid black). Removing the effect of vegetation C gain (~20 Pg C in 2100 and 40 Pg C in 2200 and
785 2300 according Koven et al., 2015), we estimate a cumulative permafrost emission for C source
786 transition regions of 30 Pg C in 2100, 110 Pg C in 2200, and 160 Pg C in 2300. These numbers
787 are on the low end but consistent with estimates of permafrost C emissions summarized by
788 Schuur et al. (2015), which range from 37-174 Pg C by 2100 and 100-400 Pg C by 2300.
789 About half of this region (3.2 million km²) shows a pattern of accelerated soil C respiration
790 following talik onset, which shifts the surface C balance of photosynthetic uptake and litter
791 respiration from net C sinks to long term net sources totaling 20 Pg C by 2300. The pattern of C
792 source transition following talik formation is most evident in warm permafrost in the sub-Arctic,
793 suggesting increased microbial decomposition with warming soils. We also find evidence of talik
794 driven soil drying near the surface associated with increased active layer thickness and higher
795 available water storage, which can lead to enhanced decomposition rates by causing soils to be
796 less frequently saturated/anoxic (Lawrence et al., 2015). At the same time, these regions show
797 high ecosystem productivity which increases roughly in proportion to respiration, and thus may.

Deleted: Experiments demonstrating the sensitivity of talik to soil drying within the active layer across soil hydrology schemes in previous (CLM4), current (CLM4.5), and newly available (CLM5) versions of CLM could provide key insight on soil thermal dynamics in frozen or partially frozen conditions.

Deleted: (

Deleted: ,

Formatted: Superscript

Deleted: Our simulations show robustly a

Deleted: across 3.2 million km² of NHL land

Deleted: appears to

809 be driven by combination of warming and increased nitrogen availability resulting from
810 permafrost thaw (Mack et al., 2004; Natali et al., 2012; Koven et al., 2015). As such, the
811 transition time to sustained net ecosystem C source is delayed by 1-2 centuries following talik
812 onset as productivity continues to outpace respiration as currently observed (Belshe et al.,
813 2013; Mack et al., 2004), with C balance transitions peaking in the mid- to late 22nd century. In
814 nearly 1/3 of these regions, an estimated 2 million km² of land, fires are a primary mechanism
815 triggering C source onset, rather than talik. Consequently, in regions of very high productivity,
816 talik appears to serve more as an indirect driver of long term C sources through accelerated soil
817 drying, rather than as a direct driver through accelerated respiration of deep soil C.

818 Our estimate of C emissions following talik onset (~20 Pg C) is low compared to the cumulative
819 emissions from all long term C source transitions (120 Pg C), but likely strongly underestimated.
820 Soil C is not permitted below 3.5 m in CLM4.5, or in most analogous models, such that potential
821 decomposition of the ~350 Pg soil organic C in deep permafrost (yedoma C, > 3 m) is not
822 accounted for (Hugelius et al., 2014; Jackson et al., 2017). This is significant for our simulations,
823 which show frequent talik formation and accelerating thaw volumes below 3 m (e.g., Fig. 3). We
824 therefore caution the reader in the interpretation of the timing and magnitude of permafrost C
825 emissions following talik onset in our simulations, which represent a lower bound of potential
826 emissions based on the current formulation of CLM4.5.

827 We identify an equally large region of land in the high Arctic, representing ~3.0 million km²,
828 which is projected to transition to a long term C source, much sooner than the sub-Arctic in the
829 absence of talik, and emit 5 times as much C by 2300 (~95 Pg C). This region, distributed across
830 northern Siberia and North America, resembles peatlands and is characterized by cold
831 permafrost, high soil C stocks and soil moisture, and low productivity. Thawing in this cold
832 northern permafrost is limited to young, shallow soils with significantly reduced contributions
833 from deeper, older C than warm permafrost, but with a factor of 2 higher C stocks. These C rich
834 soils become increasingly vulnerable to decomposition as they are exposed to increased
835 warming and drying as active layers deepen and persist deeper into the cold season. The
836 transition to long term C sources in this region peak is expected to peak between 2050 and

Deleted: s

Deleted: than the sub-Arctic and in the absence of talik

839 2100, nearly a century prior to talik driven sources in warm permafrost, and decades to
840 centuries prior to talik onset, which eventually amplifies C sources in this region.

841 These results have important implications for designing an Arctic monitoring system to
842 simultaneously detect changes in the soil thermal state and C state. In particular, C
843 observations should not be limited to warm permafrost regions of the sub-Arctic, since cold
844 northern permafrost regions are projected to become C sources much sooner and emit more C
845 even without forming talik. Our analysis of the seasonal dynamics and vertical structure of
846 permafrost thaw and soil C emissions provides a general strategy for concurrent observing
847 warm and cold permafrost based on time of year and depth of thaw.

848 Observing warm permafrost will require year round measurements of ground thermal state to
849 detect precursors to talik onset including thaw penetration at depth (~2-3 m) and late into the
850 cold season (~Jan-Feb), as well as sustained cold season C flux observations to detect changes in
851 C balance associated decomposition and respiration of deep, old soil C. Continued monitoring
852 of these depths will require sustained long term measurements from deep boreholes, and
853 increasing reliance on remote sensing technologies such as Electromagnetic Imaging (EMI). In
854 particular, EMI surveys along the continuous/discontinuous permafrost transition zones during
855 the cold season from November – March are likely to provide key thermal state diagnostics.
856 Systematic radiocarbon (¹⁴C) measurements, which can be used to partition respiration into
857 autotrophic and heterotrophic young and old soil components (Hicks Pries *et al.*, 2015), would
858 provide a valuable tool to help disentangle and track future C emissions from deep permafrost,
859 especially during the long cold season when talik enables the microbial decomposition of deep
860 old C and is the primary source of C emissions.

861 Observing cold permafrost in the high Arctic is both more urgent, due to earlier shifts in C
862 balance and larger emissions, and more complicated, due to challenging observing conditions
863 (remote, cold, and dark) and less detectable signals in thermal state (e.g., talik) and C age (e.g.,
864 depleted in radiocarbon) change. Our results suggest sustained observation of year round soil
865 thermal and hydrological profiles (soil drying; depth and duration of thaw at 1-2 meter depth)
866 using boreholes and EMI surveys, and cold season net CO₂ exchange (Sep – Oct) using
867 atmospheric CO₂ sensors and eddy covariance towers, can help detect changes in soil thaw and

868 soil vs litter respiration driving annual C balance changes. We also recommend an observing
869 network focused on regions rich in soil organic matter, where our simulations indicate
870 increased sensitivity of soil decomposition to warming.

871

872 5 Conclusion

873 Greening trends driven by high latitude warming and CO₂ fertilization have led to amplification
874 of the contemporary C cycle, characterized by increasing photosynthetic C uptake during the
875 short growing season and increasing respiration of recent labile soil C during the cold season
876 (Mack et al., 2004; Piao et al., 2008; Randerson et al., 1999; Graven et al., 2013; Forkel et al.,
877 2016; Wenzel et al., 2016; Webb et al., 2016). Our simulations of C-climate feedbacks with
878 interactive terrestrial biogeochemistry and soil thaw dynamics indicate this trend continues
879 mostly unabated in NHL ecosystems. However, sustained warming over the next 300 years
880 drives accelerated permafrost degradation and soil respiration, leading to widespread shifts in
881 the C balance of Arctic ecosystems toward long term net C source by the end of the 23rd
882 century. 6.8 million km² of land impacted in Siberia and North America will produce an
883 integrated C source of ~~90 Pg C by 2100 and 120 Pg C by 2200~~. Our projected permafrost C
884 feedback is comparable to the contemporary land use/land use change contribution to the
885 annual C cycle.

886 Our main results emphasize an increasingly important impact of NHL cold season warming on
887 earlier spring thaw, longer non-frozen seasons, and increased depth and seasonal duration of
888 soil thaw. Our simulations are consistent with soil thaw patterns observed from borehole time
889 series in Siberian and North American transects during the late 20th and early 21st centuries.
890 Patterns of deeper and longer thaw drive widespread talik, and exposes Arctic soils to increased
891 warming and drying, which accelerates decomposition and respiration of deep, old C, and shifts
892 ecosystem C balance to a state increasingly dominated by soil respiration.

893 The timing with which Arctic ecosystems transition to long term net C sources depends on a
894 number of factors including talik onset, vegetation productivity, permafrost temperature, soil
895 drying, and organic matter. The timing is most sensitive to talik onset in warm permafrost

Deleted: 11.6

Deleted: from 2010-2300

Deleted: , peaking at 0.7-0.8 Pg C yr⁻¹ in the mid- to late-
22nd century

Deleted: an emergence of

Deleted: processes driven by amplified winter warming,

Deleted: NF

903 regions in the sub-Arctic, which account for a total of 3.2 million km² of land, representing ~50%
904 of our simulated permafrost region. These regions are also the most productive, which can
905 delay the transition to net C source by decades or even centuries. As such, warm permafrost
906 regions typically do not transition to net C sources until the mid-22nd century.

907 The cold permafrost region in the northern Arctic, which accounts for an additional 3.0 million
908 km² of land, transitions to net C source in the late 21st century, much earlier than warm
909 permafrost and in the absence of talik. High decomposition rates, driven by warming and drying
910 of shallow, young C in organic rich soils, and low annual productivity make this region perhaps
911 the most vulnerable to C release and subject to further amplification with future talik onset.
912 This result is surprising given the region is dominated by tundra and underlain by deep, cold
913 permafrost that might be thought impervious to such changes.

914 Rather than thinking of the permafrost feedback as being primarily driven by a single coherent
915 geographic front driven by talik formation along the retreating boundary of the permafrost
916 zone, this analysis suggests multiple modes of permafrost thaw with a mosaic of processes
917 acting in different locations. C sink-to-source transitions are caused by active layer deepening in
918 some regions, talik-driven permafrost loss in others, fire-driven changes in other places, and
919 thaw-led hydrologic change in yet others. Our results reveal a complex interplay of amplified
920 contemporary and old C cycling that will require detailed monitoring of soil thermal properties
921 (cold season thaw depth, talik formation), soil organic matter content, soil C age profiles,
922 systematic CO₂ flux, and atmospheric ¹⁴CO₂ measurements to detect and attribute future C
923 sources. Further investigation of soil thermal properties and thaw patterns is required to
924 understand C balance shifts and potential further amplification of emissions from high northern
925 latitudes.

926

927 **Acknowledgements**

928 DML is supported by U.S. Department of Energy, Office of Biological and Environmental
929 Research grant DE-FC03-97ER62402/A0101. CDK is supported by the Director, Office of Science,
930 Office of Biological and Environmental Research of the US Department of Energy (DOE) under

Deleted: Active-layer deepening leads to C sink-to-source transitions in some regions

933 Contract DE-AC02-05CH11231 as part of their Regional and Global Climate Modeling (BGC-
934 Feedbacks SFA), and Terrestrial Ecosystem Science Programs (NGEE-Arctic), and used resources
935 of the National Energy Research Scientific Computing Center, also supported by the Office of
936 Science of the US Department of Energy, under Contract DE-AC02-05CH11231. National Center
937 for Atmospheric Research (NCAR) is sponsored by the National Science Foundation (NSF). The
938 CESM project is supported by the NSF and the Office of Science (BER) of the US Department of
939 Energy. Computing resources were provided by the Climate Simulation Laboratory at NCAR's
940 Computational and Information Systems Laboratory, sponsored by NSF and other agencies.
941 Some of the research described in this paper was performed for CARVE, an Earth Ventures (EV-
942 1) investigation, under contract with NASA. A portion of this research was carried out at JPL,
943 California Institute of Technology, under contract with NASA. © 2017. All rights reserved

944 **References**

- 945 Abbott, B. W. *et al.* (2016) 'Biomass offsets little or none of permafrost carbon release from
946 soils, streams, and wildfire: an expert assessment', *Environmental Research Letters*. IOP
947 Publishing, 11(3), p. 34014. doi: 10.1088/1748-9326/11/3/034014.
- 948 Atali, S. U. M. N. *et al.* (2014) 'Permafrost degradation stimulates carbon loss from
949 experimentally warmed tundra R eports R eports', 95(3), pp. 602–608.
- 950 Barichivich, J. *et al.* (2013) 'Large-scale variations in the vegetation growing season and annual
951 cycle of atmospheric CO₂ at high northern latitudes from 1950 to 2011', *Global Change
952 Biology*, 19(10), pp. 3167–3183. doi: 10.1111/gcb.12283.
- 953 Belshe, E. F., Schuur, E. A. G. and Bolker, B. M. (2013) 'Tundra ecosystems observed to be
954 CO₂ sources due to differential amplification of the carbon cycle', *Ecology Letters*, 16(10), pp.
955 1307–1315. doi: 10.1111/ele.12164.
- 956 Brown, J. *et al.* (2001) 'Circum-Arctic map of permafrost and ground-ice conditions, National
957 Snow and Ice Data Center/World Data Center for Glaciology, Boulder, CO', *Digital Media*,
958 available at: <http://nsidc.org>.
- 959 Christensen, J. H. *et al.* (2013) 'Climate Phenomena and their Relevance for Future Regional
960 Climate Change Supplementary Material', *Climate Change 2013: The Physical Science Basis.
961 Contribution of Working Group I to the Fifth Assessment Report of the Intergovernmental Panel
962 on Climate Change*, p. 62. doi: 10.1017/CBO9781107415324.028.
- 963 Commane, R. *et al.* (2017) 'Carbon dioxide sources from Alaska driven by increasing early
964 winter respiration from Arctic tundra', pp. 1–6. doi: 10.1073/pnas.1618567114.
- 965 Euskirchen, E. S. *et al.* (2012) 'Seasonal patterns of carbon dioxide and water fluxes in three
966 representative tundra ecosystems in northern Alaska', *Ecosphere*, 3(1), p. art4. doi:
967 10.1890/ES11-00202.1.

- 968 Fraser, R. H. *et al.* (2014) 'Warming-Induced Shrub Expansion and Lichen Decline in the
969 Western Canadian Arctic', *Ecosystems*, 17(7), pp. 1151–1168. doi: 10.1007/s10021-014-9783-3.
- 970 Goulden, M. L. (1998) 'Sensitivity of Boreal Forest Carbon Balance to Soil Thaw', *Science*,
971 279(5348), pp. 214–217. doi: 10.1126/science.279.5348.214.
- 972 Graven, H. D. *et al.* (2013) 'Enhanced seasonal exchange of CO₂ by northern ecosystems since
973 1960.', *Science (New York, N.Y.)*, 341(September), pp. 1085–9. doi: 10.1126/science.1239207.
- 974 Hicks Pries, C. E. *et al.* (2015) 'Decadal warming causes a consistent and persistent shift from
975 heterotrophic to autotrophic respiration in contrasting permafrost ecosystems', *Global Change
976 Biology*, 21(12), pp. 4508–4519. doi: 10.1111/gcb.13032.
- 977 Hugelius, G. *et al.* (2014) 'Estimated stocks of circumpolar permafrost carbon with quantified
978 uncertainty ranges and identified data gaps', *Biogeosciences*, 11(23), pp. 6573–6593. doi:
979 10.5194/bg-11-6573-2014.
- 980 Jackson, R. B. *et al.* (2017) 'The Ecology of Soil Carbon: Pools, Vulnerabilities, and Biotic and
981 Abiotic Controls', *Annual Review of Ecology, Evolution, and Systematics*, 48(1), p. annurev-
982 ecolsys-112414-054234. doi: 10.1146/annurev-ecolsys-112414-054234.
- 983 Jorgenson, M. T. and Osterkamp, T. E. (2005) 'Response of boreal ecosystems to varying modes
984 of permafrost degradation', *Canadian Journal of Forest Research*, 35(9), pp. 2100–2111. doi:
985 10.1139/x05-153.
- 986 Jorgenson, M. T. T. *et al.* (2010) 'Resilience and vulnerability of permafrost to climate
987 change This article is one of a selection of papers from The Dynamics of Change in Alaska's
988 Boreal Forests: Resilience and Vulnerability in Response to Climate Warming.', *Canadian
989 Journal of Forest Research*, 40(7), pp. 1219–1236. doi: 10.1139/X10-060.
- 990 Koven, C. *et al.* (2009) 'On the formation of high-latitude soil carbon stocks: Effects of
991 cryoturbation and insulation by organic matter in a land surface model', *Geophysical Research
992 Letters*, 36(21), pp. 1–5. doi: 10.1029/2009GL040150.
- 993 Koven, C. D. *et al.* (2011) 'Permafrost carbon-climate feedbacks accelerate global warming.',
994 *Proceedings of the National Academy of Sciences of the United States of America*, 108(36), pp.
995 14769–74. doi: 10.1073/pnas.1103910108.
- 996 Koven, C. D., Lawrence, D. M. and Riley, W. J. (2015) 'Permafrost carbon-climate feedback is
997 sensitive to deep soil carbon decomposability but not deep soil nitrogen dynamics.', *Proceedings
998 of the National Academy of Sciences of the United States of America*, 112(12), pp. 3752–7. doi:
999 10.1073/pnas.1415123112.
- 1000 Koven, C. D., Riley, W. J. and Stern, A. (2013) 'Analysis of permafrost thermal dynamics and
1001 response to climate change in the CMIP5 earth system models', *Journal of Climate*, 26(6), pp.
1002 1877–1900. doi: 10.1175/JCLI-D-12-00228.1.
- 1003 Lawrence, D. M. *et al.* (2008) 'Sensitivity of a model projection of near-surface permafrost
1004 degradation to soil column depth and representation of soil organic matter', *Journal of
1005 Geophysical Research: Earth Surface*, 113(2). doi: 10.1029/2007JF000883.
- 1006 Lawrence, D. M. *et al.* (2015) 'Permafrost thaw and resulting soil moisture changes regulate
1007 projected high-latitude CO₂ and CH₄ emissions', *Environmental Research Letters*. IOP
1008 Publishing, 10(9), p. 94011. doi: 10.1088/1748-9326/10/9/094011.

- 1009 Lawrence, D. M. and Slater, A. G. (2008) 'Incorporating organic soil into a global climate
1010 model', *Climate Dynamics*, 30(2–3), pp. 145–160. doi: 10.1007/s00382-007-0278-1.
- 1011 Lawrence, D. M., Slater, A. G. and Swenson, S. C. (2012) 'Simulation of present-day and future
1012 permafrost and seasonally frozen ground conditions in CCSM4', *Journal of Climate*, 25(7), pp.
1013 2207–2225. doi: 10.1175/JCLI-D-11-00334.1.
- 1014 Mack, M. C. *et al.* (2004) 'Ecosystem carbon storage in arctic tundra reduced by long-term
1015 nutrient fertilization', *Nature*, 431(September), pp. 440–3. doi: 10.1038/nature02887.
- 1016 McGuire, A. D. *et al.* (2012) 'An assessment of the carbon balance of Arctic tundra:
1017 Comparisons among observations, process models, and atmospheric inversions', *Biogeosciences*,
1018 9(8), pp. 3185–3204. doi: 10.5194/bg-9-3185-2012.
- 1019 Natali, S. M., Schuur, E. A. G. and Rubin, R. L. (2012) 'Increased plant productivity in Alaskan
1020 tundra as a result of experimental warming of soil and permafrost', *Journal of Ecology*, 100(2),
1021 pp. 488–498. doi: 10.1111/j.1365-2745.2011.01925.x.
- 1022 Oechel, W. C. *et al.* (2014) 'Annual patterns and budget of CO₂ flux in an Arctic tussock tundra
1023 ecosystem', *Journal of Geophysical Research: Biogeosciences*. Wiley Online Library, 119(3),
1024 pp. 323–339.
- 1025 Olefeldt, D. and Roulet, N. T. (2014) 'Permafrost conditions in peatlands regulate magnitude,
1026 timing, and chemical composition of catchment dissolved organic carbon export', *Global change
1027 biology*. Wiley Online Library, 20(10), pp. 3122–3136.
- 1028 Oleson, K. W. *et al.* (2013) 'NCAR/TN-503+STR NCAR Technical Note
1029 _____',
1030 (July).
- 1031 Parazoo, N. C. *et al.* (2016) 'Detecting regional patterns of changing CO₂ flux in
1032 Alaska', *Proceedings of the National Academy of Sciences of the United States of America*,
1033 113(28). doi: 10.1073/pnas.1601085113.
- 1034 Ping, C. L. *et al.* (2015) 'Permafrost soils and carbon cycling', *Soil*, 1(1), pp. 147–171. doi:
1035 10.5194/soil-1-147-2015.
- 1036 Riley, W. J. *et al.* (2011) 'Barriers to predicting changes in global terrestrial methane fluxes:
1037 Analyses using CLM4Me, a methane biogeochemistry model integrated in CESM',
1038 *Biogeosciences*, 8(7), pp. 1925–1953. doi: 10.5194/bg-8-1925-2011.
- 1039 Romanovsky, V. E. and Osterkamp, T. E. (2000) 'Effects of unfrozen water on heat and mass
1040 transport processes in the active layer and permafrost', *Permafrost and Periglacial Processes*.
1041 Wiley Online Library, 11(3), pp. 219–239.
- 1042 Schuur, E. A. G. *et al.* (2009) 'The effect of permafrost thaw on old carbon release and net
1043 carbon exchange from tundra', *Nature*. Nature Publishing Group, 459(7246), pp. 556–559. doi:
1044 10.1038/nature08031.
- 1045 Schuur, E. A. G. *et al.* (2015) 'Climate change and the permafrost carbon feedback', *Nature*,
1046 520(January 2016), pp. 171–179. doi: 10.1038/nature14338.
- 1047 Slater, A. G. and Lawrence, D. M. (2013) 'Diagnosing present and future permafrost from
1048 climate models', *Journal of Climate*. doi: 10.1175/JCLI-D-12-00341.1.

- 1049 Swenson, S. C., Lawrence, D. M. and Lee, H. (2012) 'Improved simulation of the terrestrial
1050 hydrological cycle in permafrost regions by the Community Land Model', *Journal of Advances*
1051 *in Modeling Earth Systems*, 4(8). doi: 10.1029/2012MS000165.
- 1052 Webb, E. E. *et al.* (2016) 'of Sustained Tundra Warming', pp. 249–265. doi:
1053 10.1002/2014JG002795.Received.
- 1054 Yi, S. *et al.* (2014) 'Freeze/thaw processes in complex permafrost landscapes of northern Siberia
1055 simulated using the TEM ecosystem model: Impact of thermokarst ponds and lakes',
1056 *Geoscientific Model Development*, 7(4), pp. 1671–1689. doi: 10.5194/gmd-7-1671-2014.
- 1057 Zhang, K. *et al.* (2011) 'Changing freeze-thaw seasons in northern high latitudes and associated
1058 influences on evapotranspiration', *Hydrological Processes*, 25(26), pp. 4142–4151. doi:
1059 10.1002/hyp.8350.

1060
|

Formatted: Space After: 6 pt

1061 **Tables**

1062 **Table 1:** Site information for long-term borehole temperature measurements along the East
 1063 Siberian Transect for the period 1957-1990. The 9 sites reported in this table, presented in a
 1064 north-to-south order, meet the criteria of at least one year of valid soil temperature data (≥ 10
 1065 months per layer, ≥ 55 months across 5 layers). Talik is observed in 4 of 9 sites, 2 of which is
 1066 observed in the first year of valid reported data. Site-specific thaw trends are provided for sites
 1067 with at least 6 years of valid data. Regional trends are calculated from all available data for 3
 1068 regional locations.

Site	Location	Date Range	Years with Valid Data	First Obs Talik	Site Trend (m mo yr ⁻¹)	Region	Regional Trend (m mo yr ⁻¹)
Drughina	145.0°E, 68.3°N	1969-1990	8	N/A	-0.083	N Siberia	-0.057
Ustmoma	143.1°E, 66.3°N	1973-1975	3	N/A	N/A		
Chumpuruck	114.9°E, 60.7°N	1981-1984	4	N/A	N/A	SW Siberia	0.019
Lensk	114.9°E, 60.7°N	1957-1990	11	1957	0.23		
Macha	114.9°E, 60.7°N	1970-1990	13	1970	0.070		
Oimyakon	114.9°E, 60.7°N	1966-1974	6	N/A	0.059		
Tongulakh	114.9°E, 60.7°N	1966-1966	1	N/A	N/A		
Uchur	114.9°E, 60.7°N	1966-1990	17	1974	0.24		
Chaingda	130.6°E, 59.0°N	1967-1990	8	1989	0.51	SE Siberia	0.51

1069

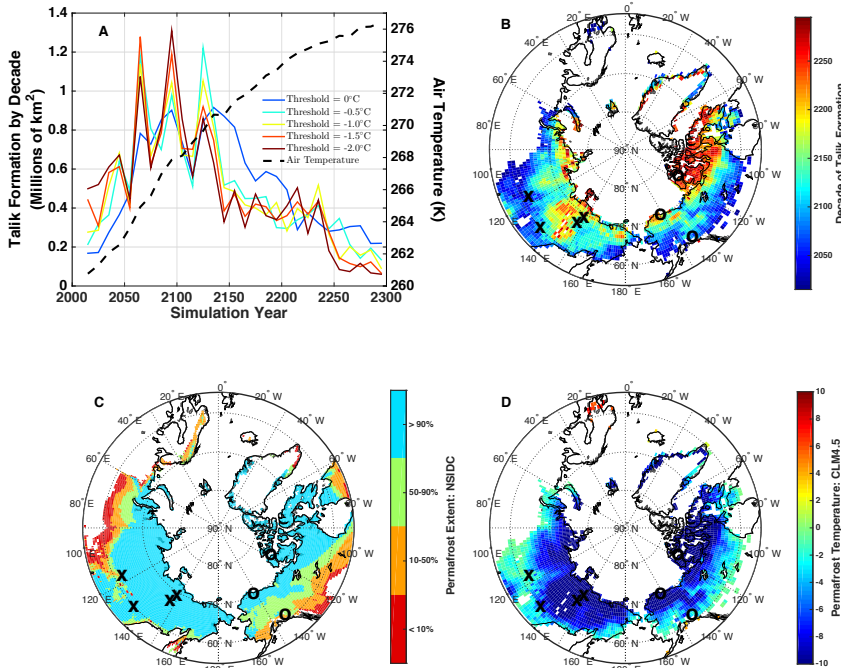
1070

1071 **Table 2:** Site information for borehole temperature measurements at 3 sites along a north-to-
 1072 south transect in North America for the period 2004-2012. Climatological soil thermal state
 1073 presented on a site-to-site basis Fig. 5 are based on all available valid monthly data for each
 1074 site, with valid data requiring at least 20 days of reported data for each layer. Layer of Deepest
 1075 Thaw represents the deepest layer in which mean soil temperature exceeds freezing ($> -0.5^{\circ}\text{C}$)
 1076 in at least 1 month. Month of Latest Thaw represents the latest month in which mean soil
 1077 temperature exceeds freezing. Here, we define May as the earliest possible month and April as
 1078 the latest possible month.

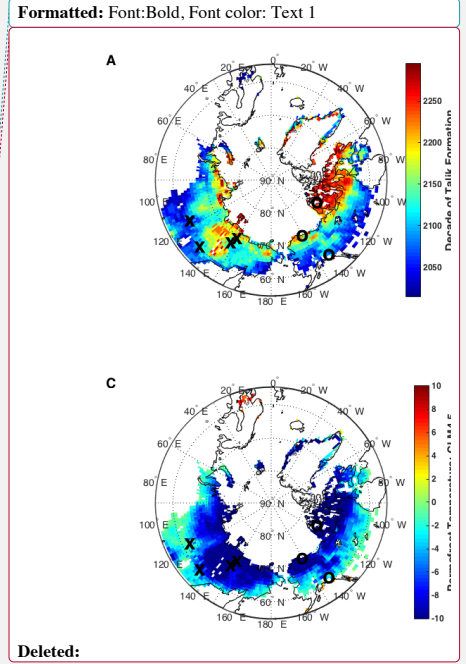
Site	Location	Date Range	<u>Soil Features:</u> <u>Surface</u> <u>organic layer /</u> <u>Soil Type</u>	Depth / Number of Layers	Layer of Deepest Thaw	Month of Latest Thaw
Mould Bay, Canada	119.0°W, 76.0°N	2004- 2012	<u>Low organic</u> <u>layer (~2 cm)/</u> <u>Sandy silt</u>	3 m / 36	0.69 m	September
Barrow2, Alaska	156.0°W, 71.3°N	2006- 2013	<u>Low organic</u> <u>layer / Sandy</u> <u>silt</u>	15 m / 63	0.58 m	October
Gakona1, Alaska	145.0°W, 62.4°N	2009- 2013	<u>Thick organic</u> <u>layer (50 cm) /</u> <u>Silty clay</u>	30 m / 35	2.5 m	February

1079

1080



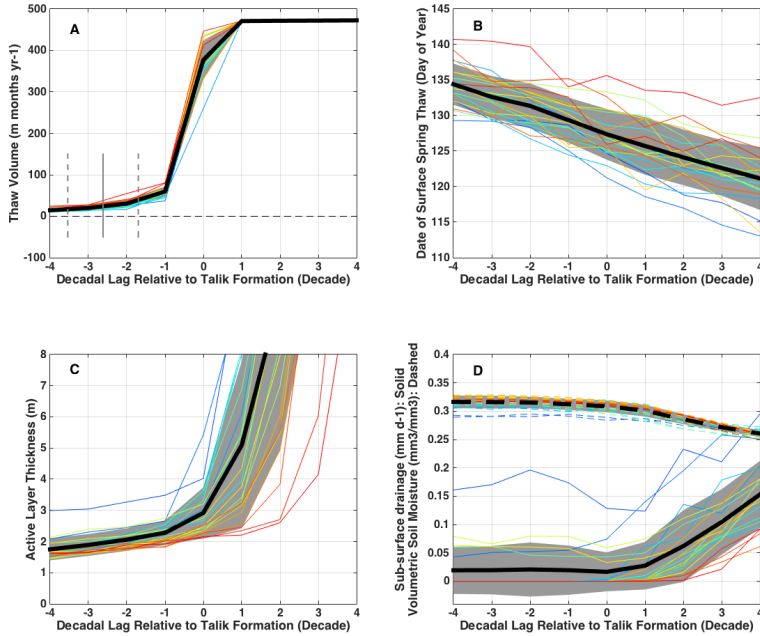
1082
 1083 **Figure 1.** Decade of projected talik formation and correlation to initial state of simulated
 1084 permafrost temperature and observed permafrost extent. (A) Time series and (B) map of the
 1085 simulated decade of talik formation are estimated from CLM4.5 as the first decade when the
 1086 mean temperature of a soil layer exceeds a freeze/thaw threshold of -0.5°C in every month.
 1087 Additional colors in A represent progression of talik onset for different freeze/thaw threshold.
 1088 (C) Initial permafrost temperature is defined as the annual mean soil temperature at 3 m depth
 1089 from 2006-2010. (D) Permafrost extent is taken from
 1090 (https://nsidc.org/data/docs/fgdc/ggd318_map_circumarctic/; Brown et al., 2001). Crosses in
 1091 A, C, D represent locations of Siberian borehole measurements along the East Siberian Transect
 1092 from 1955-1900 (Table 1). Circles represent locations of borehole measurements in Alaska and
 1093 Canada from 2002-2013 (Table 2). Dashed black line in A shows projected air temperature over



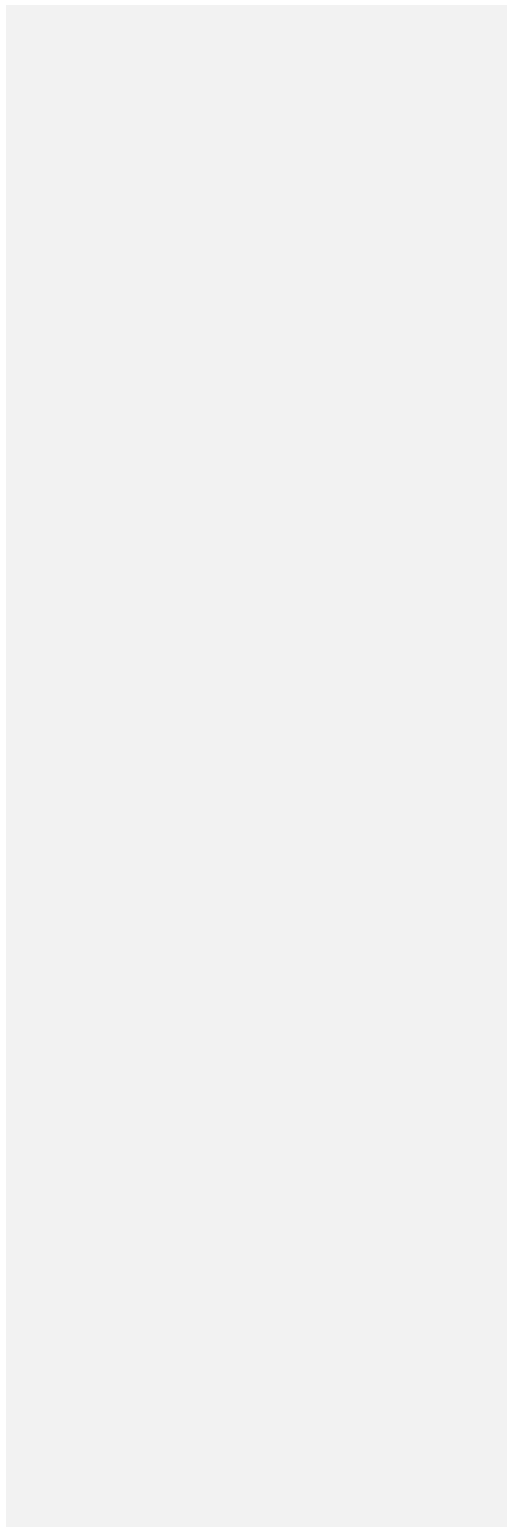
Deleted: Maps
 Deleted: time series

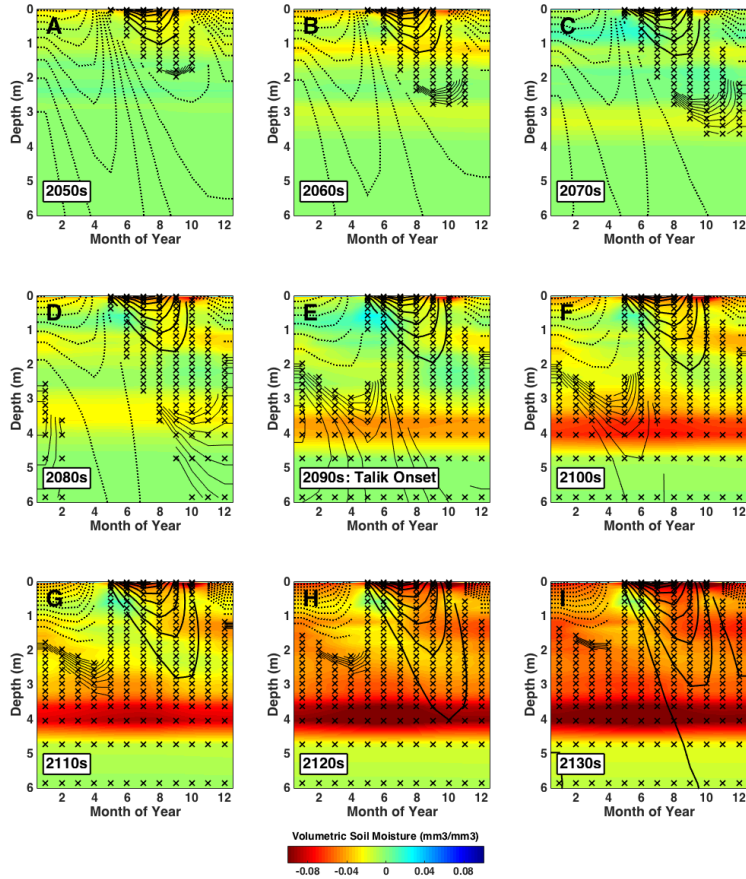
1097 the talik region. These results assume a Representative Pathway 8.5 warming scenario through
1098 2100 and an Extended Concentration Pathway 8.5 through 2300. We note that peak talik
1099 formation occurs around 2100.

Deleted: transition time



1103 **Figure 2.** Patterns showing the progression of soil thaw in the decades surrounding talik onset.
 1104 Individual lines represent averages across the subset of talik forming regions for each decade
 1105 from the 2050s (darkest red) to the 2250s (darkest blue). (A) Integrated soil thaw volume,
 1106 where the vertical solid line represents the mean timing of initial thaw at depth and late into
 1107 the cold season (Jan-Apr). Note that the upper limit to the thaw volume metric in (A) is an
 1108 artifact of the arbitrary maximum soil depth of 45.1m in CLM4.5. Other panels show (B) Date of
 1109 spring surface thaw in the uppermost layer, (C) annual maximum active layer thickness, and (D)
 1110 annual sub-surface drainage (solid) and volumetric soil moisture averaged over the soil column
 1111 (dashed) and. Grey shaded areas show the standard deviation of results for individual talik
 1112 formation decades. Mean behavior exhibits a characteristic pattern: gradual increase in thaw
 1113 volume and active layer depth prior to talik onset, abrupt shift in thaw volume, active layer
 1114 depth, followed by stabilization to constant thaw volume as soil drying and sub-surface
 1115 drainage increases.
 1116

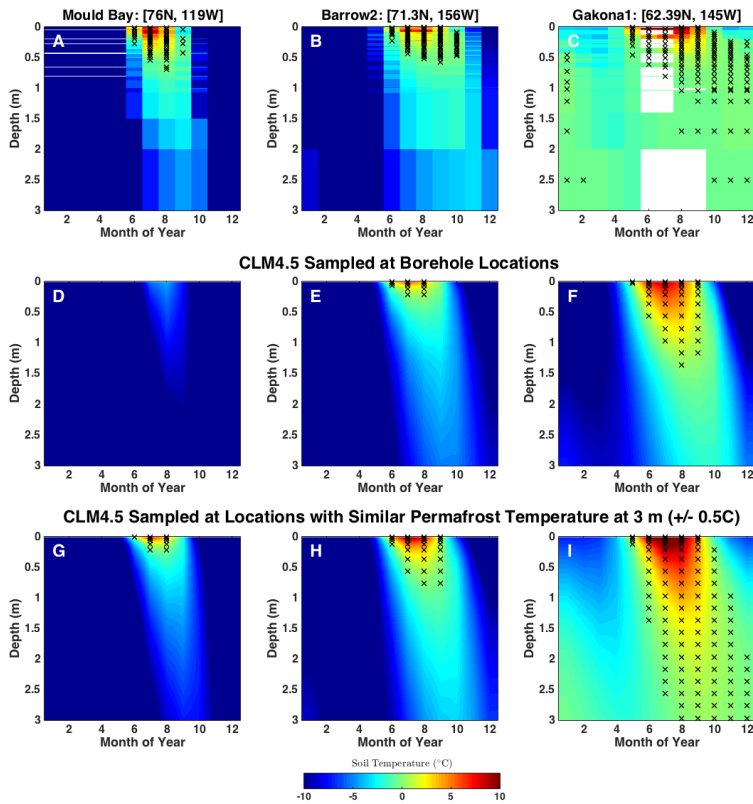




1120

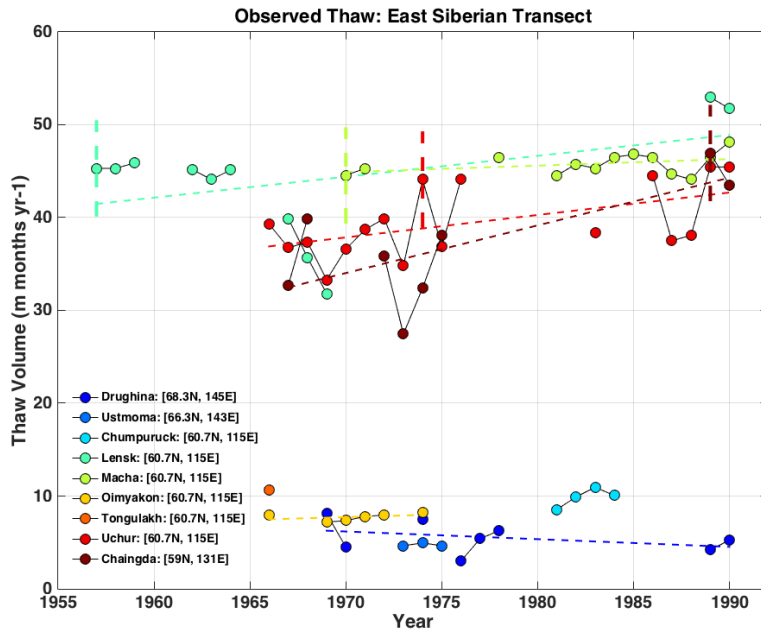
1121 **Figure 3.** Evolution of simulated decadal thermal and hydrological state as functions of month
 1122 and depth averaged across talik forming regions in the 2090s. Each panel presents decadal
 1123 average seasonal profiles in the decades surrounding talik onset from the 2050s (A) to the
 1124 2130s (I). Contours are soil temperature in 0.5°C intervals, with solid (dashed) lines denoting
 1125 temperature above (below) a freeze/thaw threshold of -0.5°C. Stars indicate “thaw” months
 1126 where soil temperature exceeds -0.5°C. Color shading is volumetric soil moisture anomalies
 1127 relative to the 2040s, where red indicates drying. Note that soil depth on y-axis is plotted on a

1128 non-linear scale. The soil thaw profile exhibits a shift from predominantly frozen and wet to
1129 perpetually thawed and drying conditions at depth while remaining seasonally frozen near the
1130 surface.
1131



1132

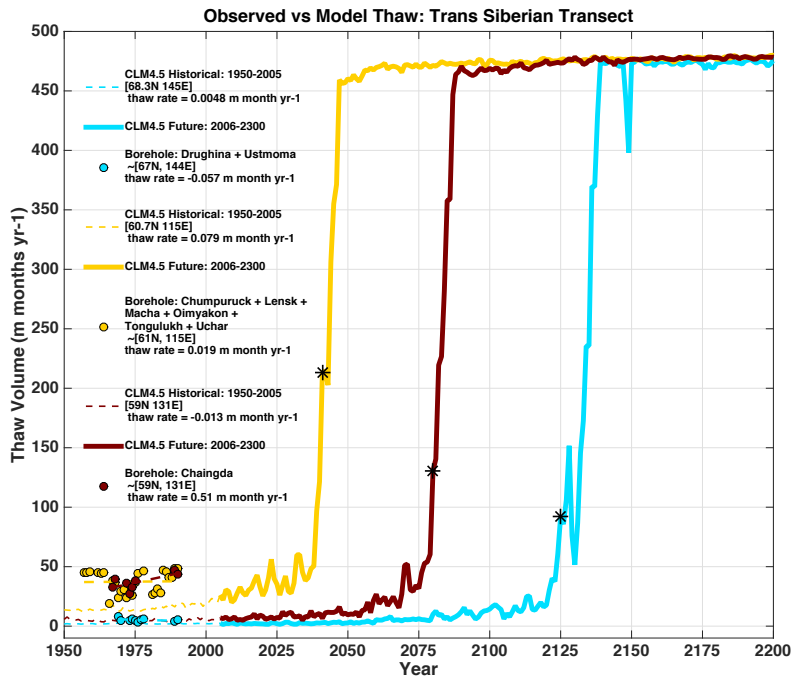
1133 **Figure 4.** Observed and simulated early 21st century soil thermal state as a function of month
 1134 and depth for the North American Transect boreholes (black circles, Fig. 1). Top Row: Observed
 1135 multi-year means for Mould Bay, Canada (2004-2012), Barrow, Alaska (2006-2013), and
 1136 Gakona, Alaska (2009-2013). The color scale shows the mean temperature and the stars mark
 1137 the months when each layer is thawed ($T > -0.5^{\circ}\text{C}$). Simulated soil thermal state from 2006-
 1138 2010 for borehole locations (Middle Row) and regions with 3 m permafrost temperature within
 1139 0.5°C of observed (Bottom Row) show similar north-to-south spatial gradient to observations,
 1140 especially for similar permafrost temperature. Note that the thaw state at Gakona, Alaska
 1141 persists at depths of 1-3 m into the deep cold season (Jan-Feb), perhaps signaling the threshold
 1142 for rapid talik formation (see Fig. 3D).



1144

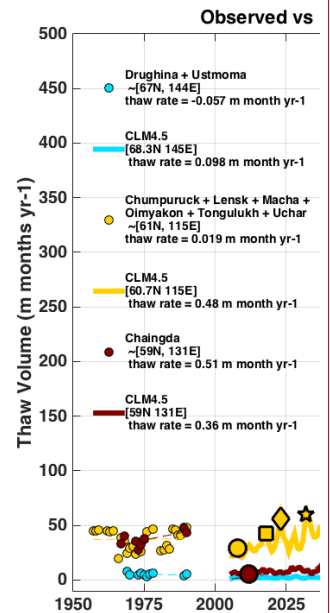
1145 **Figure 5.** Soil thaw observation time series from borehole measurements of soil temperature at
 1146 sites along the East Siberian Transect over various periods from 1957 – 1990. Site coordinates
 1147 are provided in the legend and plotted as crosses on the map provided in Fig. 1. Thaw trends
 1148 are derived from estimates of thawed volume over a depth of 3.2 m for sites with > 5 years of
 1149 data over multiple decades: Drughina, Lensk, Macha, Uchur, and Chaingda. Trend values are
 1150 reported in Table 1. Vertical dashed lines mark the onset of talik formation at Lensk (1957),
 1151 Macha (1970), Uchur (1974), and Chaingda (1989). Sites in southern Siberia show significant
 1152 negative thaw volume trends over the 20th century, representing net increases in soil thaw. The
 1153 trend at Drughina is not statistically significant, indicating that soil thaw is unchanged in
 1154 northern Siberia.

1155



1156
 1157 **Figure 6.** Comparison of observed soil thaw to historical and future simulations at sites along
 1158 the East Siberian Transect (crosses in Fig. 1). Observed thaw (filled circles) from 1955-1990 is
 1159 based on soil thaw data in Fig. 5 and on the inter-site average at 3 locations: northern Siberia
 1160 (blue), southwest Siberia (yellow), and southeast Siberia (brown). Simulated thaw from 1950-
 1161 2200 is derived from CLM4.5 and sampled at the nearest grid cell of 3 above locations. Asterisks
 1162 show simulated talik onset. Observed and simulated thaw trends are derived from soil thaw
 1163 volume, and estimated over the same period 1955-1990. We note a key discrepancy between
 1164 observed and simulated thaw volume: Simulated thaw volume is integrated over depths from
 1165 0-40 meters; observed thaw volume is integrated from 0-3.6 meters. The effect of this selection
 1166 bias is a potential low bias in observed thaw volume. In general, soil thaw is projected to remain
 1167 stable in northern Siberia but become increasingly unstable in southern Siberia.

Formatted: Font:Bold, Font color: Text 1



Deleted:

Deleted: 20th century

Deleted: (markers)

Deleted: and

Deleted: 21st century projected (solid lines)

Deleted: soil thaw

Deleted: orange

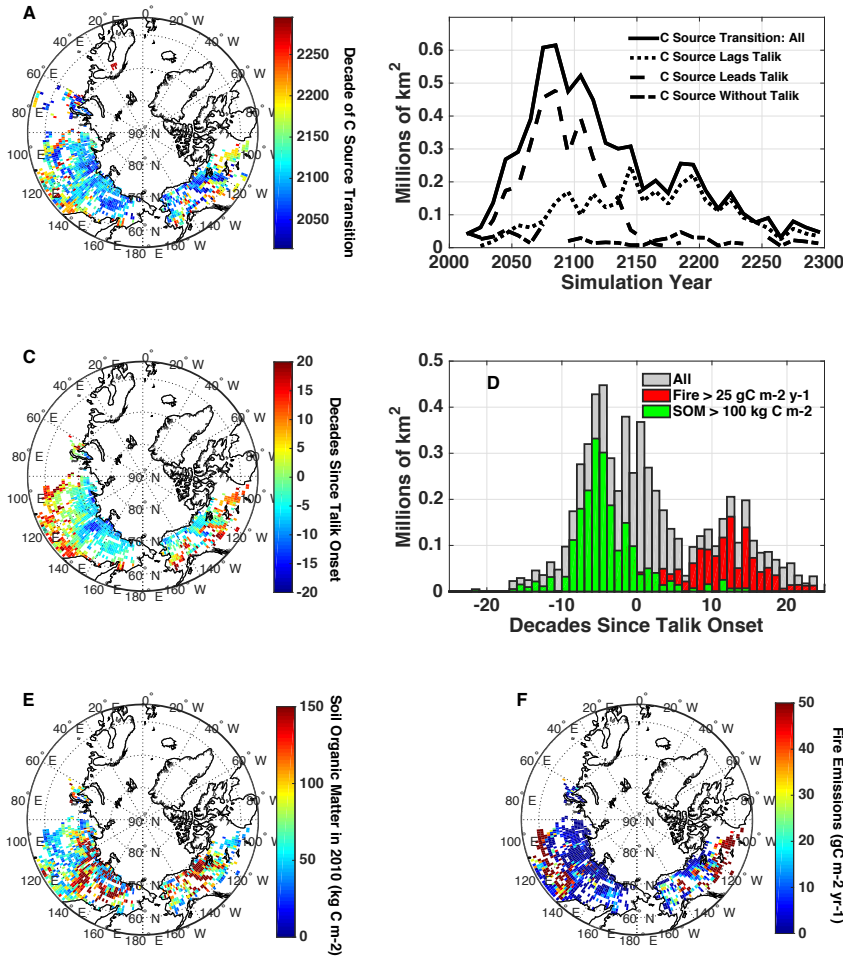
Deleted: 2006

Deleted: Markers represent thresholds for thaw onset in January (circle), February (square), March (diamond), April (star), and

Deleted: (asterisk)

Deleted: Thaw

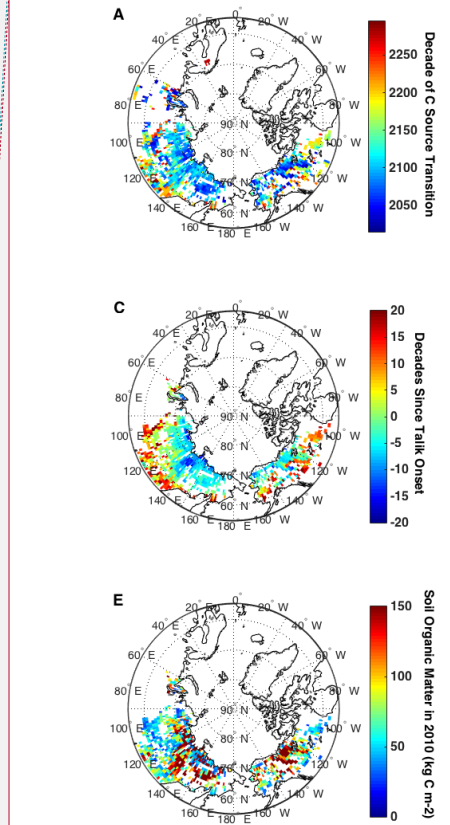
Deleted: estimates of



1183

1184 **Figure 7.** Projected decade when permafrost regions shift to long-term C sources over the
 1185 period 2010-2300, and relation to talik onset, soil C, and fire emissions. (A) Map of the decade
 1186 of transition to C source, reflected in the color code, showing earlier transitions in cold northern
 1187 permafrost. (B) The area of land that transitions peaks in the late 21st century, and is driven by
 1188 regions where the C source leads talik onset (dashed), (C) The decadal time lag from talik onset

Formatted: Font:Bold, Font color: Text 1

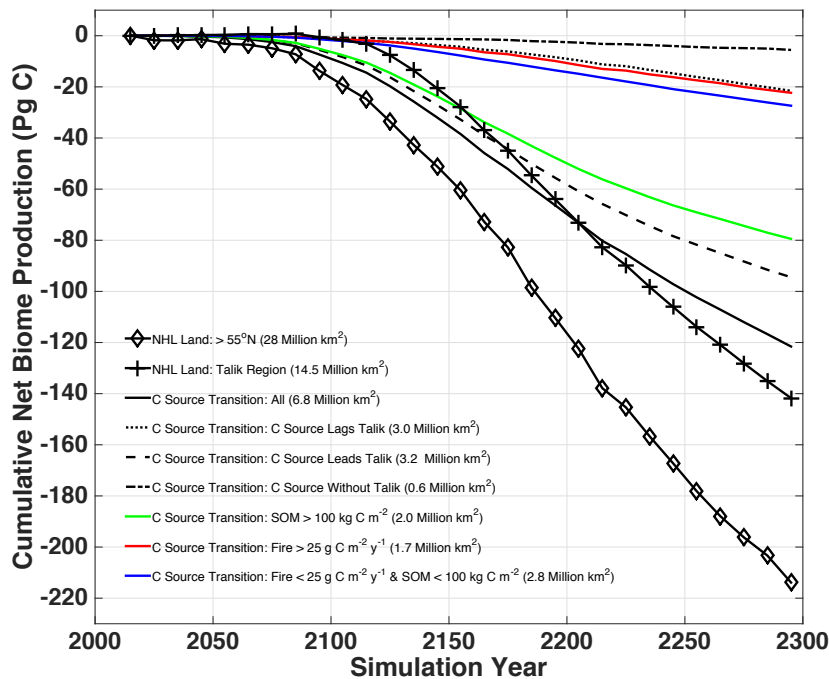


Deleted:

Deleted: . The integrated C source from these regions (magenta) peaks in the late 22nd century

1192 to C source transition shows positive lags in warm southern permafrost (C source lags talik) and
1193 negative lags in cold norther permafrost (C source leads talik). (D) Histogram shows trimodal
1194 distribution of permafrost area as a function of decadal time lag, with negative lags related to
1195 high soil organic matter (green bars and map in E), and large positive lags related to fires (red
1196 bars and map in F) but delayed by high productivity. See text for details. These results assume a
1197 Representative Pathway 8.5 warming scenario through 2100 and an Extended Concentration
1198 Pathway 8.5 through 2300.

Deleted: (Fig. 11B)

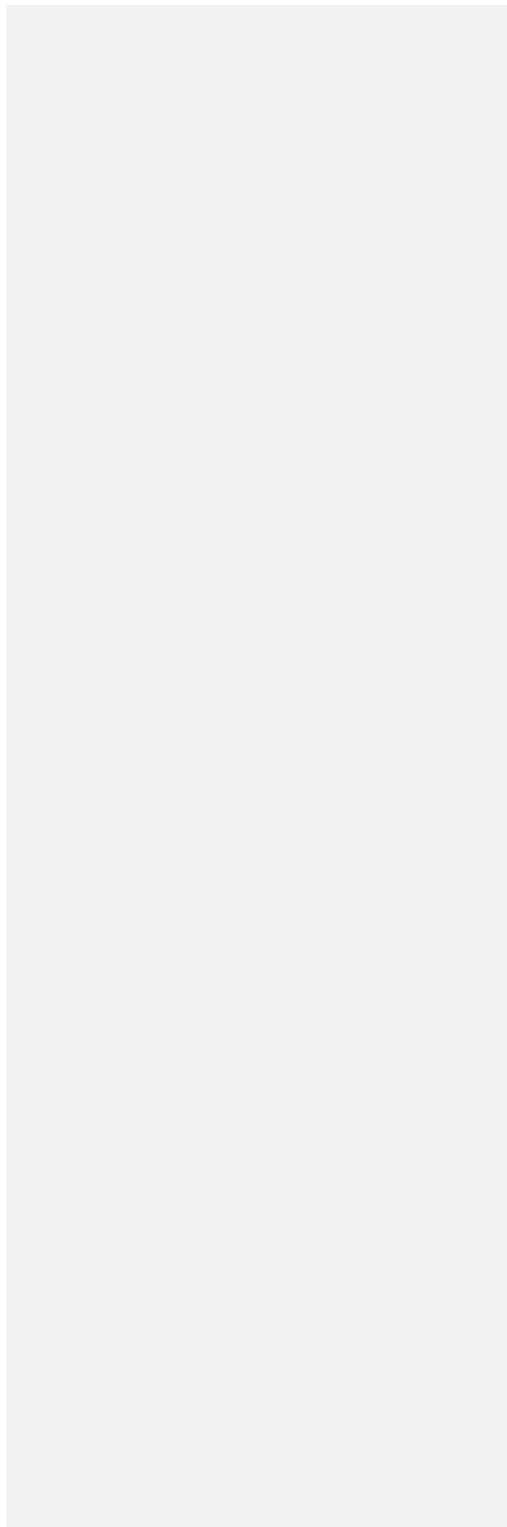


1201

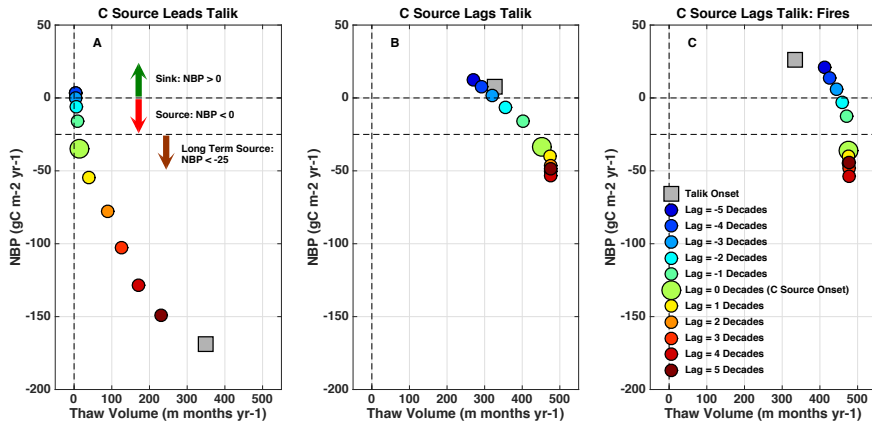
1202 **Figure 8.** Cumulative net biome production (NBP) over northern high latitude (NHL) regions (>
 1203 55°N) from 2010 to 2300. NBP < 0 represents a net C source. NHL regions are divided into the
 1204 following categories: All NHL land (diamonds), NHL land regions which form talik from 2010-
 1205 2300 (crosses), and regions which transition to long term C sources from 2010-2300 (black
 1206 solid). C source transition regions are further broken down based on the lag relationship
 1207 between talik onset and C source transition as follows: Regions where the C source transition
 1208 lags talik onset (dotted), lead talik onset (dashed), and occurs in the absence of talik (dashed
 1209 dotted). C source transition regions also divided by soil C content and fire activity: Regions
 1210 where soil organic matter (SOM) exceeds 100 kg C m⁻² (green), fire emissions exceed 25 g C m⁻²
 1211 yr⁻¹ (red), and SOM and Fires do not exceed these thresholds (blue). Regions which transition to
 1212 C sources prior to talik formation make up half of the total C source area, but account for most
 1213 of the cumulative C source (~80%) in large part due to high soil C.

1214

1215



1216



1217

1218 **Figure 9.** Net biome production (NBP) as a function of thaw volume. Symbols represent NBP
 1219 and thaw volume values averaged over regions which transition to long term C source from
 1220 2060-2140, binned into regions where the decade of C source transition (A) leads talik onset,
 1221 (B) lags talik onset, and (C) lags talik onset AND where fires exceed $25 \text{ g C m}^{-2} \text{ yr}^{-1}$. Colors
 1222 indicate decade relative to C Source transition, denoted by the large green marker, which
 1223 occurs when NBP exceeds $-25 \text{ g C m}^{-2} \text{ yr}^{-1}$ (grey horizontal dashed line). The grey square marker
 1224 indicates the mean NBP and thaw volume values during talik onset. Cases where C source leads
 1225 talik (A) show small thaw volumes during C source transition, and amplified C sources during
 1226 talik onset. Cases where C source lags talik (B-C) show large thaw volumes during C source
 1227 transition, and C sinks during talik onset.

1228

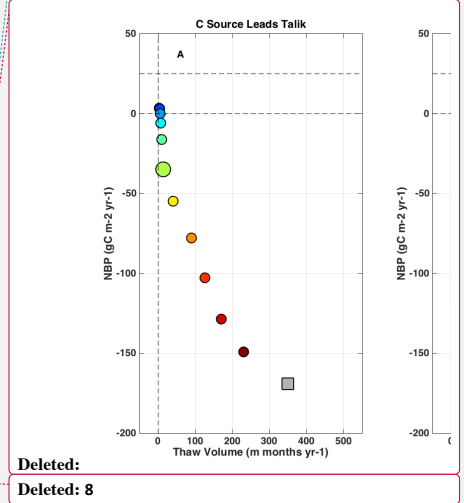
1229

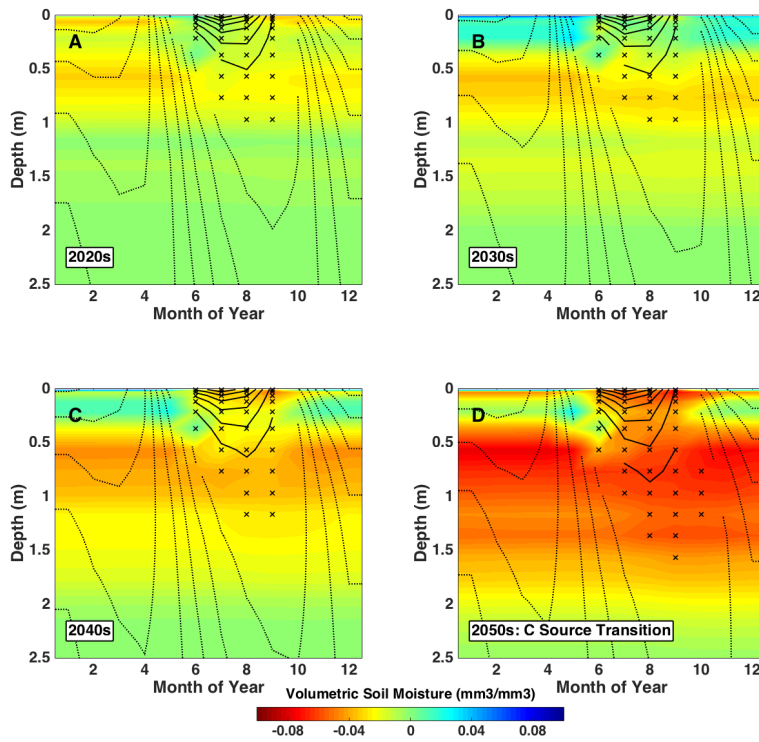
1230

1231

1232

Formatted: Font:Bold, Font color: Text 1





1236

1237 **Figure 10.** Evolution of simulated soil thermal and hydrological state, plotted as a function of
 1238 month and depth, for regions which transition to long term C sources in the 2060s but don't
 1239 form talik for another 3 decades ($\geq 2090s$). This represents cases where C Source leads talik
 1240 (e.g., Fig. 9B). Each panel presents decadal average seasonal profiles in the decades leading up
 1241 to C source transition. Shading and contour details are explained in Fig. 3. These profiles exhibit
 1242 shifts in thaw period (Oct), depth (> 1.5 m), and soil moisture (drying) in the transition decade.

1243

Deleted: 9

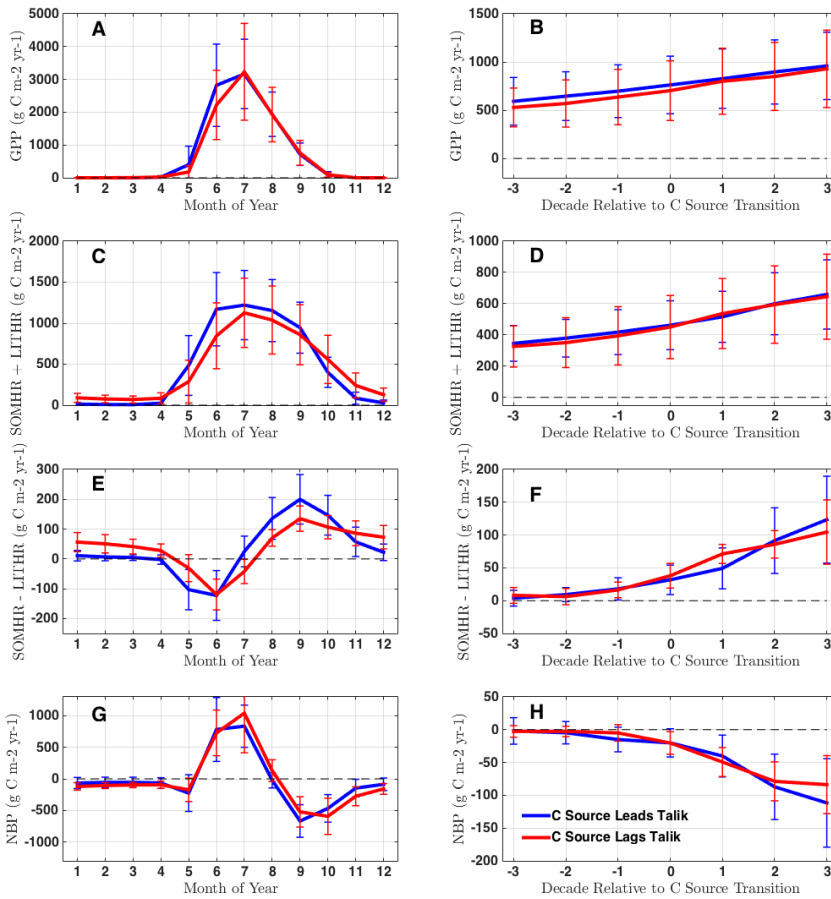
Deleted: 8

Deleted: Page Break

-

Formatted: Font:Bold, Font color: Text 1

Formatted: Font:Bold, Font color: Text 1



1249

1250 **Figure 11.** Time series of ecosystem C fluxes showing seasonal and decadal patterns during C
 1251 source transition. This present mean and standard deviations over the period 2040-2270 for (A-
 1252 B) Gross Primary Production (GPP), (C-D) Sum of respiration from soils (SOMHR) and litter
 1253 (LITHR), (E-F) Difference of respiration from soils and litter, and (G-H) Net Biome Production
 1254 (NBP) where NBP < 0 indicates source. The left columns show seasonal fluxes during the decade
 1255 of C source transition. The right column shows the evolution of decadal mean fluxes in the 3

Deleted: 2

Deleted: results

Deleted:)

1259 decades preceding and following C source transition. Regions where C source transition leads
1260 talik (blue) show similar patterns to regions where transition lags talik (red), most notably a
1261 jump in soil vs litter respiration during C source transition (F) corresponding in time and
1262 magnitude to decreasing NBP (H). The primary difference between regions is the seasonal
1263 distribution of SOMHR vs LITHR (E), which shows a large soil respiration source throughout the
1264 cold season in cases where C sources lag talik. This indicates an annual source of deep old C.

1265

1266

Deleted:). Specifically, this shows

Deleted: sudden

Deleted: (F)

Deleted: in both cases, which

Deleted: s in

Deleted: to the jump in

Deleted: NBP (H)

At first, pan-Arctic C fluxes remain neutral on average over the early- to mid- 21st century (2010-2070) as increasing productivity and C sinks dominate large scale C balance (Fig. 7B, purple). The spatially integrated pan-Arctic C balance increasingly favors net C source dominance over the next 100 years, peaking at 0.7-0.8 Pg C in the mid- to late- 22nd century, followed by gradual decline to 0.5 Pg C by 2300. The cumulative C source over the entire simulated period (2010-2300) is 11.6 Pg C.

Most

Figure 11 presents histograms of total permafrost area (Fig. 11A) and mean GPP (Fig. 11B) as a function of decades since talik onset. We removed regions with high initial soil organic matter ($\text{SOM} > 100 \text{ kg m}^{-2}$, green bars in Fig. 7D) and fire C emissions ($\text{Fire} > 25 \text{ g C m}^{-2} \text{ yr}^{-1}$, red bars in Fig. 7D) during the C source transition decade. This screening yields a more normal distribution of the decadal time lags between talik onset and C source transition (Fig. 11A), with a mean lag of 1 decade from talik onset to C source. The high standard deviation of lags (± 8 decades) reflects the skewed distribution of GPP (Fig. 11B); very low productivity in cold permafrost increases the likelihood that soil thaw will lead to C source transition, while very high productivity in warm permafrost decreases this likelihood.